An Instrument For High-Throughput Measurement of Fiber Mechanical Properties

by

Grant William Kristofek
B.S., Mechanical Engineering (2002)
Massachusetts Institute of Technology

Submitted to the Department of Mechanical Engineering
in partial fulfillment of the requirements for the degree of

Master of Science in Mechanical Engineering

at the

MASSACHUSETTS INSTITUTE OF TECHNOLOGY

February 2005

Author .....
Department of Mechanical Engineering
January 25, 2005

Certified by .....
Ian Hunter
Hatsopolous Professor of Mechanical Engineering
Professor of Bioengineering
Thesis Supervisor

Accepted by .....
Lallit Anand
Professor of Mechancal Engineering
Chairman, Department Committee on Graduate Students

An Instrument For High-Throughput Measurement of Fiber Mechanical Properties

by

Grant William Kristofek

B.S., Mechanical Engineering (2002)

Massachusetts Institute of Technology

Submitted to the Department of Mechanical Engineering
on January 25, 2005, in partial fulfillment of the
requirements for the degree of
Master of Science in Mechanical Engineering

Abstract

In this thesis, an instrument is designed and constructed for the purpose of measuring the mechanical properties of single fibers. The instrument is intended to provide high throughput measurement of single fiber geometric properties, tensile properties, elastic properties, surface roughness properties, friction properties, bending properties, and torsion properties. The instrument is capable of performing all of these mechanical measurements automatically on a large number of sample fibers which are stored in the instrument during testing.

Thesis Supervisor: Ian Hunter
Title: Hatsopolous Professor of Mechanical Engineering
Professor of Bioengineering

Acknowledgments

The process of completing this thesis has been a tremendous learning experience, and I am deeply thankful that I have been granted the opportunity to perform this work. So many fantastic people form the foundation of this work by reason of their various influences on my life along the way; and although they cannot all be thanked here individually, my sincere gratitude goes out to all of them.

I thank my teachers, both past and present, for showing me that knowledge is a gift; that learning is a joy; and that quality is a state of mind. My teachers have all been an inspiration to me in more ways than they may ever know.

I thank my colleagues at MIT and in the Bioinstrumentation Lab for their relentless commitment to science, humanity, and perfection. I have yet to encounter a problem around here at MIT that is not immediately addressed, discussed, and solved. The people at MIT are genuinely caring and deeply knowledgable; and perhaps this is because of their insatiable desire to benefit and encourage the splendor of humanity.

I thank the Course II administrative staff, especially Kate Melvin, Leslie Regan, Joan Kravit, Peggy Garlick, and Marie Pommet for keeping the wheels in motion against all odds.

I thank my advisor, Prof. Ian Hunter, for creating and inviting me to work in the most dynamic and remarkable research environment I have ever encountered, and for all of his support. There are resources in the Bioinstrumentation Lab which defy belief, and I am truly grateful that I have had the good fortune to work here.

My friends have always been indispensable in my life, and with no exception, during the process of this thesis. I would like to thank them for making life a treat and for representing for me no matter what. I would especially like to thank the Castigliones for always reminding me of the finer things in life and my musical friends who have shown me the beauty of vibrations. Everything is timing.

I thank my mom, my dad, and my family for their unconditional love and support. They have taught me about life, love, and happiness. I thank them for their perpetual

reminders to "be good and use my own brain."

Above all, I would like to dedicate this thesis to my sister, Gailin, for her general amazingness and love. She's the best sister around.

Contents

List of Figures

List of Tables

Chapter 1

Introduction

The development of any novel material depends critically on the ability to characterize its physical properties. Researchers perform a wide variety of tests on new materials to determine parameters that will help them inform their material development efforts. For any particular material under test, many test samples are required to determine these parameters with statistical accuracy. Accordingly, the cycle times required to determine the properties of a new material and advance its development are typically quite slow. A great variety of methodologies and apparatus have been developed to improve the tedious characterization process for many material types and geometries. However, remarkably little work has been done to create instruments that rapidly characterize multiple mechanical properties of fine single fibers – fibers approximately 25 - 250 μm in diameter.

1.1 Motivation

The characterization of fine fibers presents an assortment of difficult problems for materials researchers. Most notably, these fibers prove quite difficult to manipulate and measure, given their very small diameters and high length-to-diameter aspect-ratios. Additionally, fine fibers may be easily damaged. Many natural fibers, such as human hairs, cotton, and wool, exhibit structural anisotropy and are highly non-uniform from sample to sample. Extensive or careless handling of such fibers prior to

and during their testing can lead to non-classifiable damage, rendering the statistical determination of their mechanical properties impossible.

The ideal fiber testing scenario minimizes human involvement in the testing process and allows many or all of the desired tests to be performed while the fiber under test remains fixed in a single test fixture. A single instrument that is capable of automatically measuring several mechanical properties for many individual fibers on a per-fiber basis is an optimum solution to increase thoughput for fiber characterization and illicits many diverse applications.

Scientists in the hair care industry are especially interested in such an automated fiber testing instrument. When a new product or treatment has been developed, one must statistically determine its efficacy to ensure that it will not degrade or damage the hair of the customers who will use it. A number of physical parameters of treated hair must be tested, and the majority of these tests are time consuming, labor-intensive, and illicit high capital costs because many individual machines are required.

The instrument at the focus of this thesis is intended to improve the single fiber testing process for one of the leading companies in the hair care industry, Wella AG. Improvements have been made over similar instruments with respect to the number and types of tests performed, testing speed, convenience, cost, and accuracy. The new instrument is quite versatile, and it may also be used to test other natural fibers such as wool and cotton. The device may also aid in understanding the properties of novel synthetic fibers developed by textile manufacturers and research laboratories.

1.2 Prior Instrument Development

A number of machines and instruments have been developed for the purpose of examining specific mechanical parameters of single fibers. Most of these machines are not designed for testing multiple fibers automatically, and those machines which are automated require special fiber preparation procedures and perform only one or two types of test per fiber. The following sections describe some of the most advanced

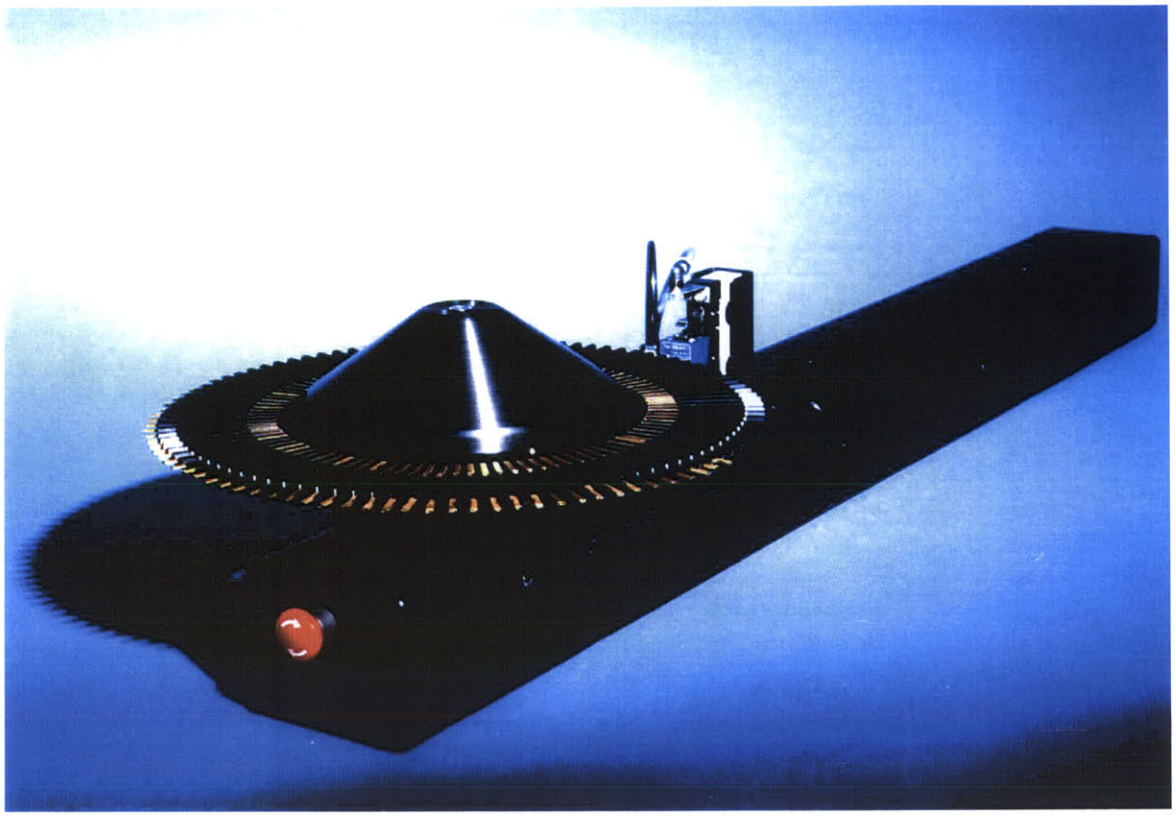

Figure 1-1: The Diastron MTT670 Automated Miniature Tensile Tester. (Taken from http://www.diastron.com, Diastron, Inc.)

instruments presently available for the automated testing of single fibers.

1.2.1 Diastron Automated Miniature Tensile Tester

Diastron Limited is an English company dedicated to developing instrumentation for materials testing. The Diastron MTT670, shown in Figure 1-1, is the current industry standard for the automated tensile testing of single fibers. Two models are available – one model is designed for tensile testing of human hairs and similar fibers, and the alternative model is configured to test non-wovens, polymer strips, and other sheet materials. The machine features automated operation for the testing of up to 100 fibers and performs automatic data analysis with WindowsTM-based software. Both models of the machine are equipped with testing protocols for measuring fiber extension, relaxation, creep, and cross-fiber adhesion [3].

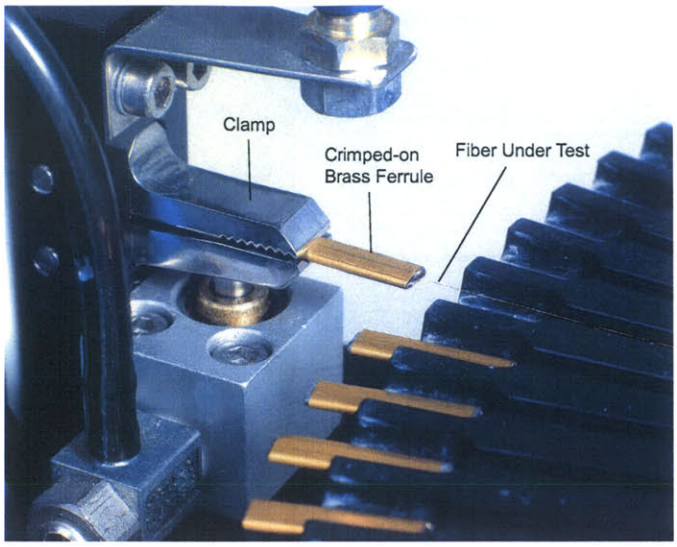

Figure 1-2: Fibers with brass ferrules crimped on for testing in Diastron MTT670. (Taken from http://www.diastron.com/, Diastron, Inc.)

Diastron also offers separate systems for analyzing the diameter, frictional properties, and fatigue characteristics of single fibers. These modules, with the exception of the diameter measurement system, are only compatible with the manually-operated versions of the Diastron tensile testing systems [3].

Additionally, all Diastron testing systems require that the fibers under test be fitted with crimped-on brass ferrules on each end as shown in Figure 1-2. The process of affixing these ferrules greatly increases the time and labor required for fiber testing.

1.2.2 Textechno Favimat-Robot

Textechno Herbert Stein GmbH & Co. KG is a German company that focuses primarily on the development and distribution of testing technology for the textile industry [4]. The Favimat-Robot is the most advanced single fiber testing system offered by Textechno. The Favimat machine facilitates four different testing protocols: a linear density test capable of measuring fiber linear density based on an acoustic excitation method; a static tensile test that examines conventional stress-strain properties such as strength, tenacity, elongation, and elastic modulus; and a textile-specific crimp test which determines fiber crimp geometry optically and crimp stability mechani-

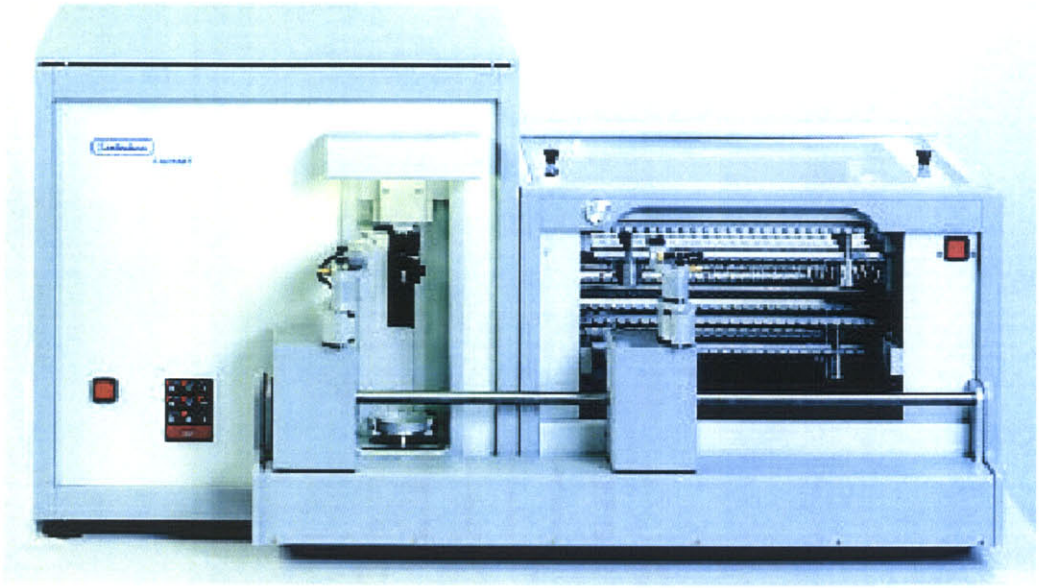

Figure 1-3: The Textechno Favimat Robot Automated Fiber Testing Machine. (Taken from http://www.textechno.com, Textechno KG)

cally. The machine requires pretensioning of the fibers for some of the tests using special tongs-shaped pre-tensioning weights [4].

The Robot is an automatic fiber feed unit designed to interface with the Favimat. Up to 450 fibers can be loaded into the Favimat machine via 18 magazines in the Robot's automatic sample changer, each of which holds as many as 25 fibers. Single fibers are transferred from each magazine to the test section of the Favimat instrument via a mechanical transfer clamp [4]. Figure 1-3 shows the Textechno Favimat Robot automatic single fiber test system.

1.2.3 Wella-developed Hair Testing Instruments

The German hair care company, Wella AG, is one of the world leaders in the science of hair testing and has developed a wide variety of instrumentation in the laboratory of their Department of Keratin Research and Efficacy Testing (*Forschung Keratin Meβtechnik*, or FKM). The techniques and methods employed in the Wella FKM are explained in detail in Section 2.3.

1.3 Approach

Many systems must be carefully designed and integrated to create an automated single fiber testing machine that operates simply and harmoniously yet is capable of measuring the many parameters essential to characterizing single fibers. The design process aimed to keep each element as modular as possible in order to minimize the effects of modifications on unrelated system functions. Furthermore, all modules were designed for simple integration with the complete system.

The first step in the creation of the automated fiber testing machine was to examine and identify the important parameters and properties of single fibers. Human hairs were the subject of the single fiber properties examination primarily because of their complex properties as compared to most other types of single fibers but also because the instrument under development for this thesis was intended specifically for testing human hairs.

Next, critical functionalities of the machine were isolated based upon the most pertinent mechanical parameters identified during the study of hair fiber properties. At this stage, an evaluation of existing technology was performed to ensure that all developed technology improved on the state of the art.

Concepts were then brainstormed for each test and for the automation mechanisms that would be used to hold, transport, load, and unload each fiber under test. These concepts were carried to working prototypes and finally to functional design modules which were integrated into the instrument. The complete automated single fiber testing system is shown in Figure 1-4 as a point of reference for the rest of the thesis.

Chapter 2 provides general background on human hair and hair testing. The information is valuable to understanding the reasoning behind many of the design decisions made during the development of the single fiber testing instrument. The morphology of hair fibers is discussed in addition to other general properties of interest to researchers in the cosmetic industry including the chemical composition and mechanical properties of hair fibers. Finally, several of the methodologies utilized by the cosmetic industry for testing hair fibers are presented in order to inspire concepts

for the development of the automated single fiber testing instrument.

Chapter 3 describes the basic considerations of single fiber testing that were used to inform the design of the testing structure of the automated hair testing machine. Overseeing principles of the instrument design are introduced and each measurement performed by the machine is detailed with respect to the desired properties to be measured, the methodology or protocol of measurement, and the user-adjustable variables for each measurement.

Chapter 4 describes the basic automation considerations which guided the design of the fiber handling architecture of the automated hair testing machine. The effective storage of single fibers to be tested is considered. Additionally, factors relating to the manipulation of fibers before, during, and after testing are discussed.

Chapter 5 describes the design and implementation of the automated fiber handling modules that comprise the automated fiber testing machine. Specific components and hardware are detailed.

Chapter 6 describes the design and implementation of the measurement modules that comprise the automated fiber testing machine. The data acquisition for the system is discussed, as well. For each each measurement system, measurement principles and design requirements are set forth; and specific components and hardware which have been utilized to implement the module are detailed.

Chapter 7 provides a brief discussion of the basic implementation of the software that governs the instrument functionality. The main computer platform, development software, user interface, and data storage strategies are presented.

Chapters 8 presents conclusions and recommendations for future work in the development of the automated single fiber testing instrument.

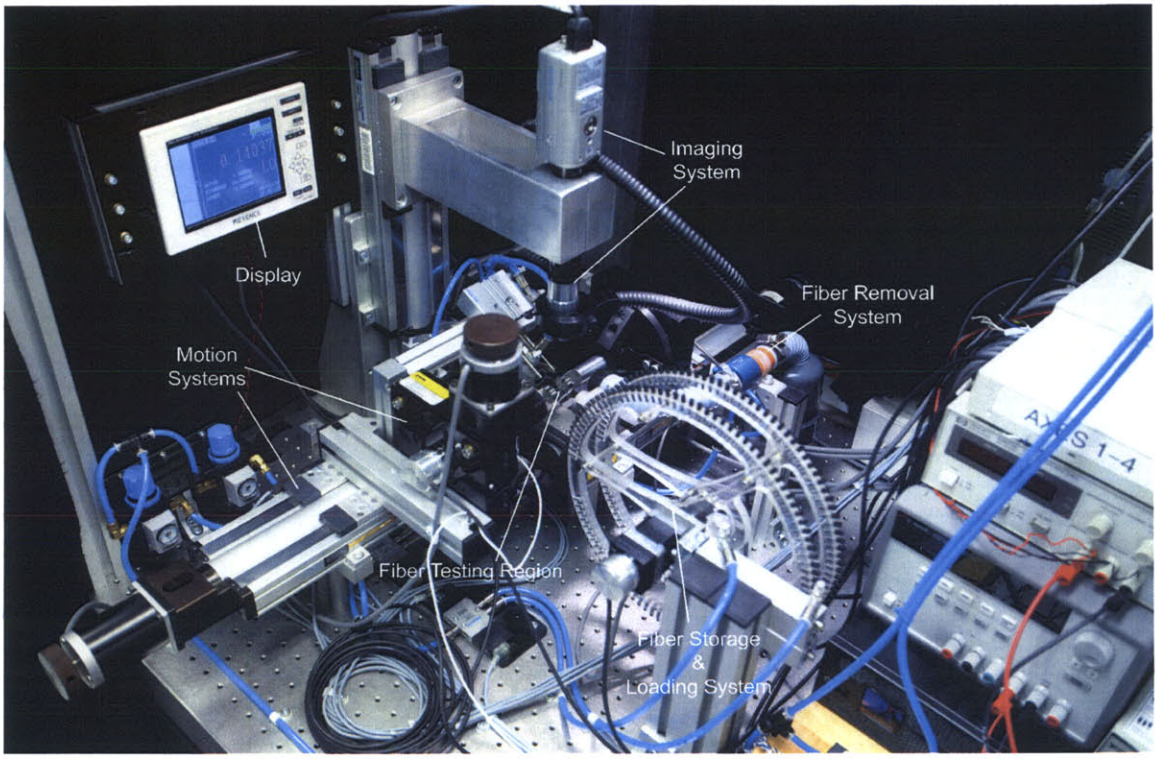

Figure 1-4: The automated single fiber mechanical testing instrument. Major modules annotated by arrows. (Photo: Kristofek)

Chapter 2

Background

The high-throughput single fiber testing instrument has been developed as a general purpose instrument to improve the state of the art in single fiber testing technology. Wella AG, a likely first user of the instrument, plans to integrate the instrument into the Wella FKM laboratory in Darmstadt, Germany. The laboratory performs efficacy testing for newly-developed hair care products such as shampoos and conditioners and for hair treatments such as bleaches, perms, and colorings. Tests are routinely performed on both single hair fibers and 100-fiber hair swatches and rely on statistical analyses of many tested samples to differentiate and quantify the effects of new products and treatments. An examination of some of the basic characteristics and properties of human hair as well as the testing methodology employed by Wella is a good starting point for understanding how the instrument has been developed and also for where future development efforts may wish to proceed.

2.1 Morphology of Human Hair Fibers

Human hair is a specialized outgrowth of the outer part of the skin called the epidermis [5] and provides protective, sensory, and sexual attractiveness functions [6]. Hair is a remarkably complex and robust natural structure. It is composed primarily of keratin proteins, which are described in more detail in Section 2.2.2, and consists of a hard outer layer of cells called cuticles, a chemically resistant epicuticle layer

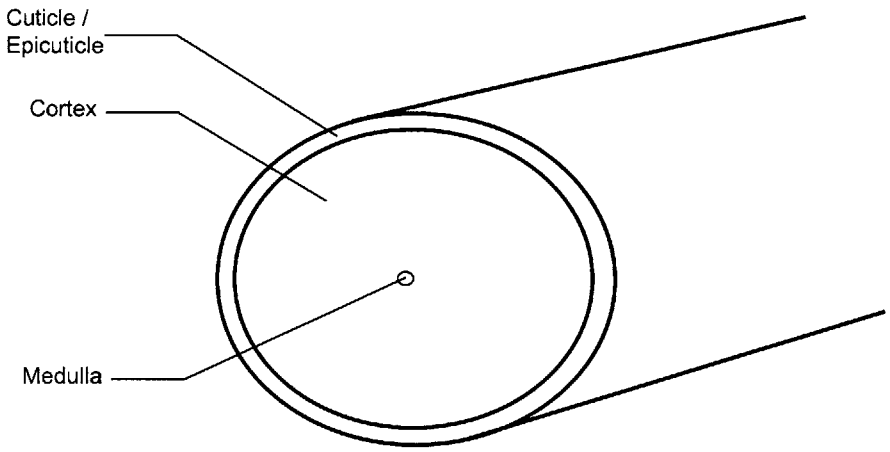

Figure 2-1: Cross-section diagram of human hair depicting primary structural elements.

over the cuticles, a fibrous inner core of cells called the cortex, and an innermost core of cells generally found only in thicker hairs called the medulla. The cellular keratin regions of the hair are bound together by the cell membrane complex which is primarily comprised of non-keratinous matter [6]. Figure 2-1 shows the locations of the primary structural components of human hair in a cross-sectional schematic.

2.1.1 Hair Growth

Human hair is grown from specialized cavities or sacs in the epidermis called hair follicles (Figure 2-2). Approximately five million of these hair follicles cover the human body, and the number of follicles typically decreases by about 10% by the time a person has reached old age. Cellular mitosis, a process of equational cell division, is the mechanism of hair growth in the hair follicle and occurs in the lowermost region of the so-called zone of differentiation [1]. It is in this area of the hair follicle where specialized cells called keratinocytes begin to differentiate morphologically and form the keratin which provides the structure of human hair [1].

According to Robbins [6], three distinct stages of hair growth have been identified. The anagen, or growing, stage of hair growth lasts for approximately 4-6 years for scalp hair and results in hairs which are typically 1 m long, but can lead to hairs as

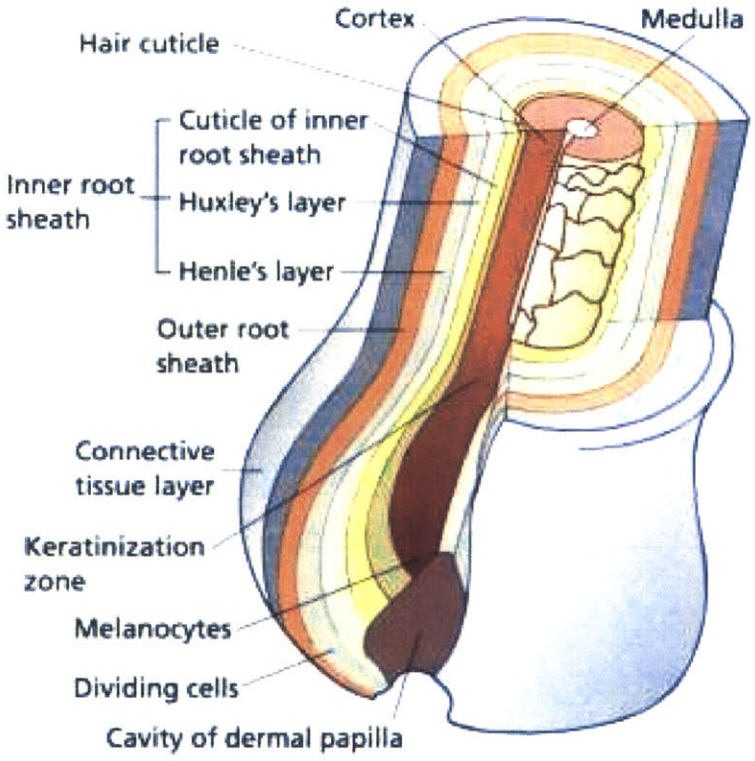

Figure 2-2: Schematic diagram of human hair follicle. (Taken from http://www.pantene.com, Pantene, Inc.)

long as 1.5 m or more. The average growth rates for scalp hairs in the anagen stage are approximately 160 mm per year for hair in the crown area, 140 mm per year for hair in the temporal area, and 100 mm per year for other hair such as facial hair in men [6]. About 90% of the human scalp hairs are in the anagen stage at any given time [1].

The catagen stage, which lasts approximately 20 days, is the transitional stage of hair growth and leads into the telogen, or resting, stage of hair growth [1]. During the telogen stage, which lasts approximately 3-9 months, hair growth stops completely. The base of the hair bulb in the follicle has atrophied during the catagen stage and new hair begins to grow beneath the telogen hair, pushing the telogen hair out. It is normal to lose approximately 100 telogen hairs per day [1].

All of these growth stages occur simultaneously during a mature individual's life to ensure that there is constantly new and healthy hair covering the head and body. However, hormonal changes occur when a person reaches his or her mid-to-late twenties, resulting in finer, shorter hair. In some individuals these hormonal changes lead to the formation of fine vellus hairs, a process commonly called balding [6]. A schematic of a human hair fiber is shown in Figure 2-3 and is notated with the main structural components which shall be described in the following several sections.

2.1.2 The Cuticle

The cuticle may be defined as the chemically resistant outer region surrounding the cortex in animal hair fibers [1]. The cuticle layer consists of hard, flat overlapping cells surrounding the central fiber core. Cuticle cells are attached at the proximal, or root, end of the hair and extend toward the distal, or tip, end. The shape and orientation of the cuticle cells accounts for the differential friction effect of hair which means that the friction from root to tip is less than the friction from tip to root [6]. Figure 2-4 shows the structure and orientation of the cuticle cells on a healthy, undamaged human hair fiber.

Individual cuticle cells are typically 0.5 μm high and between 45 μm and 60 μm long. The exposed surface of the cells is approximately 5 μm. The cuticle layer of

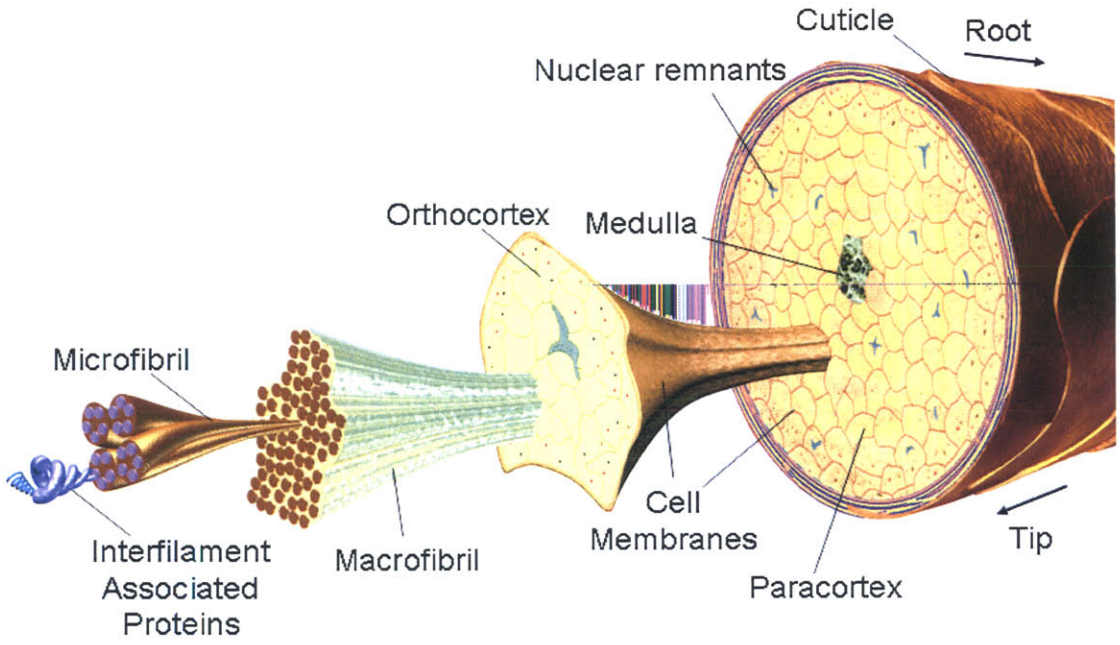

Figure 2-3: Schematic diagram of human hair with major structural components labeled. (Taken from archives, Wella AG)

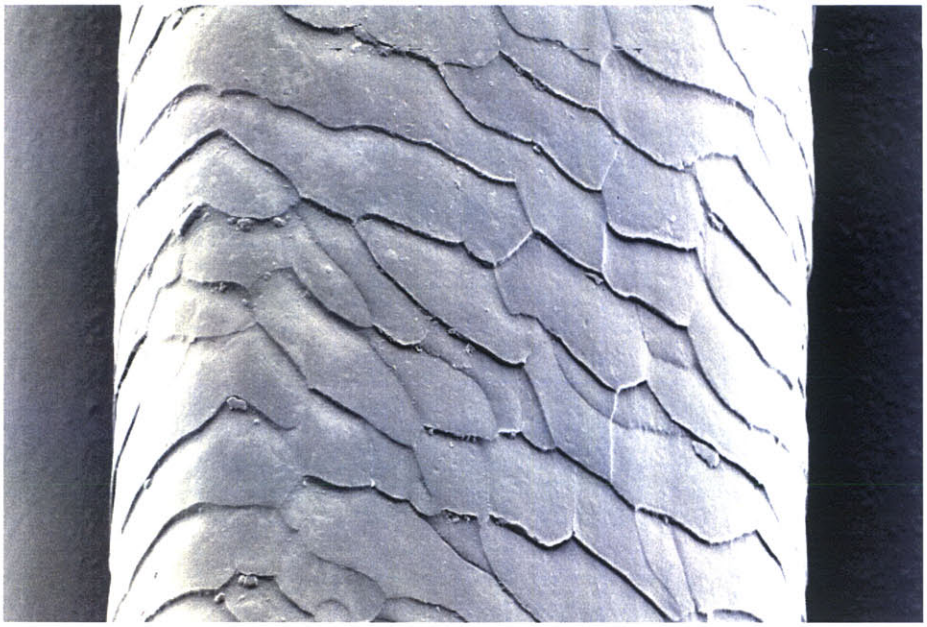

Figure 2-4: Cuticles on a hair fiber in good condition. (Taken from archives, Wella AG)

human hair is generally 5-10 cuticle cells thick. Forensic studies often analyze the cuticle layer to determine the species of origin based upon the number of cellular layers [6].

The cuticle layer is usually smooth and unbroken near the scalp, but grooming and weathering effects on the hair almost inevitably lead to cuticular damage such as lifted cuticle scales (Figure 2-5) or even complete removal of the cuticle layer in extreme cases (Figure 2-6).

The cuticle layer consists of several distinct layers. The exocuticle is the outermost layer of cuticle cells and is also the hardest and most durable layer of the hair fiber. The endocuticle is beneath the exocuticle area and is made up of softer and more pliable matter.

2.1.3 The Epicuticle

A thin material called the epicuticle covers the surface of mammalian hairs [6]. The epicuticle is approximately 5 - 10 nm thick and was first noted by Allworden [7] in

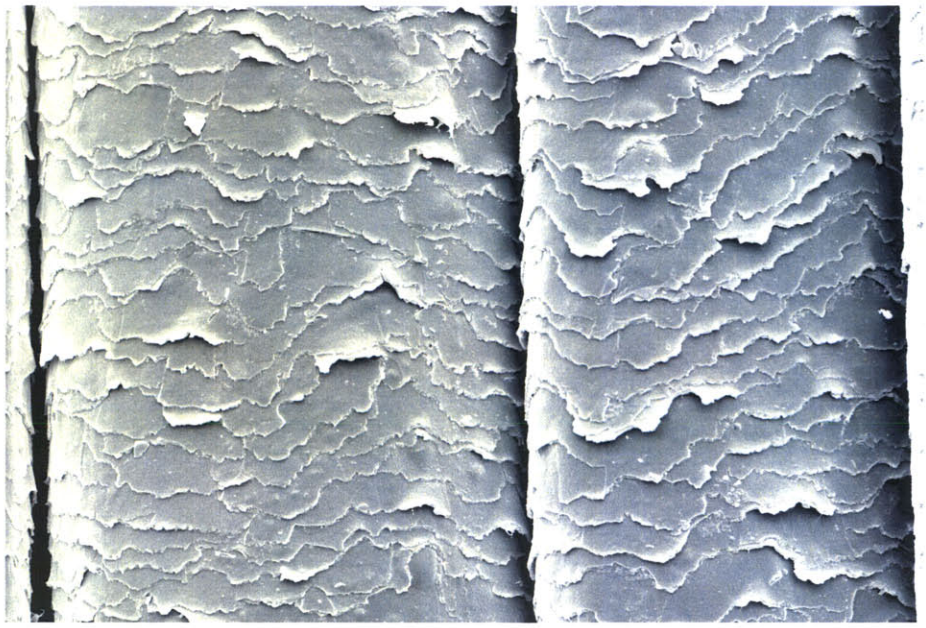

Figure 2-5: Lifted cuticles on damaged hair fibers. (Taken from archives, Wella AG)

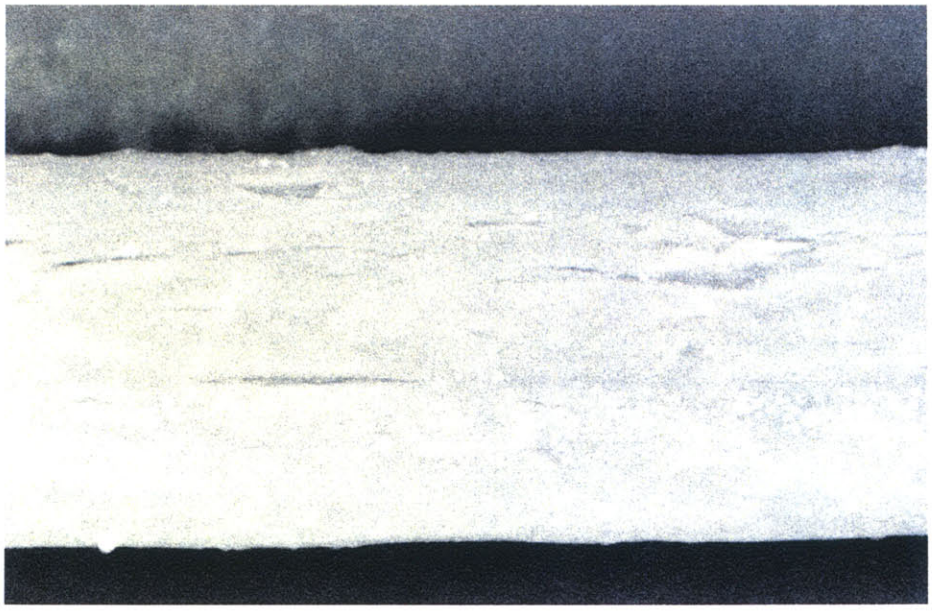

Figure 2-6: Hair fiber in highly damaged condition with cuticles removed completely. (Photo: Kristofek)

wool fibers when he observed that sacs or bubbles form at the surface of fibers treated with chlorinated water. The Allworden sacs form as a result of chlorine diffusion into the cuticle cells. Chlorine degrades proteins within the cuticle cells and produces water soluble species too bulky to diffuse out of the semipermeable cuticle membrane [1]. The subsequent swelling, produced by osmotic forces, results in the observed Allworden sacs.

It was later discovered by Leeder and Bradbury [8] that epicuticle membrane surrounds each individual cuticle cell and is not a continuous membrane covering only the outer part of the hair as was once suggested. The researchers showed this by isolating individual cuticle cells and demonstrating that single cuticle cells undergo the Allworden reaction.

2.1.4 The Cortex

The cortex region constitutes the majority of the mass of hair fibers. The remarkable mechanical strength and elastic properties of hair fibers may also be attributed primarily to the structure of the cortex. Long cords of telescopically arranged cortical cells and intercellular binding material known as the cell membrane complex make up the structure of the cortex [6]. Approximately 100 to 200 parallel cortical cells may be found in the cross-section of a typical human hair [1].

Cortical cells are between 1 μm and 6 μm thick and approximately 100 μm long, although significant variation in their size has been reported. Two main types of cells exist in the cortex. The predominant cell type found in the cortex of human hair is the paracortical cell. Paracortical cells have a high sulfur content and are typically hard in contrast to the lower sulfur content orthocortical cells. Orthocortical cells are generally found only in a narrow concentric ring at the periphery of the cortex in human hair, but may constitute as much as two-thirds of the total cortical cells present in crimped wool fibers. The cortical cells are not smooth, but instead have projections, fringes, and indentations which form a mechanically strong interdigitated microstructure in the direction of growth [1].

A substructure of several dozen macrofibrils makes up each cortical cell [1]. Each

macrofibril is comprised of hundreds of α-helical microfibrils, which are also known as intermediate fibrils. In paracortical cells, the microfibrils typically align parallel to the hair axis in a hexagonal close-packed pattern [1].

Microfibrils are very small — only 7 μm in diameter — and are therefore observable only with the aid of high magnification electron microscopy. The building blocks of the microfibrils are protein strands with total lengths of 45 μm to 50 μm, each consisting of approximately 500 amino acids. Acidic and basic forms of these protein strands form self-stabilizing α-helical pairs called protofibrils which are attached to one another by hydrogen bonds between succesive turns. These α-helical structures account for the great elasticity of hair because they can be unwound and stretched by as much as 30% without permanent damage [1].

2.1.5 The Medulla

A trabecular framework of fibrous cellular proteins called the medulla is located at the very center of many hair fibers [9]. The medulla is not present in fine animal hair fibers or in human hairs with diameters less than about 60 μm. The original biological function of the medulla is thought have been to provide warmth through enhanced thermal insulation. For example, the winter fur of deer consists primarily of medullary cells [1]. The composite of medullary cells contains a significant amount of hollow space which is ideal for trapping air for thermal insulation purposes. The medulla also often serves as a pigment reservoir and forms an inner plane of reflection within the hair fiber which is believed to contribute to the shine and luster of human hair [1]. Chemicals are more likely to degrade the protein structure of the medulla than the cortex or the cuticle [9].

2.1.6 The Cell Membrane Complex

The strength of the mechanically interlocked cellular microstructure in the hair fiber is fortified by the cell membrane complex. Cortical and cuticle cells are prevented from sliding past one another by reason of a variety of connection types. Amorphous

material known as intercellular lamellae is deposited between cortical and cuticle cells and serves as an intercellular cement. The intercellular lamellae is comprised of ultra-fine proteins, polysaccharides, and lipids [1, 9]. Another cellular connection formed in the cell membrane complex is the intercellular bridge, which resembles a welding seam and exists primarily between cuticle and perpipheral cortical cells. The connections formed by intercellular bridges are marked by their limited area of contact between neighboring cells and complete lack of cell membrane. Transmembrane proteins form the final type of intercellular connection in the cell membrane complex, acting like rivets between the respective membranes of adjacent cells [1].

2.2 General Properties of Human Hair

The remarkable properties of hair fibers have been mentioned numerous times already; however, those properties have not been defined. This section details the pertinent cosmetic and mechanical properties of hair fibers and also describes the chemical composition of hair fibers.

2.2.1 Cosmetic Properties

Water dominates the cosmetic properties of hair. Hair is insoluble in water largely because of the disulfide bonds formed by the amino acid cysteine. Nonetheless, hair is highly hydrophilic, or water-friendly, and has many sites for water molecules to anchor. Water is not absorbed into hair as in a sponge but is instead chemically bound within the fiber by weak bonds [1].

When hair is dried with heat, water on the surface is evaporated, and depending on the amount of heat applied, some of the moisture inside the fiber is evaporated as well. It is interesting to note that hair which feels dry to the touch may still contain approximately 15% residual moisture by weight. This humidity level is the normal moisture content of a newly-grown, cosmetically-unaltered hair fiber [1].

A hair fiber will equilibrate its moisture content with its ambient environment and is therefore considered to be a hygroscopic material. Hair placed in a very humid

environment above 90% relative humidity (RH) will swell up to 16% in diameter and about 2% in length. Under such high humidity conditions, hair also becomes plastically deformable and may be stretched by up to two times its original length without breaking [1].

Cosmetic properties of hair such as manageability and style retention are all affected directly by its hygroscopic behavior. For instance, the stability of water set curls results from the tension of the hair wound onto rollers while it is wet and in a plastically deformable state. When the hair is dried, usually by heat, it returns to its hard, elastic state and also shrinks slightly, causing the curls to hold shape semi-permanently [1]. Usually once hair is wetted again or experiences a very humid environment, the curls disappear.

The process of perming, or permanent curling, involves chemically breaking the disulfide bonds in the hair fiber itself to induce a plastically deformable state in the hair during which the new style is implemented. Once the hair has been styled in the chemically-weakened state, another chemical agent is used to re-form the disulfide bonds, thus permanently holding the hair in the desired style. Of course, using chemicals to physically alter the structure of hair will compromise the integrity of the hair fibers, and it is important to develop chemicals for this process that minimally affect the original properties of the hair. The automated fiber testing instrument is intended to dramatically improve the testing and development process for such chemicals by allowing researchers to rapidly test many fibers for the physical properties which may be changed or compromised following cosmetic treatment.

The temperature stability of hair is also dependent on its moisture content. Dry hair is stable to temperatures as great as 200°C, however wet hair will begin to suffer heat damage at temperatures of approximately 140°C.

Hair is an insulator material, meaning that it is highly resistant to conducting electricity. As a result of its insulating properties, hair fibers will maintain a high electrostatic charge when they are dry, and especially fine hairs will be prone to a cosmetic behavior known as "flyaway" during combing which results in the hairs literally floating away from the head and into the air. The phenomenon of "flyaway"

does not occur in moist hair because the water is able to carry away the electrostatic charge that may have built up [1].

Several of the interesting and useful properties of hair fibers are summarized Table 2.1. Knowledge of many of these properties will be critical to the development of the automated single fiber testing instrument.

2.2.2 Keratin

Human hair is composed largely of keratin. Skin, nails, hooves, claws, horns, and feathers are also made up primarily of keratin which has more than thirty distinct forms [1].

Keratin is commonly defined as an aggregate of proteins with either low or high sulfur content. In the human hair, keratin is synthesized in the keratogenous zone of the hair follicle and moves upward where it is morphologically differentiated into the various components of the fiber. About 85% of the mass of the hair fiber may be attributed to keratin proteins in the cortex [9].

The exocuticle contains keratin proteins with a high concentration of cysteine which form disulfide bonds with the A-layer of the cuticle. These disulfide bonds provide the great hardness and toughness of the cuticle. The endocuticle is composed of keratin with a much lower cysteine content and is thus softer and less durable than the exocuticle [9].

2.2.3 Chemical Composition

The chemical composition of hair fibers is dominated by carbon, which comprises about 45% of the atomic structure of hair. Oxygen accounts for approximately 28%, nitrogen 15%, hydrogen 7%, and sulfur 5%. Several essential trace elements are also present in hair fibers including iron (20 - 220 ppm), copper (10 - 20 ppm), zinc (190 ppm), and iodine (0.6 ppm) [1].

Amino acids are the principle building block of the keratin proteins found in hair fibers, and approximately 20 different amino acids are present in these proteins. The

Fiber Property	**65% R.H.**	**100% R.H.**
Mean Diameter [μm]	70	—
Density [kg/m^3]	1320	—
Linear Density [mg/mm]	6.7×10^{-6}	—
Water Uptake [% of own weight]	12-15	30
Limit of Complete Stretching Recovery [%]	—	>30
Extensibility to Break [%]	50	90
Tensile Strength [MPa]	204-254	153-178
Elastic Modulus [MPa]	10	1
Bending Modulus [MPa]	1.5-2.0	—
Torsional Modulus [MPa]	1-2	—
Melting Point [°C]	280	140
Thermal Conductivity [W/m·K]	0.3	—
Electrical Resistivity [Ohm/mm]	6×10^5	—
Transparency to Light	UV, short wave light	—
Light Reflexion (at 45°)	5.7	—
Refractive Index	1.55	—
Birefringent	yes	yes

Table 2.1: Miscellaneous mechanical, thermal, and electrical properties of human hair fibers at room temperature (25°C) in air (65% relative humidity) and in water or saturated vapor (100% relative humidity) - adapted from the text *Hair Structure* [1] by Wella AG.

predominant amino acid is the sulfur-containing cystine. Table 2.2 summarizes the chemical composition of human hair.

2.3 Hair Care Industry Methodology

The Keratin Research and Efficacy Testing Department at Wella AG has established over two dozen techniques and methods for characterizing various interesting cosmetic and mechanical properties of human hair fibers. The tests developed by Wella are capable of determining properties for single fibers as well as for multi-fiber strands, which generally contain 100 hair fibers. The tests allow researchers to evaluate the degree of hair damage in several ways; to determine different aspects of hair fiber luster; to categorize cosmetic properties such as hold level, elasticity, swelling behavior, and style volume; to understand surface properties of hair; and to observe alterations in hair color. Typically, each of these tests requires a single dedicated apparatus. Furthermore, while there is a trend to automate the testing procedures, many of the machines must be operated manually, and the test cycle time can be slow and labor-intensive. This section briefly describes some of the tests developed by Wella which have served as inspiration or motivation to the creation of the automated single fiber testing instrument.

2.3.1 Sorption Measurement

The uptake of water vapor by hair fibers is commonly determined by a procedure called sorption measurement which examines the change in fiber mass caused by water uptake [6, 10]. A sorption balance (type DVS-1, from Porotec) as shown in Figure 2-7 is used by Wella to measure the mass to a high degree of precision (1 μg). The hair material to be tested is cut into pieces approximately 2-3 mm in length, and about 10 mg are weighed in the apparatus. The mass of the sample is determined accurately via the built-in microbalance, and immediately after, the cuttings are dried for 4-6 hours in the apparatus until they have reached constant mass at 20% relative humidity.

Elements	carbon (45%), oxygen (28%), nitrogen (15%), hydrogen (7%), sulfur (5%)
Essential Trace Elements	iron (20-220 ppm), copper (10-20 ppm), zinc (190 ppm), iodine (0.6 ppm)
Amino Acids	20 different kinds; typical: sulfur-containing cysteine
Proteins	
rich in sulfur, amorphous	approx. 30%, 80-100 intermediate filament associated proteins
poor in sulfur, amorphous	approx. 20%, in endocuticle, cell membrane complex remnants of cell nuclei
poor in sulfur, α-helical, partly crystalline	approx. 50% of all proteins; keratins, at least 10 different kinds

Table 2.2: Chemical composition of human hair - adapted from the text *Hair Structure* [1] by Wella AG.

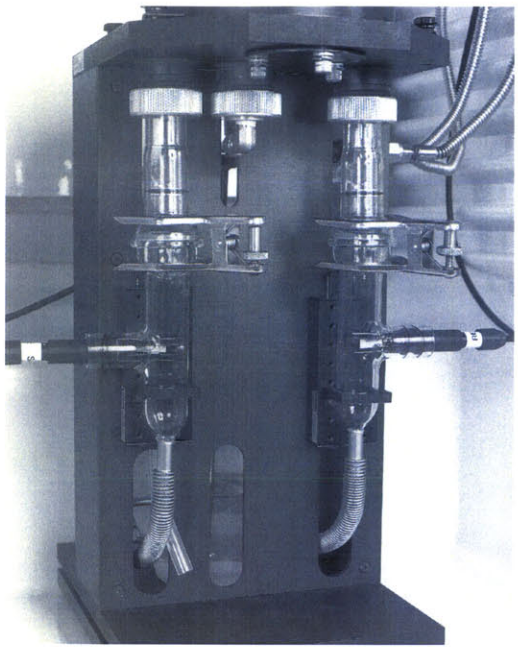

Figure 2-7: Sorption measurement test setup with the Porotec DVS-1 at Wella FKM Laboratory in Darmstadt, Germany (Taken from archives, Wella AG).

Upon completion of the drying phase, the humidity in the sample chamber of the apparatus is gradually increased to 95% relative humidity in five equal increments, and then gradually lowered again in identical increments to 20% relative humidity. The uptake and loss of humidity in the hair sample are detected as an increase and subsequent decrease in the sample mass. One measuring run is sufficient to determine the water uptake and loss data for treated and untreated hair in the relevant humidity range for quantification [10].

Figure 2-8 shows example test data comparing the vapor soprtion of untreated hair fibers to bleached hair fibers. It can be seen that the bleaching process increases the overall water vapor sorption of hair fibers significantly. One may also observe that the water sorption/desorption process in hair fibers exhibits hysteresis.

2.3.2 Shine Measurement

The shine or luster of hair is one of the most important cosmetic properties of interest to developers of hair care and treatment products. Unfortunately, the human sensory

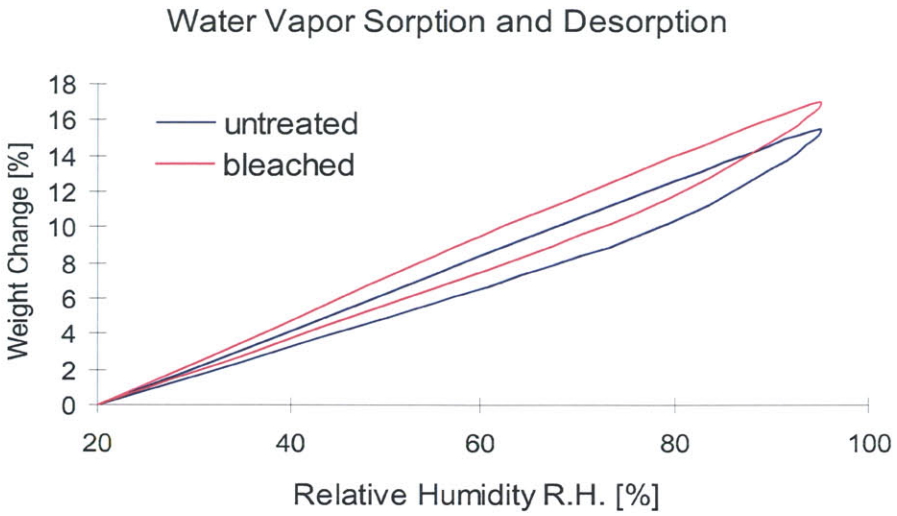

Figure 2-8: Example sorption measurement test results for bleached and untreated hair samples. (Data: Wella AG, FKM Laboratory)

perception of shine and luster is highly sensitive and developed, and instruments cannot easily measure the phenomenon. Despite the fact that numerous instrument-based methods for measuring shine have been created [6, 11], none of these methods have been standardized.

For the method utilized by Wella, a parallel beam of full-spectrum light is shined directly at the surface of a multi-fiber hair tress and the angular distribution of the reflected light is measured. The method also measures the amount of light which is diffusely scattered at or beneath the surface of the sample. The desireable characteristic of high shine intensity is indicated by a high percentage of directly reflected light and a low percentage of diffusely scattered light. It is also generally true that a narrow angular distribution range, or half intensity width (HIW), indicates higher shine, and a wide angular distribution range means less shine. Tests with human judges of hair shine have confirmed that hair tresses with a narrow HIW are more shiny [12].

The properties of the incident light strongly affect the perception of shine, and light from ubiquitous sources must be carefully excluded during shine measurement.

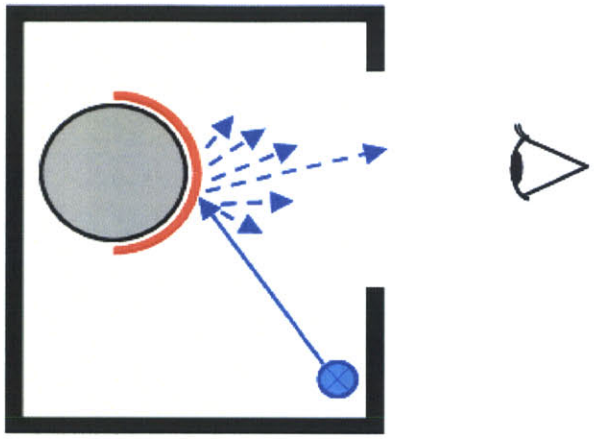

Figure 2-9: Schematic of the shine measurement test setup at Wella FKM Laboratory in Darmstadt, Germany. (Taken from archives, Wella AG)

Therefore, a black, glare-free box is used for all measurements, including those performed subjectively by eye and those performed objectively using a digital camera. The box is fitted with a tubular 60 W 220 V light bulb and each hair tress under test is wrapped around a 75 mm outer-diameter black rod mounted in the center of the box. Figure 2-9 shows a schematic of the test setup utilized at the Wella FKM laboratory for measuring and quantifying the shine intensity of human hair tresses, and Figure 2-10 shows the physical test setup. A Sony DXC-151P digital camera is used to measure the angular distribution of light. Data is recorded by an Imaging Technology Incorporated IML 150/40 Framegrabber PC card and analyzed using Optimas 5.2 image processing software [12].

Digital images of four different sample types captured by the shine box are shown in Figure 2-11, clockwise from top left: aluminum foil, red hair, blonde hair, and black hair. Upon acquisition of an image, the image analysis system measures the luminance of the reflected light in the vertical axis, which yields a distribution of light along the vertical axis of the image.

A set of curves corresponding to each of the samples tested by the image analysis system is shown in Figure 2-12. The vertical axis of the graph represents the intensity

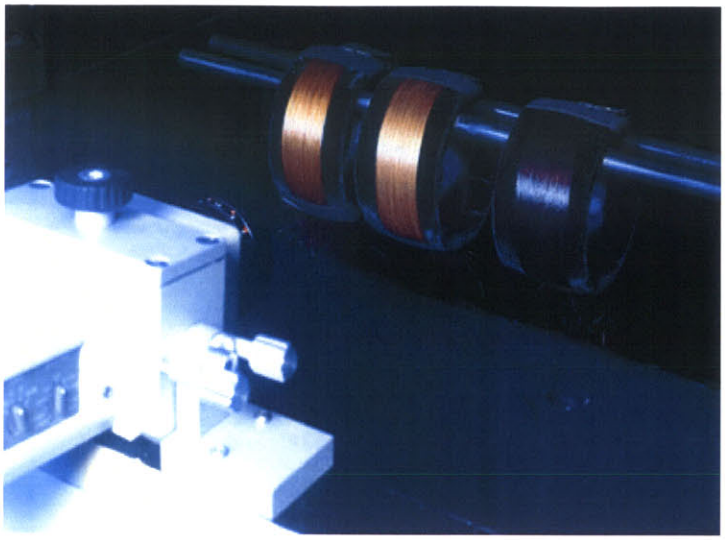

Figure 2-10: Photo of the actual shine measurement test setup at Wella FKM Laboratory in Darmstadt, Germany. (Taken from archives, Wella AG)

of reflected light and the horizontal axis represents the angle of observed intensity. For the aluminum foil (gray curve), a very slim and high peak is seen at the center of the graph. Very little off-axis reflection is observed because the incident and reflection angles are identical. For the tress of black hair (black curve) as well as the other hair samples, an angular shift of the peak is observed. This effect may be attributed to the angle of the cuticle scales, an effect which will be explained momentarily. For the red hair (red curve), a wider main peak and a small "shoulder" are present, and in the case of blonde hair (yellow curve), a very broad main peak and a very dominant "shoulder" may be observed.

In each shine measurement, the majority of light is reflected off the surface of the sample and creates the main peak on each curve. In the case of the hair tresses, a small percentage of light enters the hair and is reflected off the backside of the hair which produces the observed shoulder in those respective curves. Finally, some incident light is scattered inside and at the outer surface of the hair tresses resulting in the diffusive portion of reflected light which is observed as lower intensity light shifted angularly from the center. Figure 2-13 shows a diagram of the light paths resulting in the specular and diffuse reflection patterns described above.

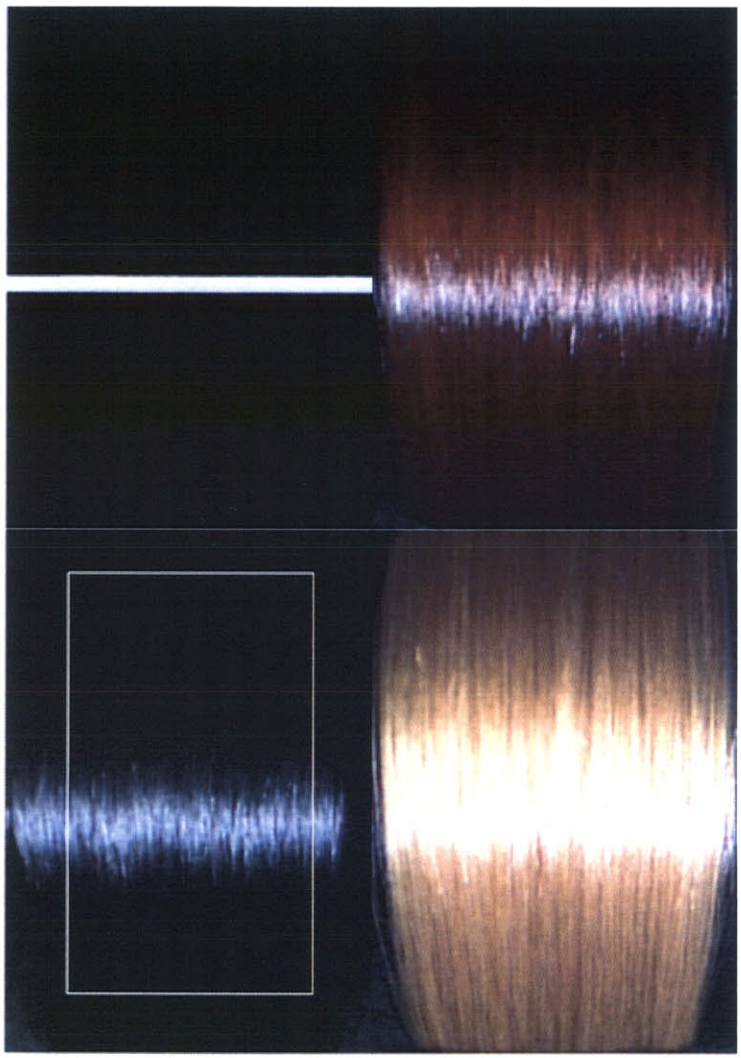

Figure 2-11: Digital images captured by the shine measurement test setup at Wella FKM Laboratory in Darmstadt, Germany. Clockwise from top left: aluminum foil, red hair, blonde hair, and black hair. (Taken from archives, Wella AG)

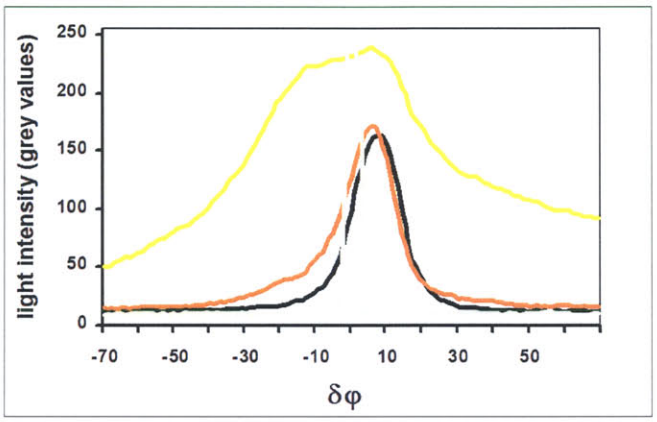

Figure 2-12: Results of analysis of digital images captured by the shine measurement test setup at Wella FKM Laboratory in Darmstadt, Germany. Light intensity is plotted as function of angle of reflection, $\delta\psi$, from the center of the shine measurement rod for Aluminum foil (*gray*), red hair (*red*), blonde hair (*yellow*), and black hair (*black*). (Taken from archives, Wella AG)

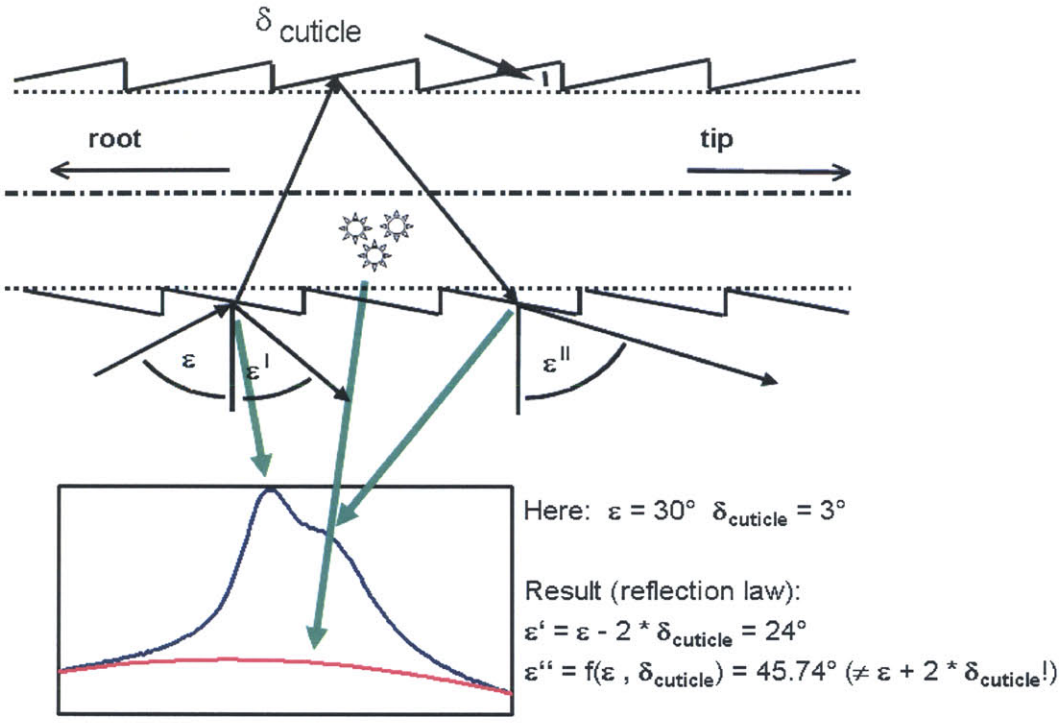

Figure 2-13: Diagram showing the light paths which result in the specular and diffuse reflectance patterns from light shined on human hair in the shine measurement method. (Taken from archives, Wella AG)

In the case of black hair, the surface reflection is very high, indicated by a rather narrow peak. In the case of blonde hair, which is more translucent, reflection from the backside of the hair is more dominant and the main peak is very broad. The color of hair therefore dramatically influences the impression of shine and luster.

A special factor called the shine number, defined as the ratio of specular to diffuse reflectance, has been created to quantify the shine measurement results. Higher shine numbers correspond to a higher degree of luster.

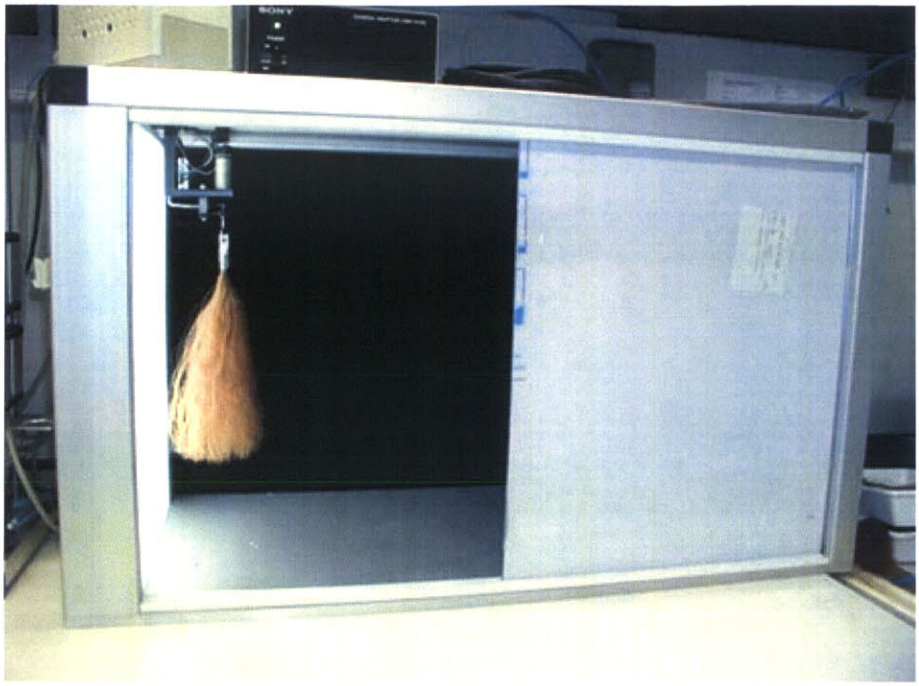

Figure 2-14: Volume measurement test setup at Wella FKM Laboratory in Darmstadt, Germany. (Taken from archives, Wella AG)

2.3.3 Volume and Body Measurement

The volume and body of a given hair style are also among the important cosmetic properties measured in the Wella FKM laboratory and are based on visible impression and tactile sensation, respectively. As with shine measurement, the volume and body tests are performed on bulk fibers in the form of 100 fiber hair swatches.

The visible volume measurement is an optically-based test performed in a specialized chamber as shown in Figure 2-14. A volume swatch is rotated 360° and 60 digital images are captured at 6° increments. The area occupied by the sample is determined for each image and the total visible volume of the hair swatch is calculated from the sum of the images [13]. A sample image captured by the visible volume measurement test setup is shown in Figure 2-15. The visible volume test is also used as a method of proving the effectiveness of anti-static treatments.

The tactile volume, or "body", of a hair sample is measured mechanically. A hair tress is drawn through a smooth metal ring of known diameter [14]. The force exerted

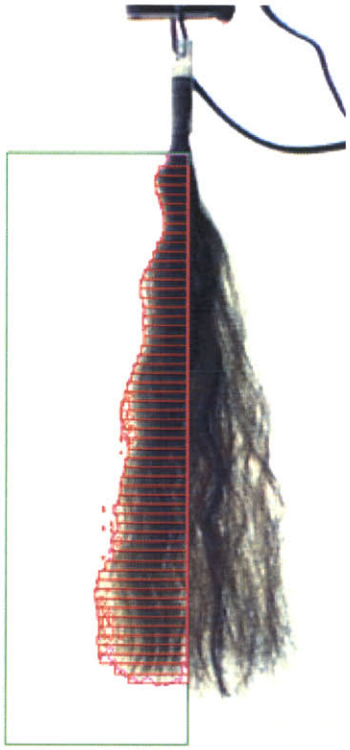

Figure 2-15: Sample image acquired by the visible volume measurement system showing the applied image analysis of style volume. (Taken from archives, Wella AG)

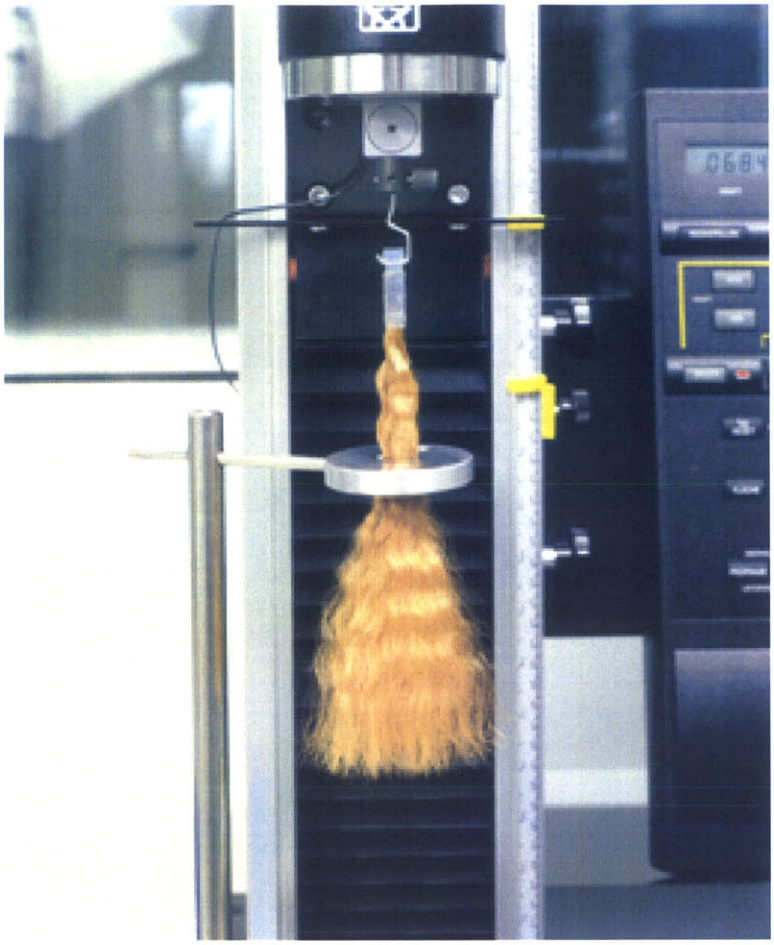

Figure 2-16: Volume measurement test setup at Wella FKM Laboratory in Darmstadt, Germany [*right*], and image acquired by the system with image analysis of style volume applied [*left*]. (Taken from archives, Wella AG)

on the tress by the ring is measured as a function of the displacement of the tress with respect to the ring. The work done in pulling the tress through the ring, calculated from the measured force and displacement values, is used as a quantitative indication of the body of the hair style. Hair tresses that require more force to be drawn through the ring are considered to have greater body due to a higher filling degree in the space of the ring and a greater resistance against deformation. The test setup used by Wella for body measurement is shown in Figure 2-16. Figure 2-17 shows sample results for body tests performed on untreated hair tresses, anti-static treated hair tresses, and anti-static treated hair tresses with volume-enhancing complex added.

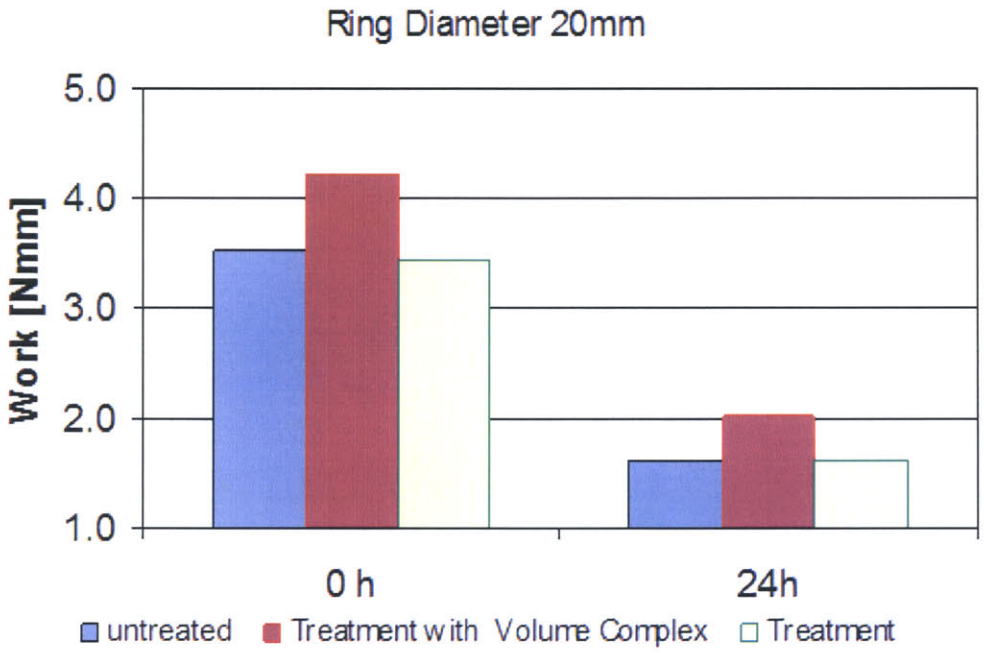

Figure 2-17: Results for body tests performed on untreated hair tresses, anti-static treated hair tresses, and anti-static treated hair tresses with volume enhancing complex. (Taken from archives, Wella AG)

2.3.4 Combing Force Measurement

Another major parameter for describing the cosmetic quality of hair is the ease of combing. Cosmetic treatments such as permanent waving, bleaching, and coloring as well as external factors such as weather exposure and frequent grooming all affect the combing ease. Each of these factors degrades the cuticle layer of the hair.

The combability of hair is generally determined by measuring the force required to slide a comb through a hair tress under defined conditions [14]. An automated device, shown in Figure 2-18 has been developed at Wella for the purpose of automatically performing combing force measurements on up to 36 hair tresses. The tresses to be tested are kept in a storage chamber. The testing device removes one tress at a time, affixes it to a load cell (HBM, Type Z6FD1), and combs through the sample at constant speed, recording the combing force as a function of the distance combed through the length of the tress. The machine then removes the tested tress and affixes the next one to be tested. A single tress is combed twenty times during a test, and the average combing force value is calculated in addition to the standard deviation. Lower combing force values indicate better care effects for the particular product under test. Hair conditioners significantly reduce the combing force values as shown in Figure 2-19.

subsectionBreaking Force Measurement The structural integrity of hair may be determined by measuring the force required to break single fibers [6]. Wella conducts all of its single fiber breaking tests using the Diastron MTT600 miniature tensile tester described in Section 1.2.1.

For the breaking force measurement, a set of twenty-five single fibers are taken from a hair tress. A small brass ferrule is affixed to each end of every fiber before testing to facilitate manipulation by the testing apparatus. Next, the cross-sectional dimensions of each fiber are measured using a laser micrometer. The working principle of the laser micrometer is described in Section 6.3.2.

After the fiber dimensions have been measured, the fibers are arranged in the slots of the 100-position carousel system of the Diastron MTT600 for automated

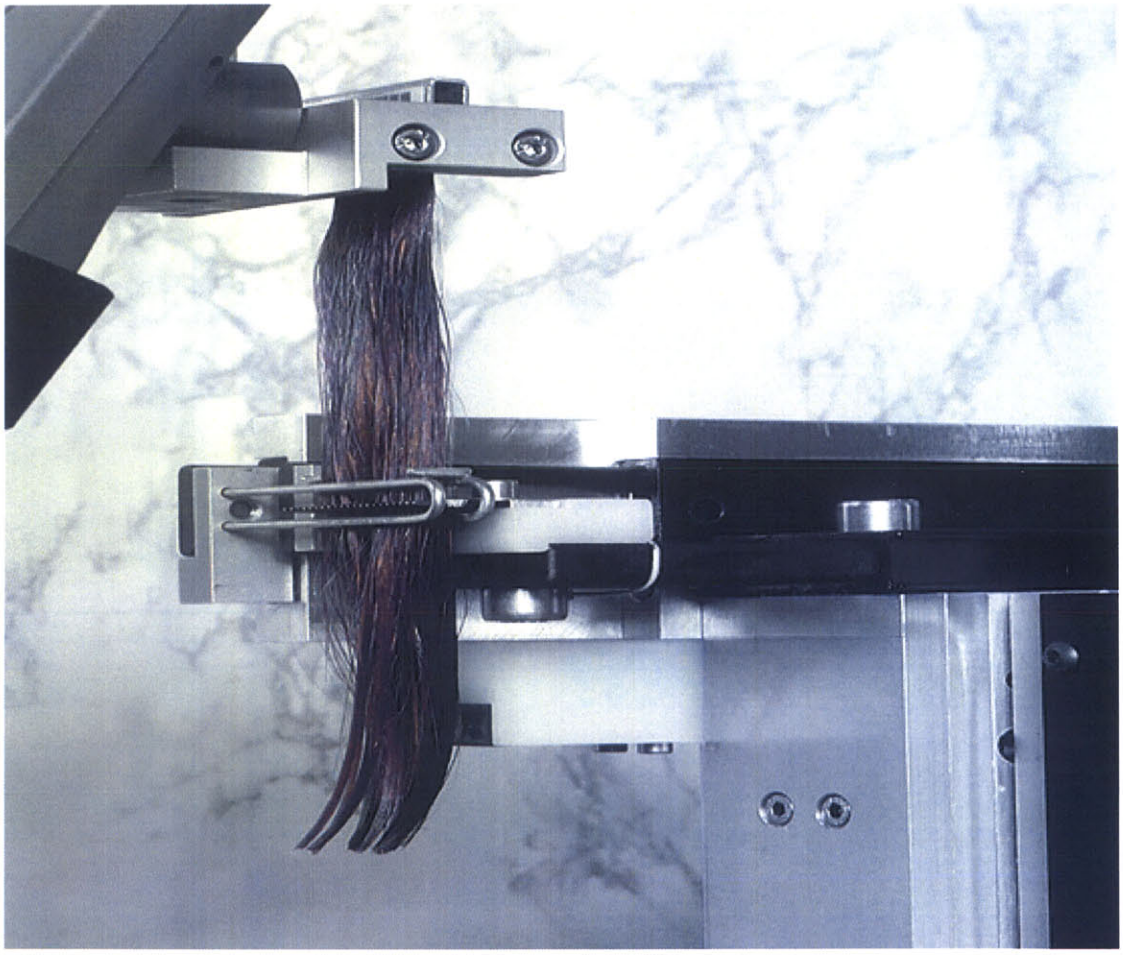

Figure 2-18: Automated combing measurement device at Wella FKM Laboratory in Darmstadt, Germany. (Taken from archives, Wella AG)

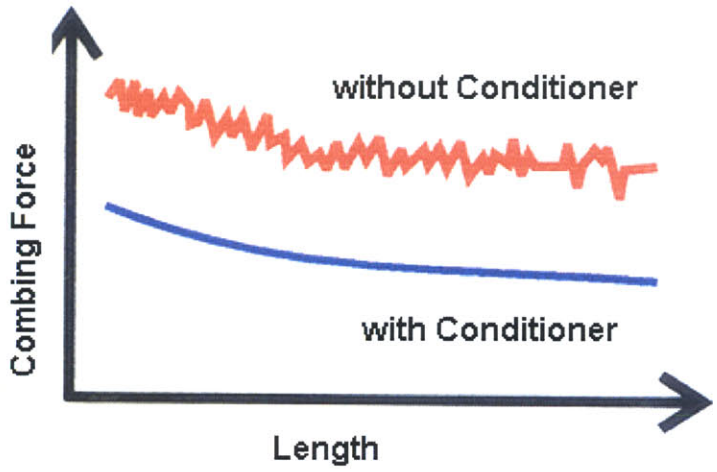

Figure 2-19: Results of combing force measurements for hair with and without conditioning treatment applied. (Taken from archives, Wella AG)

measurement of breaking force . Each fiber is stretched at a constant velocity of 0.17 mm/s until the breaking point is reached. The force exerted on each fiber at the breaking point is normalized by the previously measured cross-sectional area of the fiber to attain the tensile strength of the fiber. Multiple fibers are tested to generate an average breaking force value. For further discussion on the calculation of the tensile strength of single fibers, see Section 3.2.4.

2.3.5 Friction Breakage Measurement

Another measure of the structural integrity of hair is the resistance against breakage due to friction. The friction breakage measurement is performed on single fibers and is referred to as the flexabrasion test by Wella. The principle of the measurement is to subject single fibers to a cyclic low-level mechanical stress and to measure the number of cycles required to break the fiber [15].

As with the breaking force measurement, the flexabrasion test is perfomed by an automated machine and requires each fiber to be fitted with brass ferrules for the purpose of handling and manipulation.

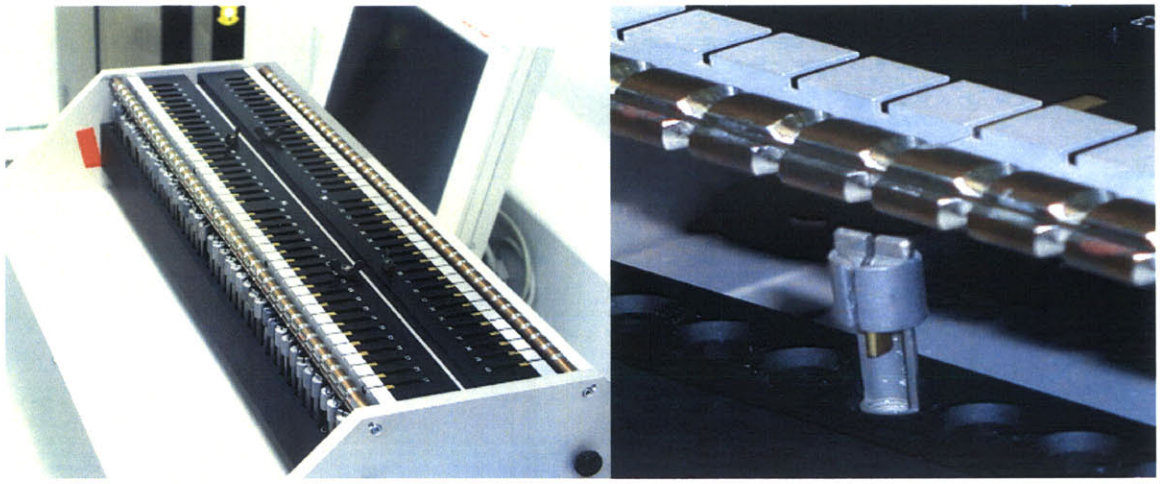

Figure 2-20: Automated friction breakage measurement device at Wella FKM Laboratory in Darmstadt, Germany. (Taken from archives, Wella AG)

Each single fiber is attached at one end to an oscillating motor in the instrument. Each fiber is then draped over a small diameter stainless steel rod. A small mass is affixed to the hanging end of the fiber. The instrument, shown in Figure 2-20, is capable of performing many cyclic breakage tests in parallel.

The results of the friction breakage measurements are evaluated using a Weibull reliability analysis. According to Weibull, the failure frequency of hair breakage can be described by

$$H = 1 - e^{-(\frac{X}{\theta})^b}, \tag{2.1}$$

where H is the failure frequency normalized to $1 = 100\%$ failure, X is the life variable which is equal to the number of cycles to fiber breakage, θ is the characteristic life corresponding to the number of cycles to breakage for 63.2% of the fibers, and b is the shape parameter corresponding to the gradient of the linear equation [16]. For analysis, Equation 2.1 is linearized as

$$\ln \frac{1}{1-H} = b(\ln x - \ln \theta) \tag{2.2}$$

and $\ln \frac{1}{1-H}$ is plotted against $\ln X$. A linear regression is performed on the plot, and the characteristic life θ is determined from the axis intercept $\ln \theta$. The shape factor b is determined from the linear gradient of the plot. Hair samples which are found

to have a higher characteristic life are deemed to have a higher resistance against breakage.

2.3.6 Curl Retention Measurement

The stabilization of a hairstyle with styling products, especially as the style is exposed to varying levels of air humidity, is quite important to consumers and is typically quantified by measuring the curl retention properties [14]. The principle of the method consists of treating human hair tresses with the products to be tested and then performing a water set on the tresses. The curled tresses are then exposed to a defined climate at increased humidity. The loss of shape of the curl as it is subjected to the higher humidity environment, known as the dropping out effect, is measured as a function of time over a time period of up to 24 hours.

Treated hair tresses are wound onto a standard rod of known diameter as shown in Figure 2-21, dried, and then unwound again. A 50 mg mass is attached to each curled tress and the tresses are suspended vertically as shown in Figure 2-22 at a known climate of constant temperature and humidity. The length of the tresses is determined by means of a measuring gauge at defined times.

The percentage of curl retention can be calculated from the following equation:

$$\text{Curl retention} = 100 \ln \frac{l_o - l_t}{l_o - l_1} \tag{2.3}$$

where l_o is the length of the initial tress prior to curling, l_t is the length of the stretched tress measured at relevant time increments, and l_1 is the initial length of the curled tress.

Analysis of the results of the curl retention test for treated and untreated hair tresses shows the degree of the stabilizing effect of the product under test.

2.3.7 Swelling Measurement

The permanent waving process of hair includes various chemicals and physical reactions, especially pronounced swelling [6] which is mostly due to the reduction of cystine to cysteine and the breakage of bonds in the cortex this process involves.

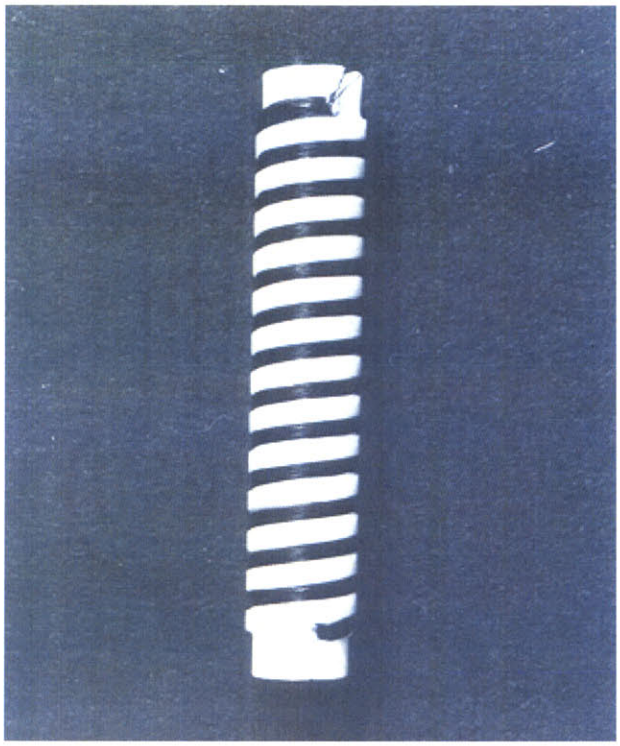

Figure 2-21: Standard rod used for performing the water set of hair tresses in the curl retention measurement. (Taken from archives, Wella AG)

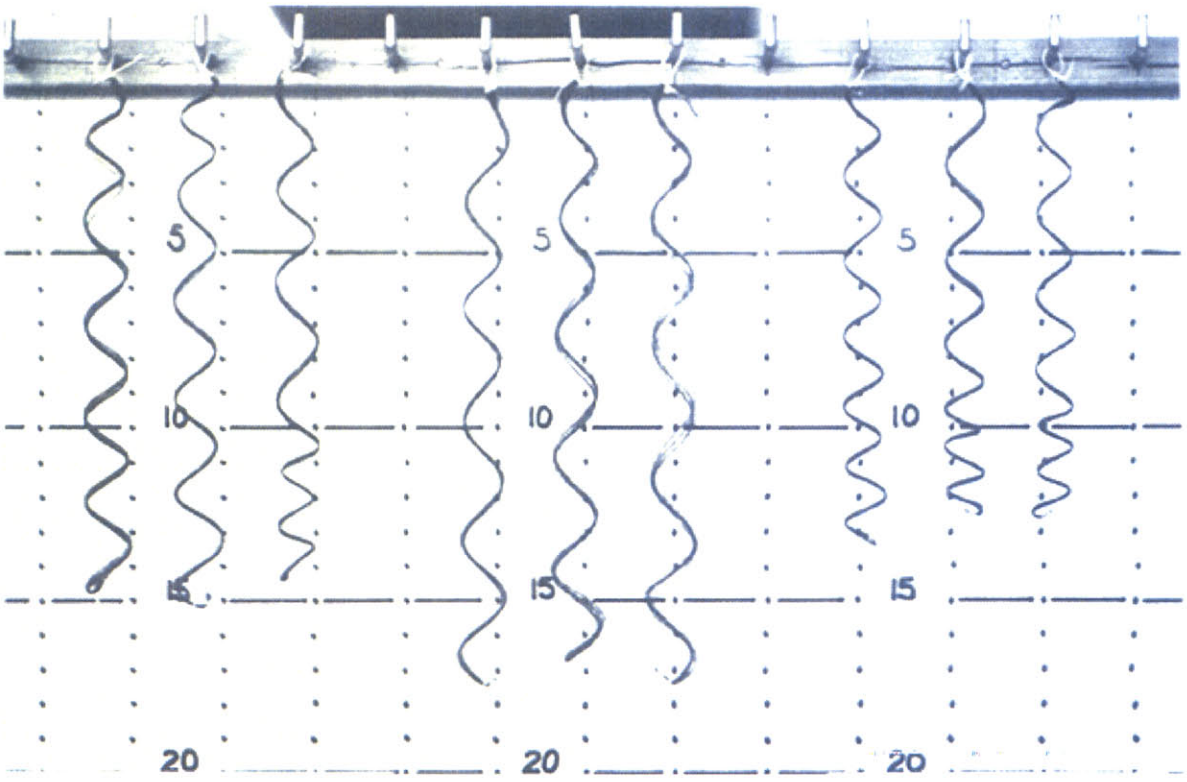

Figure 2-22: Array of hair tresses suspended vertically in the curl retention measurement. (Taken from archives, Wella AG)

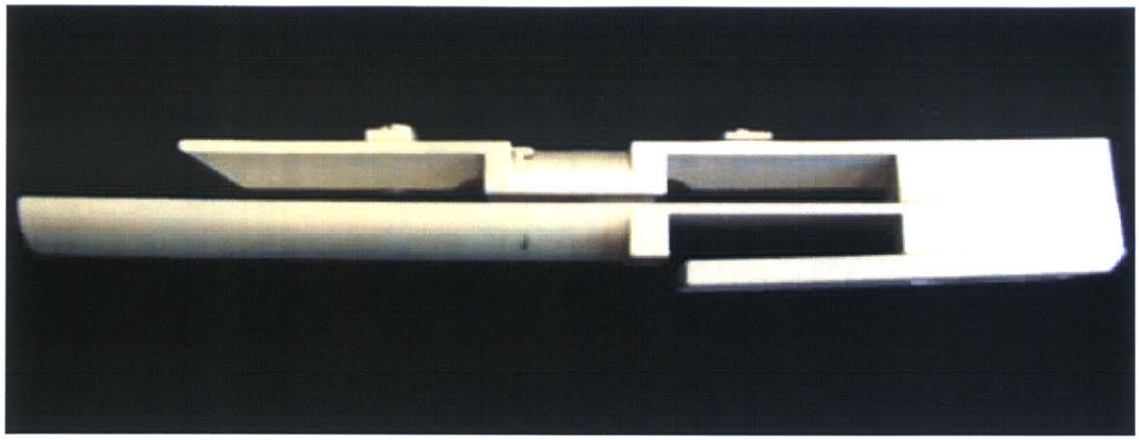

Figure 2-23: Swelling measurement device at Wella FKM Laboratory in Darmstadt, Germany. (Taken from archives, Wella AG)

The swelling and de-swelling processes (de-swelling due to the neutralizing phase) can be measured by means of a so-called measuring rod. For this purpose a hair tress is wound onto that rod under defined conditions (similar to winding on a permanent waving roller) in a way that all phases of the permanent-waving treatment can be carried out while the tress is wound on this rod (Figure 2-23).

Due to swelling and contraction during the permanent waving process, the wound hair exerts a radial pressure on the rod which changes the position of a moveable beam which is an element of the measuring rod. The change of the position is continuously measured with an inductive distance sensor and represented as a function of time (Figure 2-24). The higher the signal from the rod, the higher degree of swelling of the hair.

2.3.8 Elasticity Measurement

Another cosmetic criterion essential to the consumer is the elasticity of the hair, also called "bounce." The elasticity is especially relevant in connection with permanent waving preparations and hair styling products.

Prior to the elasticity measurement, the tresses of human hair are subjected to a curling treatment. Hairs treated with hair styling products are subjected to a water set curling procedure while permanent waving preparations are subjected to

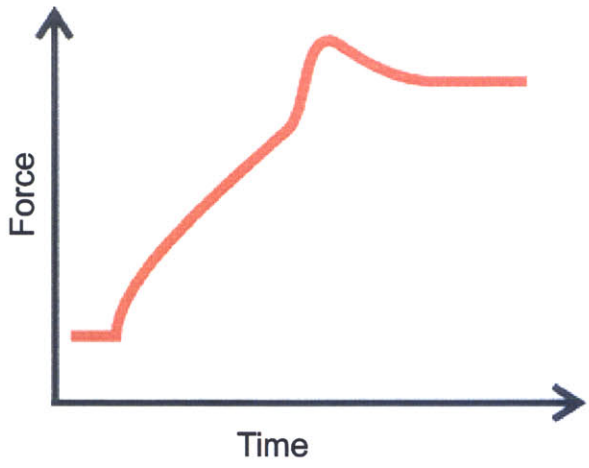

Figure 2-24: Example results of swelling measurement curve plotted as force versus time. (Taken from archives, Wella AG)

curling via the appropriate permanent waving procedures. Afterwards, a curled tress is fixed to a measuring apparatus and vibration is generated mechanically. The tress is allowed to oscillate passively, and the decay of the curl vibration is recorded by means of a rotational position sensor [17].

The angular position of the sensor signal is recorded by PC and evaluated. The free damped vibration of the curl is defined by the frequency and amplitude of oscillation.

2.3.9 Bending Stiffness Measurement

The appearance and properties of a hairstyle are essentially caused by certain properties of the individual hairs forming that style [18, 14]. The bending stiffness of the individual hair is an important parameter, for instance, for the volume of the hairstyle and the feel of the hair [19].

Scott *et al.* (1978) have described bending stiffness measurement according to the so-called *balanced fiber method* in which defined weights are affixed to the ends of individual hairs. These hairs are placed on their center on a fine wire hook [19]. The distance between the two ends of the hanging fiber is a measure for the bending

stiffness, since hairs having a lower degree of bending stiffness bend more and therefore their ends are less wide apart. Apart from this, the bending modulus can be calculated as well, by taking boundary conditions, such as the fiber cross-sectional area and the mass of the weights into account.

Another method to determine the bending stiffness, which is commonly applied in textile fiber testing, is based on vibration. According to that method, the individual hair fiber is set into vibration, usually by using an acoustic source such as a loud-speaker or voice coil actuator. The bending modulus is calculated from the resonant frequency of the fiber, taking the appropriate boundary conditions into account [20].

The principle of the method detailed here is to fix the upper end of a single hair in a clamp and to slowly push the fiber downward onto a force meter which records the force required to achieve a slight bending. Bending is generally achieved by a few millimeters of compressional displacement. Based on the force values obtained from the bending of the single hair fiber, the bending tension is calculated for each single hair according to the Euler equation for beam bending deformation and the appropriate boundary conditions [21]. The Euler equation for beam bending is detailed in Section 3.2.5. Figure 2-25 shows an apparatus designed by Wella for automated measurement of bending stiffness.

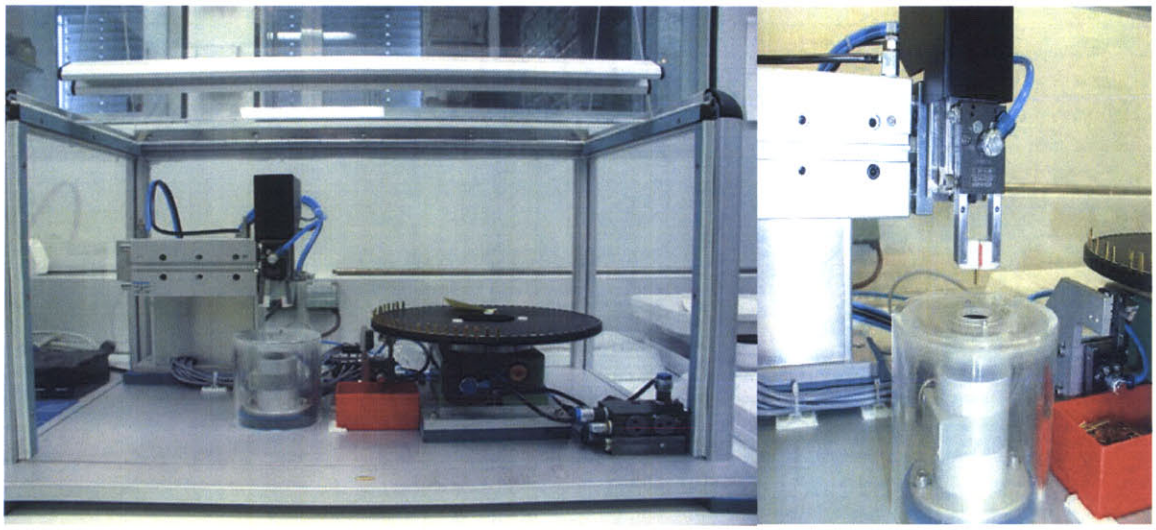

Figure 2-25: Automated bending force measurement device at Wella FKM Laboratory in Darmstadt, Germany. (Taken from archives, Wella AG)

Chapter 3

Single Fiber Testing Considerations

The automated single fiber testing instrument has been designed to be a solitary machine for measuring several of the most useful mechanical properties of single fibers. In order to thoughtfully approach the design process and to gain understanding of one of the most complex fibers found in nature, the principal structural properties of human hair fibers were detailed in Chapter 2. Additionally, several test methods and instruments typically used for measuring properties of both individual and bulk fibers have been described in an introduction to the state of the art in hair fiber testing. The survey of hair fiber testing technology was intended to guide the incorporation of existing concepts into the new instrument and to recognize where new ideas may be necessary or beneficial.

This chapter details a number of basic considerations which have informed the design of each testing module in the automated hair testing machine. Fundamental principles of the instrument design are introduced. Also, each measurement performed by the machine is detailed with a discussion of the desired properties to be measured, the methodology or protocol of measurement, and the variables for each measurement which may be adjusted by the user to tailor a test to his particular needs.

3.1 Principles of Test Methodologies

An instrument or machine cannot be efficiently and effectively designed until certain basic principles of its ultimate functionality are established. The automated single fiber testing instrument has been designed with the end goal of automatically testing single fibers for the following properties: cross-sectional geometry, surface roughness, friction, tensile strength, elastic modulus, bending modulus, and torsional modulus. Wella considers these to be the most important parameters for characterizing single hair fibers [22].

Simplicity of the overall instrument has been preserved by adhering to several key considerations while designing the machine to encompass measurement of each fiber mechanical property. The most pervasive objectives during the machine development process have been to achieve statistical differentiation between sample sets, to modularize the test procedures, to minimize the number of sensors required, and to minimize the number of moving elements required to perform each of the necessary measurements.

3.1.1 Achieve Statistical Differentiation

The properties of fibers can vary widely. Hair fibers, specifically, can exhibit considerable variation between samples even if the fibers have been sampled from the head of a single individual. Therefore, the properties of many fibers must be measured in order to determine characteristic fiber properties or to distinguish between the effects of various treatments on fibers under test. The machine has been designed with ample capacity, testing up to 100 single hair fibers without reloading. The minimum number of fibers required for statistical differentiation between treatments is detailed in Section 3.2 for each specific test.

The capacity of the instrument to achieve statistical differentiation for large sample sets will also be beneficial for establishing the mechanical properties of novel fibrous materials.

3.1.2 Test Method Modularity

Conventional fiber measurement instrumentation might necessitate the use of a unique device to measure each property of an individual fiber or set of fibers. In contrast, the single fiber testing instrument has been designed with the ability to measure several properties within one apparatus and is thus more efficient from many perspectives including space, labor, and time requirements. The increased functional capacity provided by the instrument becomes far more practical if the user is given the option of selecting which specific test or tests he would like to perform. Therefore, the tests must be modular.

The protocol for each test has been carefully planned for isolation from other tests in the instrument's test regimen. Modularity has been established such that the parameters required for determining a particular fiber property may all be measured within that single test. Furthermore, duplicate parameters required by multiple tests are not measured by the machine more than once. For instance, a user may wish to measure the bending modulus and tensile strength of a set of fibers. Both measurements call for identical knowledge of fiber geometry, however, the test procedures involve different force measurements. The instrument will measure fiber geometry only once for each fiber under test in such a scenario.

A user will thus be able to choose to perform a single test, a specific sequence of selected tests, or a complete test battery sequence on a single fiber or up to 100 fibers with no redundancy and with maximum time efficiency. It must be noted that, although specific tests may be chosen, the order in which the tests are performed is fixed. The prearranged test sequence prevents a user from ordering selected tests in a way that might either prematurely damage the fiber under test or the instrument itself.

3.1.3 Minimize Number of Sensors Required

The instrument has been designed to minimize the total number of sensors required for measuring the desired fiber properties. Just as duplicate measurements of parame-

ters for multiple tests introduce time expense to the testing cycle, duplicate sensors for measurement of similar parameters introduce expense in the form of cost and complexity.

Each test has been designed to use a minimum number of sensors, and where possible, a single sensor is employed to measure parameters needed to determine more than one property.

3.1.4 Minimize Number of Moving Elements

The number of moving elements required to perform all of the tests has been carefully considered in order to reduce overall cost and complexity. All of the tests may be performed while the fiber is secured in a single test fixture in order to minimize the physical manipulation of the fiber under test. An additional motivation for reducing the physical manipulation of the fiber is to minimize damage to the fiber resulting from handling.

A fiber testing system which performs multiple tests on a fiber in a single fixture has many major advantages over a system involving several different machines. Repeatability is improved, error due to handling is reduced, capital and operational costs are reduced, and efficiency may be increased substantially.

3.2 Measurement Method Development

Each measurement method has been evaluated based upon the desired properties, the parameters which must be measured to determine the desired properties, the number of fibers which are to be measured to achieve statistical differentiation, the methodology or protocol of the test, and the variables which the user may adjust to customize the test to his specific needs.

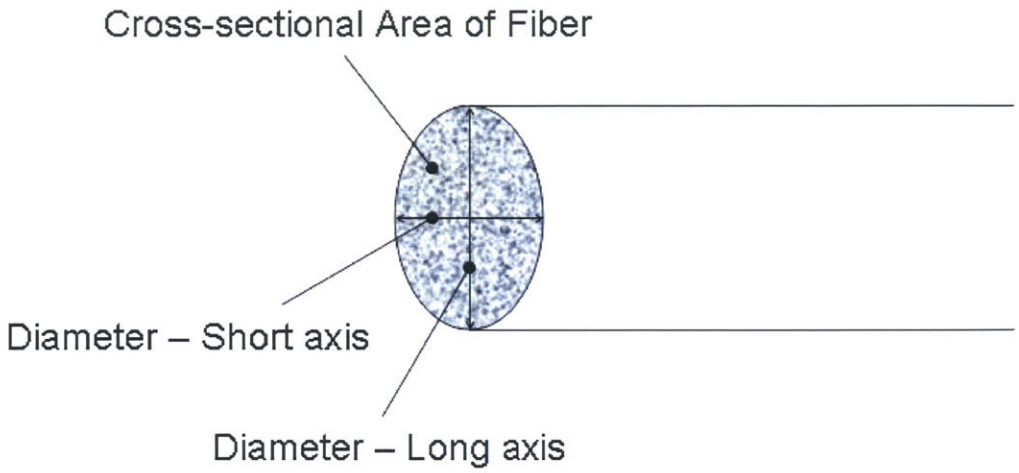

Figure 3-1: Schematic of the cross-section of a fiber showing dimensions of interest.

3.2.1 Cross-sectional Geometry

The cross-sectional geometry must be known in order to determine many other mechanical properties of a fiber and is therefore of great importance to researchers. For the purposes of this investigation, the cross-sectional geometry is defined by the dimensions of a fiber perpendicular to the long axis of the fiber as illustrated in Figure 3-1.

Cross-sectional Geometry – Desired Properties

Geometric properties of interest to researchers include the variation of diameter along the fiber axis, the degree of twist along the fiber axis, the average values of fiber diameter and fiber cross sectional area at specific regions along the fiber, and the fiber ellipticity, or the ratio of the long axis diameter to the short axis diameter. Another interesting geometric measurement which is currently unavailable on other commercial fiber testing instruments is the variation of diameter along a fiber axis during stretching. Active monitoring of diameter during manipulation of the fiber

would permit calculation of the Poisson's ratio, ν, of a fiber as it is being stretched. The Poisson's ratio is defined as

$$\nu = -\frac{\epsilon_T}{\epsilon_x} \tag{3.1}$$

which is the negative of the ratio of transverse deformation ϵ_T to axial deformation ϵ_x of a material as it is stretched [23].

Cross-sectional Geometry – Measured Values

The cross-sectional geometry module of the automated single fiber testing instrument must be capable of measuring the diameter of the fiber under test, the position along the fiber axis, and the angle of rotation of the fiber axis.

Cross-sectional Geometry – Methodology / Test Protocol

The method presently used by Wella to measure the cross-sectional geometry of hair fibers determines the major and minor axes of a fiber by scanning multiple times during a 180° rotation of the fiber at a single position. The standard position for the measurement is at the center of the hair fiber being tested. However, a modified version of this test could perform the same 180° rotational scan at multiple points along the fiber.

The modified protocol, depicted in Figure 3-2 performs 10 measurements along the fiber axis. At each measurement point, the fiber is rotated 180° to find the short or long axis, and 50 diameter measurements are recorded per position. Further study might involve scanning along the fiber on the short and long axes to estimate the degree of twist of the fiber.

Another protocol is suggested as an alternative to the fiber geometry measurement method employed by Wella. The new proposed method scans along the length of the loaded sample fiber at an initial orientation defined as 0° with a user-defined linear resolution between each diameter measurement location. The fiber is then rotated to a second orientation 90 from the initial scan axis and is again scanned along its length with measurements occurring at the same user-defined measurement points

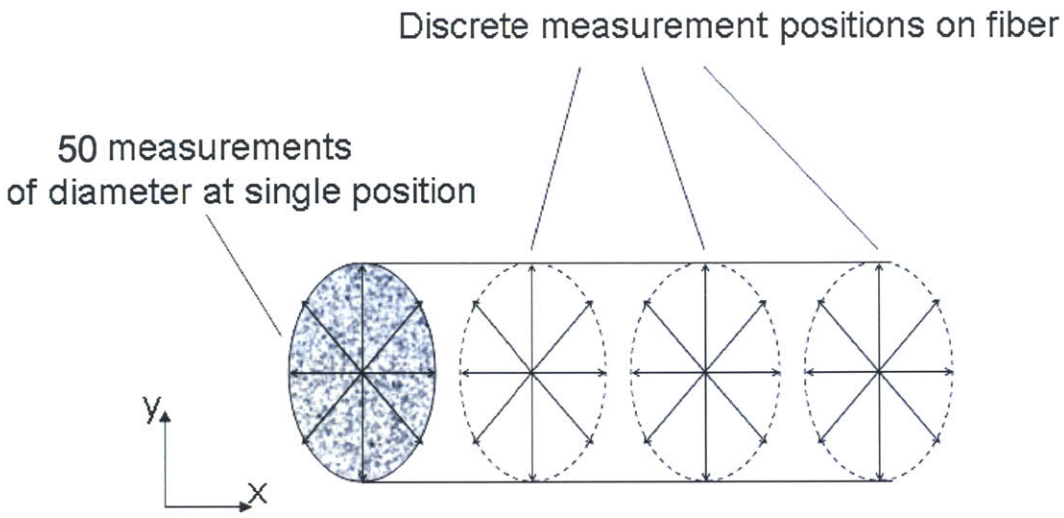

Figure 3-2: Schematic of Wella method for measuring the cross-section of a fiber.

and resolution. The schematic in Figure 3-3 shows how the geometry of a fiber will be measured by this methodology.

Cross-sectional Geometry – User Variables

When a user is determining his test protocol for the diameter and cross-sectional geometry measurements, it is important that he is able to choose a methodology that will determine results in a meaningful way. The user shall be able to choose between either of the proposed geometry measurement methods described above. He shall also be able to vary the number of measurement points, $n_{samples}$, along the length of the fiber or the resolution, R, of the measurement points. These two latter values are related by the length, l_{fiber}, of the sample

$$R = \frac{l_{fiber}}{n_{samples}}. \tag{3.2}$$

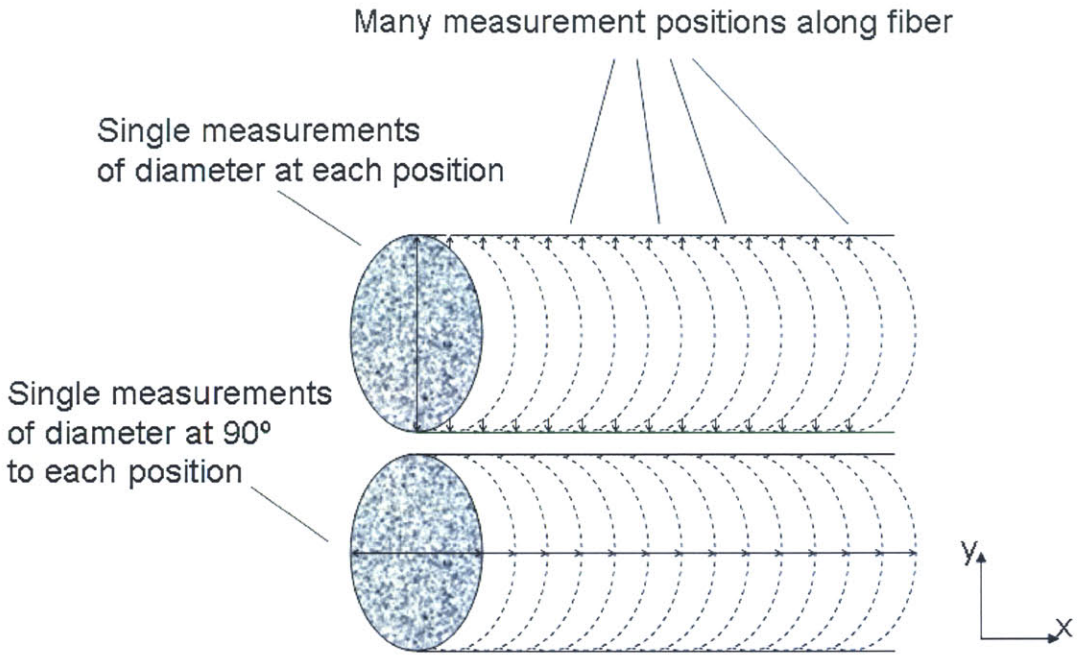

Figure 3-3: Schematic of proposed method for measuring the cross-section of a fiber.

3.2.2 Surface Roughness

Surface roughness is a quantitative measure of the profile of a surface. It is a very important property for understanding how a fiber will feel to the touch and how it will interact with other fibers and materials. Perhaps because it is very difficult to examine the profile of fibers without the aid of atomic force microscopes, no instruments have been designed to automatically measure the surface roughness characteristics of small single fibers [22].

Surface Roughness – Desired Properties

Surface roughness is a quantitative measure of the geometric contour of a surface. The roughness of a surface under test is typically determined by the tactile stylus method in which a 2-dimensional profile is measured mechanically by scanning a cantilever tip over a surface [24]. The position of the scanning probe along the surface is recorded while the vertical deviations of the probe from a reference position are measured. Figure 3-4 shows a schematic of the basic principle of surface roughness measurement.

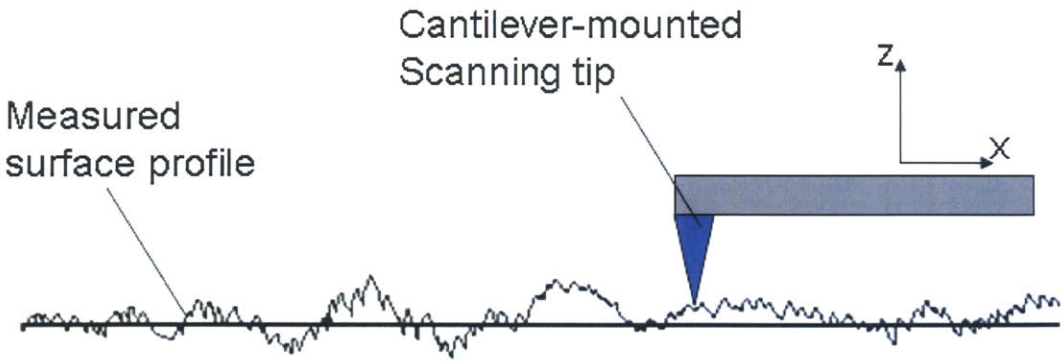

Figure 3-4: Schematic of two-dimensional surface roughness measurement.

A profile is usually represented graphically as a plot of the surface height versus scan position. Average surface roughness, R_a, is one of the most common parameters used to evaluate material roughness profiles. R_a is defined by the integral of the absolute value of a surface profile measured over an evaluation length, l, as

$$R_a = \frac{1}{l} \int_0^l |z(x)| dx. \tag{3.3}$$

The average roughness is the total area of the peaks and valleys divided by the evaluation length. For most material surfaces R_a is expressed in μm [25].

The information from the roughness measurement of hair fibers that is specifically pertinent to Wella is the average roughness of the cuticle scales. As mentioned in Chapter 2, the exposed surface of the cuticle is typically only 5 μm long. Therefore, there is a good chance that measurement of the surface roughness of individual cuticle cells is not physically possible with a mechanical method and existing instrumentation. If this is found to be the case, the total average roughness along the fiber axis is desired [26].

Periodic	***Non-periodic***		***Cut-off***	***Eval. Length***
Irregularity [mm]	R_z [μm]	R_a [μm]	λ_c [mm]	L_s/L_m [mm]
>0.01 to 0.04	Up to 0.1	Up to 0.02	0.08	0.08 / 0.4
>0.04 to 0.13	>0.1 to 0.5	>0.02 to 0.1	0.25	0.25 / 1.25
>0.13 to 0.4	>0.5 to 10	>0.1 to 2	0.8	0.8 / 4
>0.4 to 1.3	>10 to 50	>2 to 10	2.5	2.5 / 12.5
>1.3 to 4	>50	>10	8	8 / 40

Table 3.1: Cutoff Value Selection Table for ISO 4288 surface roughness measurement of periodic and non-periodic surface profiles of varying evaluation lengths [2].

Surface Roughness – Measured Values

In order to determine the average roughness of a fiber surface according to the classical definition, two major parameters must be measured by the instrument. Assuming a mechanical measurement technique is used, the horizontal position of the roughness sensor along the fiber and the vertical position of the roughness sensor on the fiber must be measured synchronously.

It will be important to hold the fiber sample stable during testing and also to define the reference position of the vertical position sensor repeatably for each fiber under test.

Surface Roughness – Methodology / Test Protocol

Standard protocol for surface roughness measurement requires a lightly loaded cantilever, with approximately 0.7 - 2 N contact force at the tip, to be scanned at a constant scanning rate over an appropriate evaluation length [27].

International standard test parameters for scanning rate, evaluation length, and filter cut-off frequency have been determined experimentally and published in standard ISO4288 [2], and are dependent on the spacing of profile irregularities and on whether a profile is periodic or non-periodic. Table 3.1 below summarizes the ISO4288 standards.

Surface Roughness – User Variables

To accommodate a variety of potential fiber roughness scenarios, the user of the instrument must be permitted to vary several parameters of the surface roughness test. The sampling and evaluation length of the fiber under test shall be variable to permit examination of the surface roughness for numerous areas of a fiber. The maximum evaluation length shall be limited by the length of the fiber under test, and the sampling lengths shall conform to the values shown in Table 3.1.

The scan rate for measurement shall be variable within the limits defined by ISO4288 standard. Therefore, for evaluation lengths less than approximately 3.8 mm, the velocity of measurement shall be $v_{meas} = 0.1$ mm/s, and for evaluation lengths greater than approximately 4.0 mm, the velocity of measurement shall be $v_{meas} = 0.5$ mm/s.

Finally, because surface roughness is a quantitative measure of a profile based upon subjective constraints, the cut-off frequency shall be adjustable by the user as well. Allowable values for cut-off frequency shall also conform to the ISO4288 standard. Of course, the instrument may be modified to conform to any other standards based upon the specific needs of the end user.

3.2.3 Friction

Friction is the force that resists motion when one body slides over another [28]. The friction properties of fibers provide many useful insights for researchers about how fibers will interact with other fibers and various material surfaces.

Friction – Desired Properties

According to the classical laws of friction formulated by Leonardo da Vinci and later by Amontons, the frictional force, F_f, necessary to slide one surface over another is proportional to the normal load, N, pressing the two surfaces together [28], as

$$F_f = \mu N. \tag{3.4}$$

A proportionality constant known as the coeffiecient of friction, μ, relates the perpendicular friction force to the applied normal force. The coefficient of friction is typically independent of the measured area of contact; however, the true area of contact between surfaces may change with increased normal force and cause the coefficient of friction to change [6].

Two distinct coefficients of friction reflect the fact that different frictional forces arise when initiating sliding movement and when maintaining sliding movement. The static coefficient of friction, μ_s, is a measure of the force required to start surfaces sliding, and the kinetic coefficient of friction, μ, is a measure of the force required to maintain sliding movement between surfaces [28]. According to Amonton's law, the coefficient of static friction is greater than the coefficient of kinetic friction for most surface pairs [6].

In order to understand the friction properties of fibers, the coefficients of static and kinetic friction must be determined for a variety of conditions defined by the user to suit his needs.

Friction – Measured Values

Determination of both coefficients of friction, μ_s and μ_k, for a single fiber will require at least one moving axis with the ability to measure the position of the axis as it moves. The normal force of contact between the fiber under test and the surface of interest must be measured as well. It is also possible for the normal force value to be a constant as long as it is well known. Finally, the resultant frictional force perpendicular to the normal force and parallel to the direction of sliding motion between the contact surfaces must be measured.

Friction – Methodology / Test Protocol

Numerous experimental methods have been described for measuring the friction of fibers, and each is designed to accomplish a unique measurement objective.

One method mentioned in the literature involves a twisted pair of single fibers. The fiber pair is twisted twice and pulled from opposite ends of each fiber. The force

way that tests of fibers treated with different hair cosmetic products may result in statistically significant differences.

Users of the instrument will be permitted to vary the rate of sliding within a set of allowable values ranging from 0.17 mm/s up to 4.17 mm/s. Also, the normal load applied to the single fiber shall be variable in a range to be specified by the user.

Finally, the friction measurement should allow the user to choose the type of material he wishes to put in contact with the fiber under test. Some materials commonly used for friction tests with bulk fiber strands include steel, aluminum, wool, and plastics such as nylon [6].

3.2.4 Tensile Properties

The tensile properties are a collective measure of the deformation effects of stretching a fiber. When any elastic material is strained, or deformed, there is a corresponding stress, or tendency to recover the normal condition [6]. In general, measurements of fiber tensile properties are expressed for elongations of a fiber in the long dimension, and are most often performed using load-elongation methods, otherwise known as stress-strain methods [6].

Tensile Testing – Desired Properties

During a tensile stress-strain test, a sample of known length (in this case a fiber) is carefully gripped at both ends and stretched at a prescribed rate while the load on the fiber is precisely monitored [6]. Data from the tensile test are used to determine a number of fiber properties including tensile stress, elastic limit, maximum elongation, modulus of elasticity, proportional limit, reduction in area, yield point, and yield strength. Tensile tests performed at elevated temperatures provide creep data [32].

One of the most important properties to measure during the test is the tensile stress of the single fiber. The tensile stress, σ_t, at any point on a fiber may be defined as

$$\sigma_t = \frac{F_l}{A_c}, \tag{3.6}$$

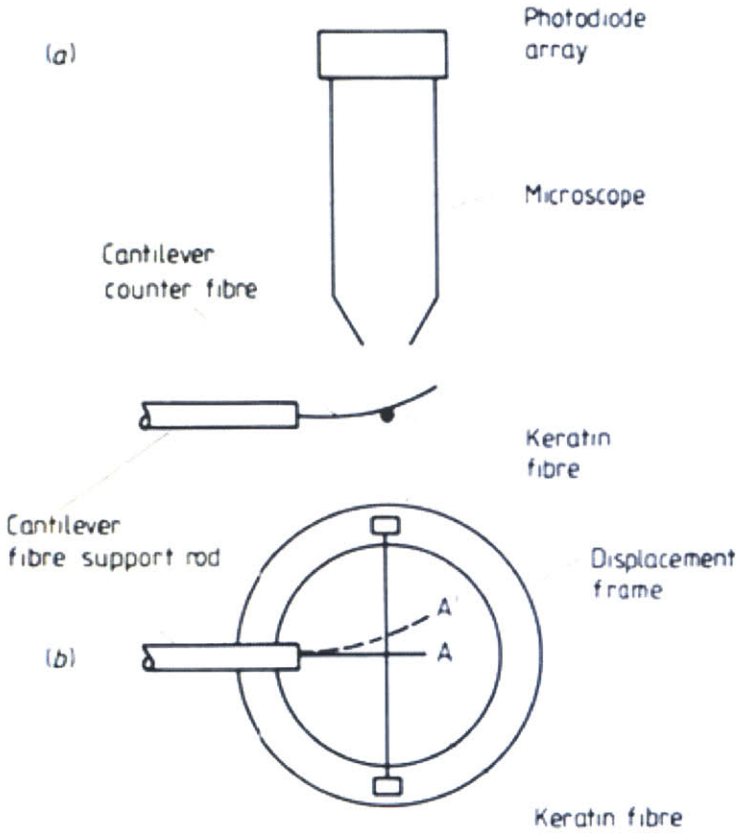

Figure 3-5: Schematic diagram of monofilament static friction test setup. (Briscoe *et al.*, 1985)

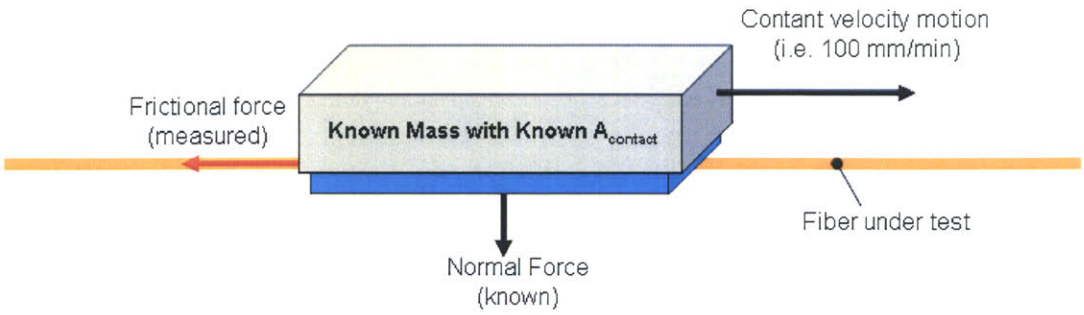

Figure 3-6: Schematic for single fiber friction measurement adapted from DIN53375 standard for multifiber hair friction measurement.

considered to be valid for the load ranges used in studies on human hair fibers [6].

It has been shown experimentally that different rubbing speeds in the range greater than 250mm/min do not appreciably affect the coefficients of friction [18].

A new method proposes that an element with a known surface contact area and normal force is moved axially along the single fiber surface while a sensitive force transducer measures the reaction force generated by the sliding contact.

This method is the most feasible to implement in an automated fashion. An additional linear axis may be added to move the measurement system into and out of the testing zone. Furthermore, it may be possible to eliminate the need for an additional sensor if the load cell for the tensile measurements is used for measuring the friction force rather than a separate unit. Figure 3-6 provides a schematic drawing of how this friction measurement method might be implemented in the single fiber testing instrument system.

Friction – User Variables

In the past, Wella has mainly performed friction measurements on bulk fiber samples and has had very little experience testing the friction properties of single fibers. Therefore, the user variables for friction measurement must be defined in such a

due to the contact between the fibers is measured as they are pulled apart and is considered to be the friction. The method does not have a capacity to measure the normal force of contact between the fiber surfaces and therefore does not satisfy the requirements to measure the coefficients of friction.

Another method devised by Briscoe et al. [29] measures the static friction between fibers in a so-called monofilament sliding experiment. A pair of polyethene pereph-thalate (PET) fibers (or PET/glass and PET/human hair) is configured orthogonally. One fiber, called the trapped fiber, is suspended at both ends in tension as shown in Figure 3-5. The bending moment of the other fiber is used to provide a very small normal force on the order of 0.07 μN up to 0.78 μN. The force between the fibers at the point of contact is called the auto-adhesive force and is proportional to the static friction between the fibers under test. The method is very sensitive, but requires a complex optical system to measure the bending of the non-trapped fiber [29].

Capstan-based methods have been devised by Schwartz and Knowles [30] and Scott and Robbins [31]. The apparatus used by the former researchers drapes a fiber with equal weights on each end over a cylinder of known diameter. One end of the fiber is placed on a torsion balance to measure the frictional forces as the cylinder is moved against the fiber [30].

The method developed by Scott and Robbins [18] involves the use of a commercially available Instron tensile tester. The root end of the fiber is attached to the load cell of the Instron, and the fiber is wrapped around two mandrels which are attached to the crosshead on the non-load cell side of the Instron. The crosshead is moved downward, and as the mandrels move downward against the fiber, the resulting tension is recorded and considered to be the friction of the fiber against the mandrels. The method determines the kinetic coefficient of friction according to the relationship in Equation 3.5

$$\mu_k = \frac{1}{\phi} \ln \frac{T_2}{T_1} \tag{3.5}$$

where ϕ is the total angle of fiber wrap in radians, T_1 is the tension in the fiber before passing over the mandrel rod, and T_2 is the tension in the fiber after passing over the mandrel rod. The equation assumes that the friction is independent of load which is

where F_l is the load measured along the axis of the fiber, divided by the cross-sectional area, A_c, of the sample under test at the region of interest as in Equation 3.6 [23].

The stress in a fiber is related directly to the amount of deformation, or strain, in the fiber. For the purposes of fiber tensile property measurement, strain, ϵ, may be defined as

$$\epsilon = \frac{\delta L_f}{L_f}, \tag{3.7}$$

where δL_f is the change in length of the fiber sample divided by the original length of the sample, L_f [23]. Stress is generally measured as a function of strain.

Consequently, another important fiber property called the modulus of elasticity, or Young's modulus, may also be derived from the tensile stress-strain test. Certain materials are said to be elastic; and these materials behave linearly in a certain region known as the Hookean region. In this region, a linear increase in deformation of the material leads to a linear increase in the stress experienced by the material [6]. Materials in the elastic region always return to their original state when the load is removed. The elastic modulus, E, relates the stress and strain as

$$E = \frac{\sigma_t}{\epsilon}, \tag{3.8}$$

and is measured as the slope of the linear portion of the stress-strain curve [23].

The proportional limit, σ_{PL}, is defined as the last point on the load-elongation curve for which stress is proportional to strain. The elastic limit, σ_{EL}, is defined as the greatest stress a material can withstand without any permanent deformation occurring upon release of the load. The ultimate tensile stress, σ_{ULT}, corresponds to the maximum stress experienced by a fiber during a loading cycle; and the yield stress, σ_Y, corresponds to the stress at which a fiber breaks [23].

The maximum elongation is defined as the length to which a fiber may be extended before it breaks. Reduction in area is defined as the ratio of the cross-sectional area of an elongated fiber to the original cross-section area. Finally, creep is general term which refers to the continued deformation of a material under load. Creep is a time-dependent phenomenon [23]. Hair fibers, for example, experience creep [6].

Tensile Testing – Measured Values

Many properties of a single fiber may be determined from a tensile test, yet remarkably few measurements are required. The load on the fiber must be measured during the elongation. Also, the elongation of the fiber must be measured precisely. Finally, as the load on the fiber and the deformation of the fiber are measured, the time of the measurement must be recorded if creep is to be determined.

Tensile Testing – Methodology / Test Protocol

There are a number of potential methods for acquiring the data necessary to derive the tensile properties of single fibers. Two primary methods, one time-controlled and the other position-controlled, are considered for the design of the single fiber testing instrument.

The time-controlled method is the approach currently in practice at Wella. The Wella system is based on the Diastron MTT600 and does not have feedback available to control position with great accuracy. A hair which has been fitted with crimp ferrules is loaded into the Diastron test system and stretched until the fiber breaks. Motion of the testing axis in the Diastron machine is provided by a stepper motor, and the distance traveled is measured by counting the motor steps from an initial position. The machine travels with a constant speed while recording the force values from a load cell mounted in line with the fiber under test. The recording of the force values commences when an initial force value is passed. Exact positioning of the fiber by this method is difficult because stepper motors are naturally prone to skipping steps, and errors arise if the machine jumps one or a few steps [22].

An improved alternative method proposed for the automated single fiber testing instrument is based on precise position control. In this case, the tensile test involves stretching a single fiber in a manner similar to that described for the time-controlled method except that the position of the moving axis is monitored separately from the motion source. Therefore, the actual displacement of the fiber under test may be known very precisely even if the motion system does not provide precise motion.

Tensile Testing – User Variables

The range of valuable information that the tensile test may provide also means that users may wish to adjust many variables to suit their particular testing requirements. The tensile extension rate is an important variable parameter because fibers may respond differently depending on how quickly they are deformed. Typical extension rates for fiber testing vary from about 1mm/min for a slow test to as much as 0.67 mm/s for a fast tensile test. The standard extension rate used by Wella to test human hairs is 0.17 mm/s.

A great deal of data may be generated by a tensile test and therefore the sampling rate must also be adjustable by the user to limit data sets based upon specific positional or temporal resolution needs. The Diastron machine acquires data at a rate of 3.47 Hz at an extension speed of 0.17 mm/s. It would be ideal to surpass this rate with the automated single fiber testing instrument to allow finer measurements.

3.2.5 Bending Properties

The bending properties of fibers are difficult to define precisely. The bending of structures typically involves a combination of compressive and tensile loads which are difficult to quantify in a consistent way across the wide variety of fiber types and structures. For the purposes of the instrument designed for this thesis, the bending properties of fibers are determined from a measurement based on the classical definition of column buckling.

Bending – Desired Properties

When a fiber is bent, internal forces are generated as shown in the schematic of Figure 3-7. Some of these forces are compressive forces and some are tensile forces. All of the forces are governed loosely by the modulus of elasticity of the fiber. The modulus of elasticity is not uniform throughout the material, however, because many fibers are anisotropic. Hairs are an example of such fibers.

The primary property of interest for the fiber bending tests, the bending modulus,

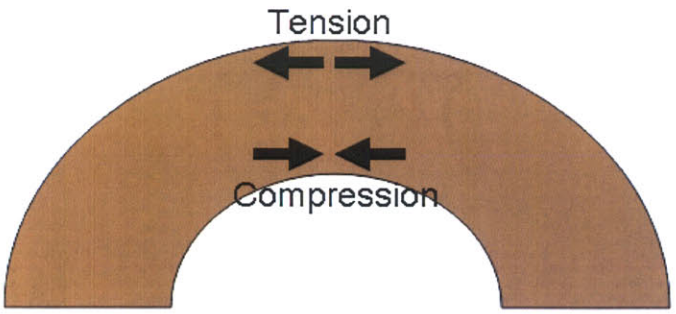

Figure 3-7: Diagram of internal forces generated in a fiber during bending measurement.

is actually an artificial term which accounts for the fact that the bending of anisotropic fibers such as hairs leads to the calculation of a modulus of elasticity unique and different from the elastic modulus measured from stress-strain tests.

The Euler column buckling load may be used to approximately determine the bending modulus of fibers [33]. In simple terms, the Euler column buckling load is a measure of the onset of instability of a column placed under compression. When applied to the measurement of buckling in a fiber, the equation states that the load, P_e, which causes the onset of buckling, or instability, in the fiber is related to the bending modulus of elasticity, E_b, of the fiber, the minimum principal second moment of inertia, I, of the fiber, and a shape factor, λ, related to the length, L_f, of the fiber as

$$P_e = \frac{\pi^2 E_b I}{\lambda^2}. \tag{3.9}$$

The minimum principle second moment of inertia for an elliptical fiber is defined as

$$I = \frac{\pi d^3 D}{64}, \tag{3.10}$$

where d is the small diametric dimension of the fiber and D is the large diametric dimension of the fiber. The shape factor λ is dependent on the boundary conditions

of the defined as

$$\lambda^2 = \frac{L_f^2 A}{I}, \tag{3.11}$$

where L is the length of the fiber and A is the minimum cross-sectional area of the fiber [23, 33].

Bending – Measured Values

In order to determine the bending modulus from the Euler buckling approximation, the instrument will be required to measure the appropriate cross-sectional dimensions of the fiber under test, the length of the fiber under test, and the load at which buckling initiates. The buckling load will be defined as the first maximum load experienced by the fiber during compression.

Bending – Methodology/Test Protocol

Fiber bending modulus tests performed at Wella are typically performed on fibers which are free at one end and fixed at the opposite end. The particular testing configuration conforms to the boundary conditions set forth above for the Euler beam buckling equation.

Ideally, the fiber will be able to remain in the grippers during the entire testing regimen. Therefore, the bending modulus measurement will occur with the fiber under test mounted in the grippers. Compression of the fiber will be achieved by advancing one of the grippers toward the other. During this process, the load on the fiber will be measured as a function of the compressed position and time. The fixed-fixed boundary conditions for the proposed measurement technique are slightly different and require calculation of the bending modulus based upon a modified buckling load equation [23]. The corresponding equation is

$$P_e = 4\frac{\pi^2 \mathrm{E_b I}}{\lambda^2}. \tag{3.12}$$

Bending – User Variables

Users of the instrument shall be permitted to vary the rate at which the compression of the fiber occurs during the bending test. There is a strong likelihood that the rate of measurement may affect the measurements. The distance to which the fibers are compressed will also be adjustable by the user.

3.2.6 Torsional Properties

The torsional properties of fibers are the final property which the automated single fiber testing instrument shall be responsible for measuring. The torsion test may be defined as a method for determining the behavior of materials subjected to twisting loads [32].

Torsion – Desired Properties

The torsion test shall be concerned primarily with measuring the torsional modulus of elasticity for single fibers. The torsional modulus of elasticity, G, of a fiber may be defined [23] via the general torque-angular displacement relationship

$$\tau = GJ\alpha \tag{3.13}$$

where τ is the torque exerted on the fiber; G is the torsional modulus of the fiber; J is the polar moment of inertia of the fiber and is proportional to the outer diameter, D_o, of the hair as

$$J = \frac{\pi}{32} D_o^4. \tag{3.14}$$

The variable α relates the angle of twist θ of the fiber, in radians, to the length between torque application points L as

$$\alpha = \frac{\theta}{L}. \tag{3.15}$$

Torsion – Measured Values

In order to determine the torsional modulus of a single fiber, the fiber must be subjected to a twisting load. The important values to be measured are the angle of fiber

twist, the length of the fiber, and the value of the applied load.

Torsion – Methodology/Test Protocol

Most of the traditional methods for measuring the torsional modulus of single fibers, especially hairs, have been related to the so-called torsional pendulum method. The torsional pendulum method involves suspending a small pendulum from a fiber that may be set into free rotational oscillation. By determining the period of oscillation of the pendulum and other geometric properties of the fiber, the torsional modulus may be calculated [14].

A new method is proposed for the single fiber testing instrument that will allow the fiber under test to remain fixed in the grippers during the measurement. The new proposed method involves rotating the ends of the fiber while the middle of the fiber is fixed and prevented from rotating. As ends of the fiber are rotated, a reaction force is generated at the fixed contact point at the middle of the fiber. This reaction force may be measured by a highly sensitive force transducer. The angle of rotation of the ends of the fiber may also be measured. Because the other geometric characteristics of the fiber may be measured as well, the torsional modulus may be calculated without removing the fiber from the testing region.

Torsion – User Variables

The torsion measurement proposed for the instrument is new and untested. Therefore, in order to make the test a valuable one for researchers, many parameters of the test shall be variable. Users shall be permitted to adjust the angle and rate of rotation of the ends of the fiber, the amount of tension in the fiber, the length of the fiber, and the force with which the element to prevent fiber rotation contacts the fiber under test.

Chapter 4

Automation Considerations

One of the principle advantages of the single fiber testing instrument, apart from its versatile functionality, is automated operation. In this chapter, the important design considerations which affect the automatic operation of the machine have been identified and explained in order to accomplish the objective of high-throughput testing of many fibers. For simplicity and clarity, the automated functionality of the machine has been divided into four focused tasks: pre-test fiber storage, pre-test fiber handling, in-test fiber handling, and post-test fiber disposal.

4.1 Pre-test Fiber Storage Considerations

The efficacy of the instrument relies on the ability to perform a wide array of tests on multiple sets of single fibers. Therefore, the instrument must be able to store many fibers as effectively as possible. The successful storage system must have ample capacity, must be simple and efficient to load, and must not compromise or damage the fibers before or while they are tested.

Storage Capacity

Many of the tests performed by the automated single fiber testing instrument will require that multiple fibers be tested in a single round of testing. Users may wish to generate statistical data for a set of many similar fibers, or they may wish to perform

a barrage of similar tests on a set of several unique fibers for comparison purposes. In many instances, a user may only wish to measure the properties of one single fiber. Nevertheless, versatility is important for maximizing the end user's ability to fulfill his personal testing requirements. The storage system should be intuitive and flexible enough to allow the user to accommodate most testing scenarios.

Wella recommended a preliminary specification that the instrument should be capable of performing multiple repetitions of the same measurement using at least 30 different hair fibers [34]. However, in order to improve efficiency and to compete with other commercially available single fiber testing instruments, the instrument shall be able to test up to 100 single fibers without reloading. Additionally, the fiber storage positions shall be numbered so that the user may easily account for the location of each specific fiber and the number of fibers which have been loaded prior to testing.

Fiber Loading

The procedure of loading fibers for testing has presented significant problems in the past for other single fiber testing instruments. Therefore, the design considerations for fiber loading have been regarded as an opportunity to greatly improve the state of the art in fiber testing.

Most others fiber testing systems require some sort of preparation of the fibers to be tested. The Diastron MTT600 automated tensile tester and the Textechno Favimat Robot single fiber testing instrument are both among the most advanced commercially available instruments for the automatic testing of single fibers. However, both instruments require the user to prepare each fiber under test with special clamped-on fasteners prior to loading into the instrument.

The procedure of affixing special fittings to either end of every fiber for testing has many obvious disadvantages. First, the process is time consuming, labor intensive, and tedious. Secondly, error may be introduced if the exposed length of each fiber varies from sample to sample. Finally, the fiber may be damaged in an unrepeatable way if the clamps are affixed too tightly or inconsistently. A special machine is under development by Wella and the Fraunhofer Institute for Manufacturing Engineering

and Automation to automate and standardize the formerly manual process of affixing brass ferrules [22].

A better solution for the automated single fiber testing instrument under development is to make the loading procedure as straightforward and effortless as possible. The fibers should be loaded directly into the instrument storage zone by hand without the need for any modification to the fiber. No special fasteners should be required. The system should be ergonomic and easy to load by hand, should hold the fibers to be tested securely in place, and should allow hairs to be removed easily for testing.

Minimize Damage to Fibers

Another important consideration for the fiber storage system is to minimize or eliminate the potential for damage to fibers before they are tested. Any deviation of a fiber from its natural form may cause significant variations in measurement results. Damage is most likely to occur if the fibers are exposed to rough surfaces or sharp edges. Therefore, the storage system should be free from any such features.

Also, some fibers that will be tested in the machine will be coated with surface treatments. As a result, the storage system may become contaminated, and all fibers loaded for subsequent tests may become damaged or compromised by such contamination. For instance, hair fibers that will be tested in the machine will be treated primarily with two product types: rinse-off and leave-on treatments. Rinse-off treatments will not pose any problem of contamination to the storage surfaces; however, it is possible that certain leave-on treatments will leave trace amounts of residue, such as cationic polymer layers, on the grip surfaces. The storage system should be designed such that it may be cleaned easily by some of the proposed methods for cleaning these residues. These methods include cleaning with short intensive bursts of high-pressure water, a similar spray of alcohol, or manual cleaning of the fiber storage zones with a sterile wipe at the end of each round of testing [22].

Finally, it has been mentioned earlier that other single fiber testing systems require the additional step of affixing specialized clamps to each fiber prior to testing. By eliminating this procedure and allowing the user to load the fibers directly by hand,

the human handling of the fibers is reduced significantly. This approach will further help to minimize the potential for fiber damage.

4.2 Fiber Handling

Once the fibers have been loaded into the storage system by the technician, the instrument should be able to effectively handle them in a completely autonomous way. The handling of the fibers shall involve manipulation prior to testing, during testing, and after testing. Several considerations for each stage of fiber manipulation must be addressed to ensure that the handling of each fiber is consistent and reliable.

4.2.1 Pre-test Fiber Handling Considerations

Before a fiber may be tested, it must first be transferred from the storage zone to the testing zone. There are several factors which must be addressed to ensure that the handling of the fibers in the pre-testing stage is optimally planned.

One of the most important pre-test considerations to bear in mind is that the fibers must be placed with great precision. The fibers which are to be tested by the instrument are very small, with some dimensions of interest in the sub-micron range. In order to be effective, the fiber handling system will be responsible for accurately and repeatably loading fibers into the testing region.

Additionally, the objective of the single fiber testing instrument is to improve the efficiency of fiber testing by increasing throughput. The pre-test fiber loading system must be fast.

Furthermore, the loading system must be robust against failure. An automated system should not require any attention from a human user during its automatic cycle. Many different types of fibers may be tested by the instrument. In the axial dimension, these fibers may be straight, curly, or wavy; and the fiber cross-sections may be thick, thin, round, elliptical or even completely asymmetric. The instrument should be able to accommodate a wide range of fiber types without failure. It should also be able to handle or even avoid the scenario of an imperfectly loaded fiber.

Finally, it is important that the fiber handling system does not damage the fibers as it transfers them from the storage zone for testing. It has been mentioned several times that damage to a fiber may result from many sources including excessive handling and contact with rough, sharp, or contaminated surfaces. When loading fibers for testing, each of these potential damage sources must be minimized as much as possible.

4.2.2 In-test Fiber Handling Considerations

Once a fiber has been loaded into the testing region of the instrument, measurements may be performed. A number of new considerations arise for the in-test portion of the fiber handling system. Most importantly, the fiber must be gripped in some fashion for each test in the test regimen. Also, the in-test fiber handling system is responsible for the motion that will ultimately translate into all of the fiber measurements. Thus, in-test motion considerations must be discussed as well.

Fiber Gripping

The gripping of the fiber during the test comprises a major component of the in-test fiber handling system and has a great deal of influence on the ultimate quality of the tests which will be performed by the single fiber testing instrument. Ideally, the instrument should be able to perform all of the requisite tests while the fiber remains in a single set of grips. The advantages of a consolidated test region are manifold. The time required to test each fiber may be minimized by eliminating the time that would otherwise be spent transferring the fiber to alternative test regions for various tests. Also, the complexity of the machine is decreased through shared functionality. Finally, the potential for damage to the fiber under test as a result of handling between testing regions is eliminated.

In order to function repeatably and reliably, the gripping region must observe several mechanical considerations. One of the most common pitfalls of nearly all mechanical testing is that the sample is not held securely. Therefore, it will be

Figure 4-1: Contrary linear motions required by automation system.

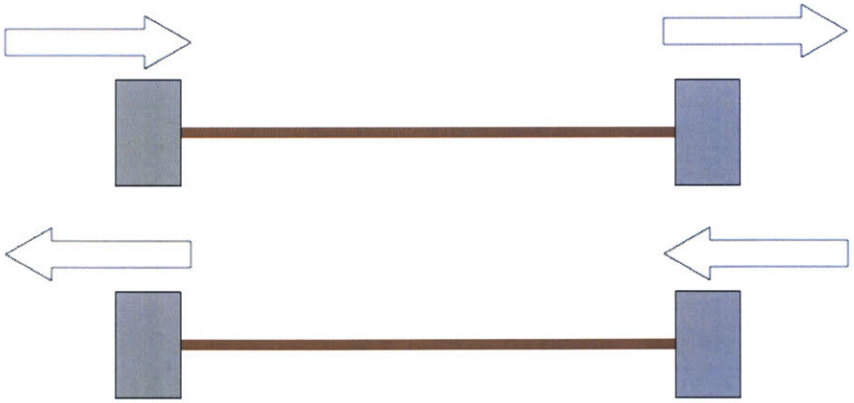

Figure 4-2: Uniform linear motions required by automation system.

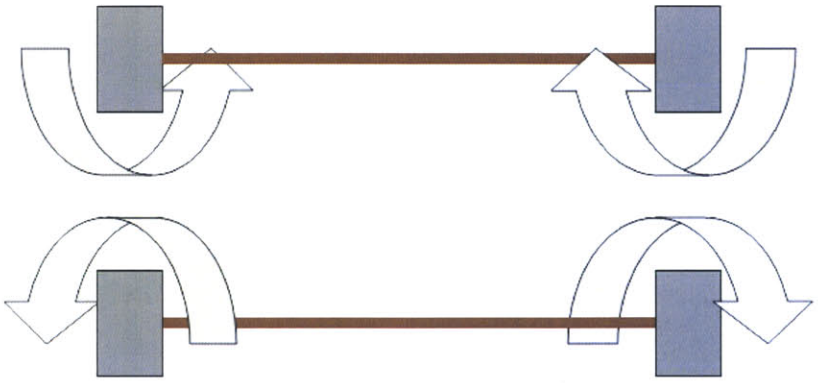

Figure 4-3: Contrary rotary motions required by automation system.

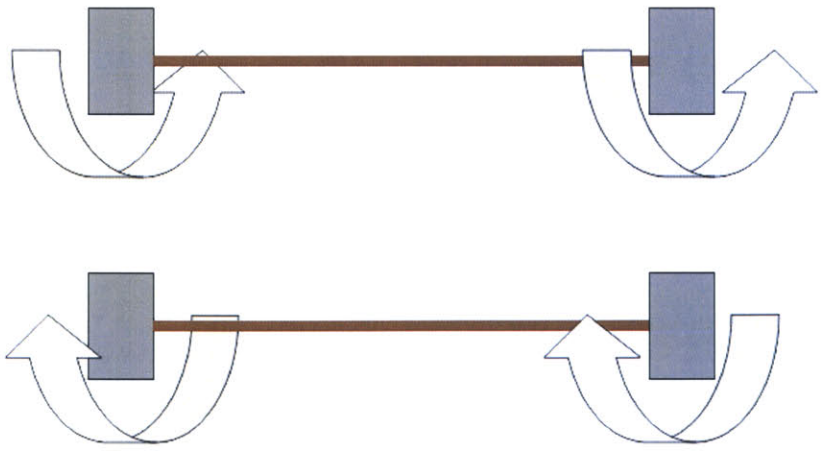

Figure 4-4: Uniform rotary motions required by automation system.

very important for the gripping region to hold the fibers securely without slipping. Slipping of the fiber must be prevented axially as well as rotationally to support all of the possible tests.

Additionally, the gripping region must be designed to minimize mechanical damage to the fibers. Damage to the gripped fiber may result from the usual sources of grip surface contamination, contact with sharp edges and rough surfaces, and extensive manipulation. Another factor which arises for the gripping region is that the fiber must be gripped tightly enough to prevent slipping during testing, however not so tightly that the fiber may be damaged.

In-test Motion

During the testing phase, the instrument will be responsible for automatically performing all necessary measurements on the single fiber under test. The instrument must therefore provide capacity for moving the fiber, and a number of appropriate motion-related considerations must be addressed.

The test procedures will involve examining each fiber from multiple perspectives, and the instrument must be able to move the fiber suitably. The fiber will be stretched and compressed along its axis for the tensile and bending modulus tests, respectively. Therefore, the instrument must be able to provide contrary motion along the fiber axis as shown in Figure 4-1. The instrument must also provide uniform transport of the fiber for the friction and surface roughness measurements as shown in Figure 4-2. Uniform movement of the fiber may also be necessary for moving the fiber between various zones such as those for loading and testing.

For the diameter measurement, the fiber must be uniformly rotated about its axis, and the instrument must provide a means to rotate the fiber accordingly as shown in Figure 4-3. The torsion test will require that the fiber be twisted about its axis as well, requiring that the rotational system be able to provide contrary rotation as shown in Figure 4-4.

All of these linear and rotational motions must be very precise and repeatable. Precise axial positioning that is greater than the order of the features to be measured

is important to ensure accurate measurement results, and each fiber must be moved in an identical fashion to produce repeatable results. Furthermore, the motions must be smooth and free of jitter or vibration that might affect the sensitive measurements. Finally, the motion systems must be fast in the linear and rotational directions for rapid positioning between tests and loading cycles.

4.2.3 Post-test Fiber Handling Considerations

After a round of testing is performed on a fiber, that fiber will be handled by a post-test fiber handling system. The system will be responsible for removing and storing the tested fiber.

Fiber removal

The final step in the testing cycle is to dispose of the tested fiber. Tested fibers must be removed from the testing zone so that subsequent fibers may be tested. The principal objective of the waste fiber removal step is to ensure that all remnants of the tested fiber are expelled. To guarantee that the machine will operate smoothly, each fiber to be tested must be presented into an identical testing environment. Therefore, regardless of the state of a fiber after it has been tested, it must be removed from the testing zone completely. Additionally, the fiber removal system may be required to automatically clean the testing region if it has been contaminated during testing.

Disposed fiber storage

The waste fiber removal system is also responsible for storing the removed fibers for ultimate disposal. Access to the disposal system must be convenient and simple.

Chapter 5

Automation System Design and Implementation

The preceding chapters have provided background, motivation, prior art, and design considerations for the construction of the automated single fiber testing instrument. Chapters 5 and 6 discuss the actual design and implementation of the instrument. The chapters are subdivided into two broad sections. Chapter 5 describes the design and implementation of the automated modules of the instrument. Chapter 6 discusses the design and implementation of components related to the measurement modules of the machine. Because of the high level of component integration in the instrument, certain areas of the two chapters may contain minor overlap of information.

The automation system of the single fiber testing instrument integrates many elements to provide effective automated functionality. This chapter describes the early prototypical designs as well as the final designs for each automation subsystem. The pre-test fiber loading system is discussed first. Next, the pre-test fiber storage system is explained. Afterwards, the design of the in-test motion system is detailed. Finally, the post-test fiber disposal design is presented. For each automation subsystem, specific devices and components which have been implemented are described.

5.1 Pre-test Fiber Handling System

The pre-test fiber handling system is responsible for presenting each single fiber to the testing region of the instrument so that it may be tested. The handling system is comprised primarily of a fiber loading system and grippers which are responsible for holding the fiber during testing. Several novel methods were considered for handling the fiber loading procedure. Additionally, multiple iterations of gripper design were carried out. An effective method was ultimately chosen based upon experimentation.

5.1.1 Fiber Loading Methods

Several options were examined to accomplish the task of handling small single fibers. Existing methods were considered first. The solution utilized by most commercial fiber testing systems, such as those marketed by Diastron, Inc. and Textechno KG, is to affix special fittings onto the ends of the fibers thus making them far more convenient to manipulate mechanically. This solution is effective, but it is also quite labor intensive. Therefore, a number of novel methods were considered as alternatives to the industry standard.

Air was considered as a potential means to transport the fibers into the testing region. Air transport by means of vacuum was investigated first. The system proposed the use of vacuum-pressure to extract individual fibers from a storage chamber into a smooth circular hose which then transported them to the testing region.

In order to keep the fibers under control such that they could be delivered to the testing zone precisely, the orifice at the end of the vacuum hose must be very small. Effectively, the degree of precision with which the fiber may be directed corresponds to the size of the outlet orifice, which means that the orifice would have a maximum diameter of approximately 500 μm. The air flow rate through the vacuum hose is approximately proportional to the cross-sectional area of the hose and to the pressure of the air in the hose. Because the exit orifice must be so small, the pressures required to generate a flow rate adequate to move the fiber are unreasonably large.

In addition to the issues of pressure and flow rate, the vacuum-based system does

not present an easy solution for how to extract one fiber at a time or how to position the fiber precisely once it has been transported to the testing region.

Another prospective means of fiber transport is also based on air, but instead utilizes compressed air to push the fibers through a transport hose into the testing region. Identical issues to the vacuum-based system arise with this option. The fibers are difficult to control, and the pressure required to generate flow rates that could cause the fibers to move through the transport hose are too great if the orifice is constructed small enough to direct the fiber to a desirable position.

Electrostatic manipulation of the fibers was also briefly considered as an option for fiber transport and handling. Many fibers such as hair are highly resistive to the flow of electricity. Because charges are unable to move easily within such non-conductive fibers, they can become quite electrostatically charged, or covered with stationary charge. The charged fibers may then be manipulated by other charged objects. For instance, oppositely charged objects will attract the fibers when placed in close proximity while similarly charged objects will repel the fibers. The electrostatically induced cosmetic phenomenon of static flyaway in hair results when an object such as a plastic comb or balloon is rubbed in contact with the hair. Charges of equal and opposite magnitude are generated on both the comb and the hair surface because of the difference in the affinity of each of these materials for electrons [6]. It was desired that the electrostatic charges on the fibers might be used either to separate the fibers, as occurs when hairs on a head experience static flyaway, or to actually manipulate the fibers in a controllable fashion. Some bench level experiments were performed using a high voltage power supply to generate static electrical charges on hair fibers. The studies indicated that the level of charge on the fibers could not be controlled enough to move the fibers in a repeatable fashion. The weights of the fibers were often greater than the achievable electrostatic forces, so the fibers were dropped prematurely. Furthermore, some of the tests to be performed by the instrument involve examining fibers in a saturated humidity climate. Fibers which are wet are far more conductive than dry fibers and will therefore not easily maintain static electrical charge.

Magnetism was also initially considered as a means of fiber manipulation. The proposed mechanism considered using the fields of permanent magnets or electromagnets to guide the fibers to the testing region. The most obvious dilemma associated with magnetic fiber handling is that the fiber must either be magnetic itself or have some magnetic element attached to it to allow it to be moved by a magnetic field. Recalling that two of the principal design considerations associated with the fiber handling system were to make the system universally repeatable for most fiber types and to eliminate the need for attaching foreign objects to the fibers, this method was eliminated as a possibility.

Mechanical manipulation ultimately proved to be the most reliable and effective means of fiber handling. The method proposed physically holding the fiber at either end and moving it about the instrument in a purely mechanical fashion using only actuators and mechanisms. It was found that fibers could be mechanically transferred from a standard pre-loading configuration to a standard loaded position more easily than by any other method. The mechanical handling of the fibers allowed the greatest variety of fibers to be tested by the machine because, unlike the other proposed methods, the method is largely independent of any special properties of the fibers. The final design of the mechanical loading mechanism is described later in this chapter.

5.1.2 Grippers

Based upon the selection of a system in which the fibers are transported mechanically, the most logical solution for holding the fibers during testing imitates the naturally effective gripping action of a human hand. The grippers were designed to have two basic states: open and closed. The open state allows a fiber to be inserted, and the closed state provides the force necessary to hold the fiber during the test regimen and to prevent it from slipping.

Gripper Design Requirements

The gripper force required to prevent slipping was estimated from the ultimate tensile strength of an average 70 μm diameter human hair fiber. The ultimate tensile strength of such a fiber, as shown in Table 2.1 is 254 MPa, which corresponds to a breaking load of 0.997 N for the given fiber dimensions assuming a round fiber cross-section. This means that the grippers must provide at least enough clamping force on the fiber to prevent it from slipping at a load of approximately 1 N.

The frictional interface between the fiber and the grip surface determines the amount of actual resistance to fiber slipping; and depending on whether the fiber is coated with a friction-reducing treatment, the coefficient of friction may vary substantially. Therefore, the gripper system has been designed with a clamping surface optimized for increasing the coefficient of friction with the fibers under test, even if the fibers have been treated. A safety factor of 10 has also been introduced for the clamping force requirement. This corresponds to 10 N of clamping force on the fiber in the testing position, allowing for a variety of fibers and testing procedures while preventing slipping of the fiber as much as possible. It shall also be possible for the user to vary the amount of gripping force by changing the force-generating element of the gripper prior to a round of testing.

The grippers have been designed to ensure that each fiber is positioned and held precisely upon loading. The grippers open easily with little mechanical effort, and the opening action does not damage the sensing elements of the test system to which the grippers are coupled. Finally, the grippers have been designed for minimum overall weight. The weight of the grippers is of major concern to the mechanical testing setup because the inertia of any components inline with the fiber under test will have a direct effect on the quality of the measurements.

Gripper Actuation

Actuation of the grippers emerged as a critical consideration during the design process. The grippers could be opened and closed by an onboard actuator similar to many

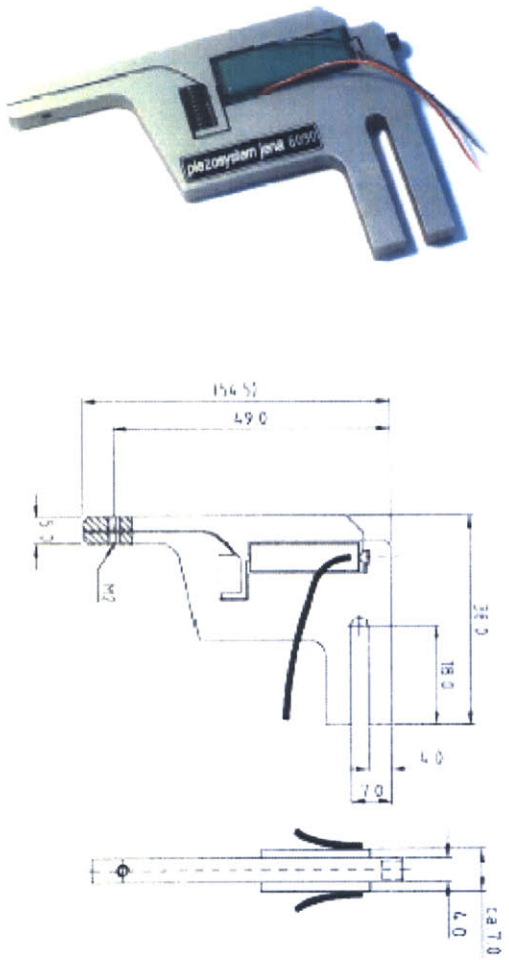

Figure 5-1: Piezosystem Jena Grippy 3 piezo-actuated gripper. (Taken from http://www.piezojena.com, Piezosystem Jena)

commercially available grippers. One inspiring gripper design developed by Piezosystem Jena [35] utilizes an integrated piezo element to generate opening and closing gripping functions as shown in Figure 5-1.

Other commercially available miniature grippers from Techno-Sommer and Festo, as shown in Figure 5-2, use integrated pneumatic-mechanical mechanisms to generate gripping functionality. Pressurized air is used to drive a piston which either opens or closes the gripper, and a spring provides the opposite action depending on the user-selected configuration [36]. A gripper from Newport, shown in Figure 5-3, also utilizes pneumatic air pressure to drive the gripping functions. Even the smallest of

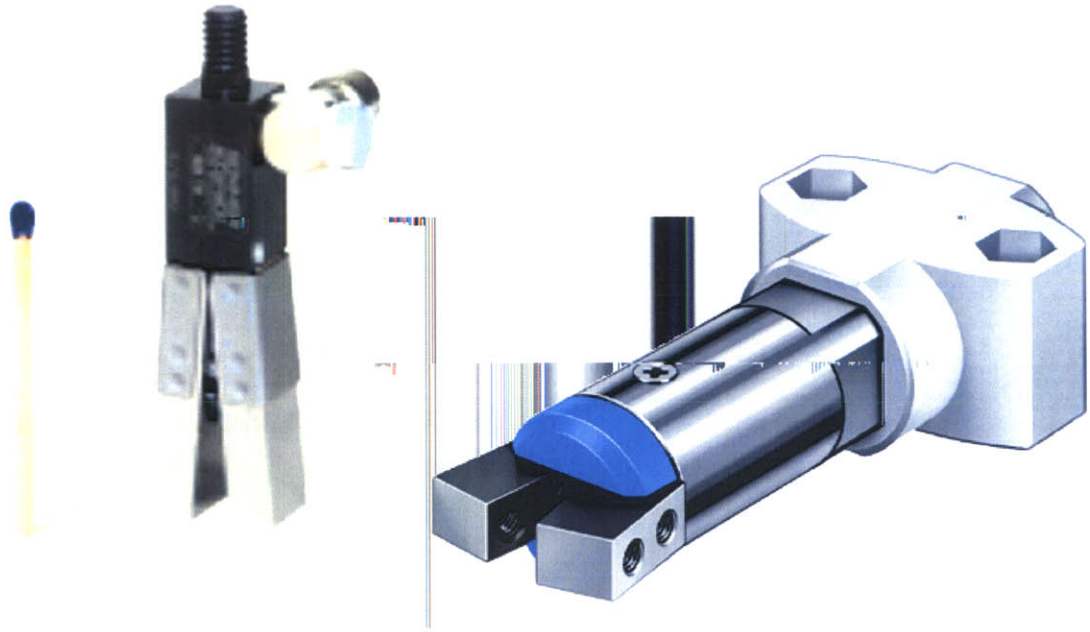

Figure 5-2: Techno Sommer micro-gripper (*left*) and Festo micro-gripper (*right*), both pneumatically actuated.
(Taken from http://www.techno-sommer.com, Techno Sommer &
http://www.festo.com, Festo)

these grippers is too bulky and heavy for use in the single fiber testing instrument, however.

Another option is to integrate passive actuation into the gripper. The essence of this concept is to use an active element which is not attached to the gripper to open the gripper so that the fiber may be positioned inside, and to use a passive element such as a spring or elastomer to close the gripper and generate the clamping force on the fiber. The passive gripping concept offers the advantages of lighter weight, smaller overall dimensions, and simplicity over the alternative options of actuator-integrated grippers. Thus, the grippers have been designed to support active opening from a decoupled actuator and passive closing with an integrated actuator.

Figure 5-3: Newport pneumatically-actuated grippers. (Taken from http://www.newport.com, Newport)

Gripper Design - Iteration 1

The first iteration gripper design attempted to account for all of the design requirements set forth above, but areas for improvement were discovered upon testing the prototype with actual fibers. The design, shown in Figure 5-4, was based upon a flexure-based structure for simple single piece construction. A compression spring was utilized to provide the passive closing force to press closed a flexure cantilever beam that served to grip the fiber under test. The gripper could be opened by pushing on a pin that passed through a channel in the main gripper structure and pushed against the spring-loaded cantilever beam. The design was configured such that the pin doubled as a positioning guide for fiber placement. The grippers could be opened actively, the fiber could be brought into contact with the pin, and then the active opening force would be removed and the gripper would close and secure the fiber passively.

Prototypes of the grippers were manufactured from two different materials: epoxy resin and aluminum. The grippers were first formed from a UV-light curable epoxy

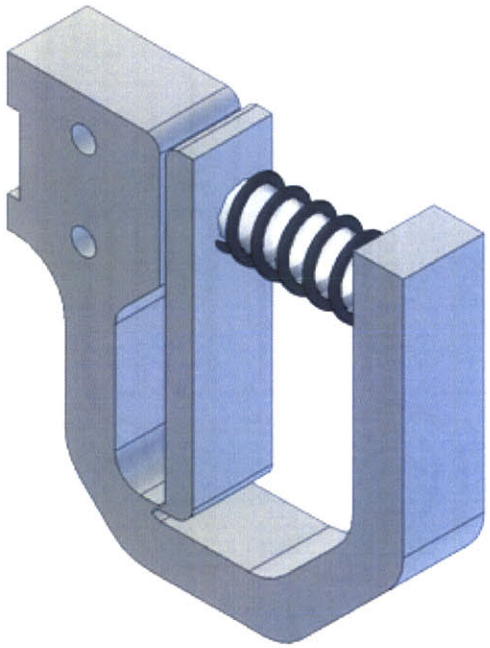

Figure 5-4: Solid model rendering of first iteration gripper design.

resin (Accura SI 40 Nd) using a 3D Systems Viper stereolithography (SLA) machine. The 3D Systems machine is a rapid-prototyping tool that is capable of producing complex, high resolution parts [37].

The epoxy resin version of the gripper was useful for determining the basic functionality of the mechanism. It was found that the design was effective at holding the fiber, but the geometry of the flexure system caused a good deal of stiction as the gripper was pushed open. Also, the resin-constructed prototypes all broke at the flexure junction after only a few open-close cycles. Despite the fact that the SLA produces parts quickly, the cured resin material has similar properties to brittle plastic and therefore cracks easily when it is cyclically stressed.

A second prototype of the first iteration gripper was manufactured from 6061-T6 aluminum. Aluminum is a lightweight metal which is far more capable of handling cyclic stress than the epoxy resin. It is often used for manufacturing flexure systems [38]. The aluminum gripper was cut from a solid block of aluminum by means of wire electrical discharge machining (EDM). The EDM process makes use of the erosive effects of an electrical discharge to remove material from a workpiece and is a forceless process with no contact between the workpiece and the machining electrode [39].

The aluminum gripper design proved to be more effective for holding hair fibers and other fibers than the resin prototype because the EDM machining process leaves all machined surfaces with a very fine and uniform surface finish. The roughness of the surface is dependent on many factors including the material being machined, the rate of machining, and the type of wire used. Therefore, further optimization of the surface could be performed later. Nonetheless, the gripper surface greatly improves friction generation and therefore reduces the clamping force necessary to hold the fiber in the grippers. Unfortunately, the aluminum gripper was also more likely to cause damage to the fiber because of the sharp edges created by the EDM process. These edges could be carefully filed smooth to reduce such damage to the fibers.

Each prototype had distinct drawbacks stemming from the material of construction as well as the machining technique used. The first iteration grippers were not optimized for size, and could be smaller. The grippers were asymmetric and would

likely contribute asymmetric off-axis loading that could affect the instrument measurements. Also, it was noticed that the pin which was used to open the grippers and guide the fiber before closing often pinched the fiber. Finally, the pin experienced stiction while opening the gripper as it contacted the walls of the guide channel, unnecessarily increasing the amount of force required for that function.

Gripper Design - Iteration 2

A second iteration gripper was designed to solve some of the problems associated with the first generation gripper design. The new gripper, shown in Figure 5-5, was designed to be much smaller in overall size. The symmetry of the gripper was improved by moving the center of mass of the unit closer to the gripper core. The flexure was redesigned to allow greater deflection during the opening and closing actions in hopes that the issue of fatigue fracture at the flexure might be prevented. The new gripper design was also much lighter than the previous version. Finally, the issue of the pin pinching the fiber during opening was solved by creating a small insert for the pin on the cantilever arm of the flexure so that the pin could no longer pinch the fiber.

Prototypes of the second iteration gripper were only manufactured from epoxy resin using the 3D Systems Viper SLA. The new design improved on most of the shortcomings of the preliminary design, but in fact worsened the machinability of the part. Therefore, the rapid prototyping tool was the most appropriate method for constructing a prototype for testing.

The second iteration prototypes functioned better than the first iteration prototypes. The grippers opened more easily and consistently. The grippers were also less prone to breaking at the flexure point from the cyclic stress of opening and closing, although the problem persisted and simply manifested itself at a delayed time. Finally, the fiber pinching problem present in the first generation grippers was remedied by the solution of passing the positioning pin through the open-close guide channel and into the cantilever beam.

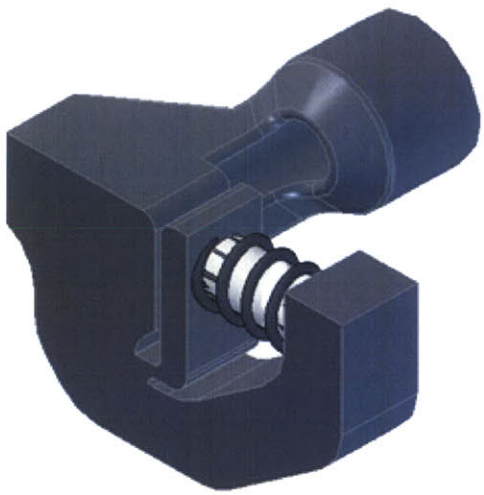

Figure 5-5: Solid model rendering of second iteration gripper design.

Gripper Design - Final Iteration

The final iteration gripper design set out to encompass all of the lessons learned from the first several gripper prototypes and aimed to make the system easily machinable. In a major improvement over the prototype designs, the final gripper design replaced the original flexure-based system with a mechanical hinge joint. The new design maintained the positioning pin for precisely loading the fiber in the center of the gripper, but decoupled the pin from the functionality of opening the gripper.

The opening function in the new gripper design would instead be carried out by pushing on the half of the hinged gripper structure not directly attached to the instrument. This design modification was additionally motivated by the fact that the point of contact of the lever arm for opening the gripper was moved to a point further away from the axis of rotation than the point at which the gripper applied force to the fiber. Therefore, the passive closing force which the gripper applied to the fiber became greater than the force required to open the gripper.

Additionally, rather than using a linear spring to produce the closing force, a torsional spring was utilized. The design has been configured so that a user may remove the grippers from the instrument and increase or decrease the degree of gripping force as necessary by simply changing the torsion spring. The standard gripper configuration applies approximately 10 N of gripping force at the point at which the fiber is gripped. The use of torsion springs permitted further miniaturization of the design as well. The mass of the gripper was reduced, and the center of mass could be positioned precisely at the center of the unit by utilizing a cylindrical form factor.

The final iteration gripper prototype was manufactured from stainless steel on the EDM, principally because of time considerations. The EDM is capable of machining steel much more quickly than aluminum [39]. In a production version of the instrument, the grippers will be made from aluminum which is nearly 3 times less dense than stainless steel [40] and will result in a highly effective yet very light, low-inertia gripping unit.

The final version of the gripper, shown in Figure 5-6, works quite well. It is able to

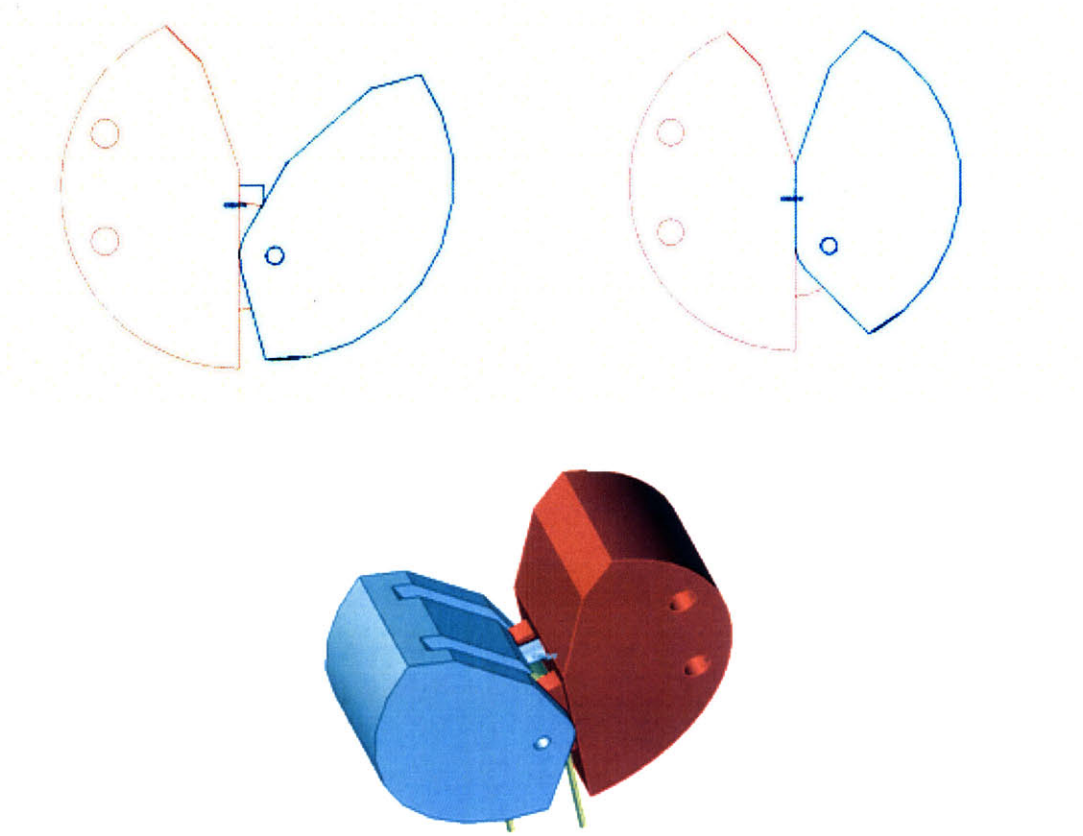

Figure 5-6: Solid model renderings of final iteration gripper design. Gripper is shown clockwise from top left: open and closed in wireframe; and in isometric solid view.

hold a variety of fibers without slipping, loads easily and repeatably, is easy to modify for special testing purposes, and is convenient to clean in the event of contamination.

5.1.3 Pre-test Fiber Storage Design

As discussed in Chapter 4, the fibers must be loaded into the instrument by a technician and stored by the instrument prior to testing. Several options for fiber storage have been considered. Each option has relative merits, but ultimately, one of the simplest designs proved to be the most effective mechanism for organizing fiber storage.

Prototype Fiber Storage Methods Overview

Early fiber handling methods based on air flow, electrostatics, and magnetism suggested fiber storage concepts in which fibers would be loosely and randomly gathered in some sort of container. Though such a storage method is attractive from a convenience standpoint, the stochastic nature of fibers immediately indicated the inadequacy of this method.

A more attractive method of fiber storage is to place the fibers by hand directly into some sort of magazine or carousel which holds them in a standardized configuration. As required by the design considerations, each fiber must be loaded into the storage unit easily by hand without the need for any special fixtures on the fibers. Each fiber must be held securely until testing and must be removed easily by the fiber handling system for testing without damaging that fiber or disturbing the other fibers awaiting testing.

It was determined that the best way to hold the fibers for loading into the designed grippers was to stretch them very slightly so that they were taut across an appropriate width span. The width of the taut fiber would be determined approximately by the length of the fiber to be tested minus the width of the gripping surfaces as shown in Figure 5-7.

Fiber Storage Method Design - Iteration 1

One of the first magazine designs was loosely inspired by the bandoliers used by soldiers to hold bullets. In the design, a three-sided semi-rectangular frame with square cross section was formed with small notches cut into the opposite sides as shown in Figure 5-8. The notches were as small as the fibers to be tested and designed with tapered faces to hold fibers of different sizes snugly as shown in Figure 5-9. Also, the notches were spaced approximately 3 mm apart to allow easy loading by hand.

The design was meant to automatically load the fibers into the instrument one at a time by indexing the magazine into the gripping zone as shown in Figure 5-10. The notches were angled at 45° so that only one degree of motion (up and down) of the

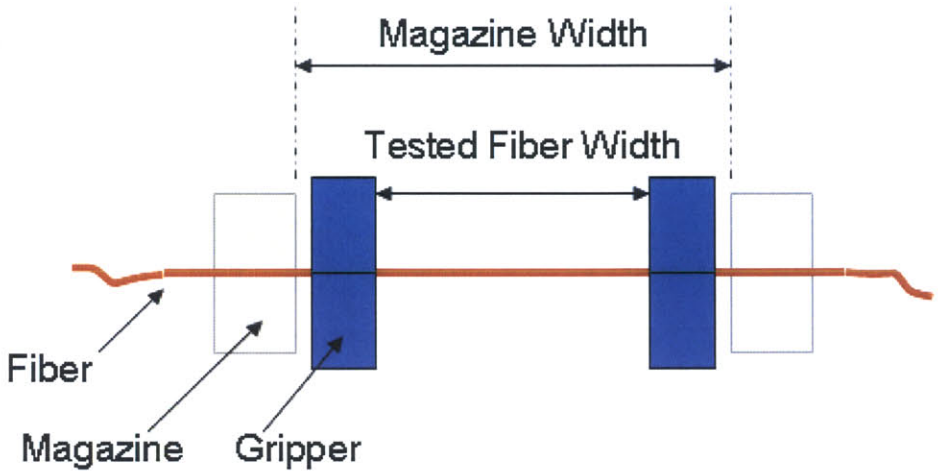

Figure 5-7: Schematic of proposed fiber loading configuration.

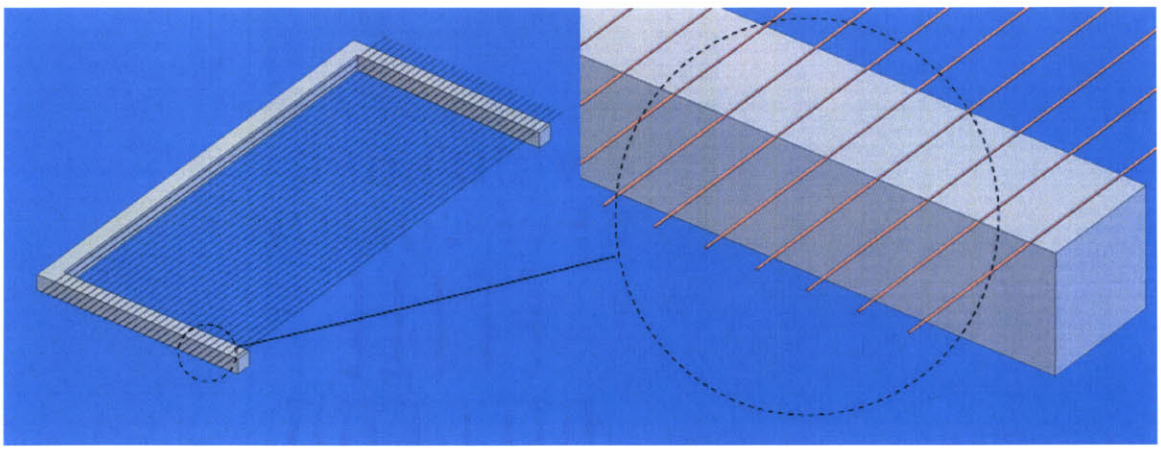

Figure 5-8: Solid model renderings of first iteration magazine design. Zoomed-in view indicated by dotted circles.

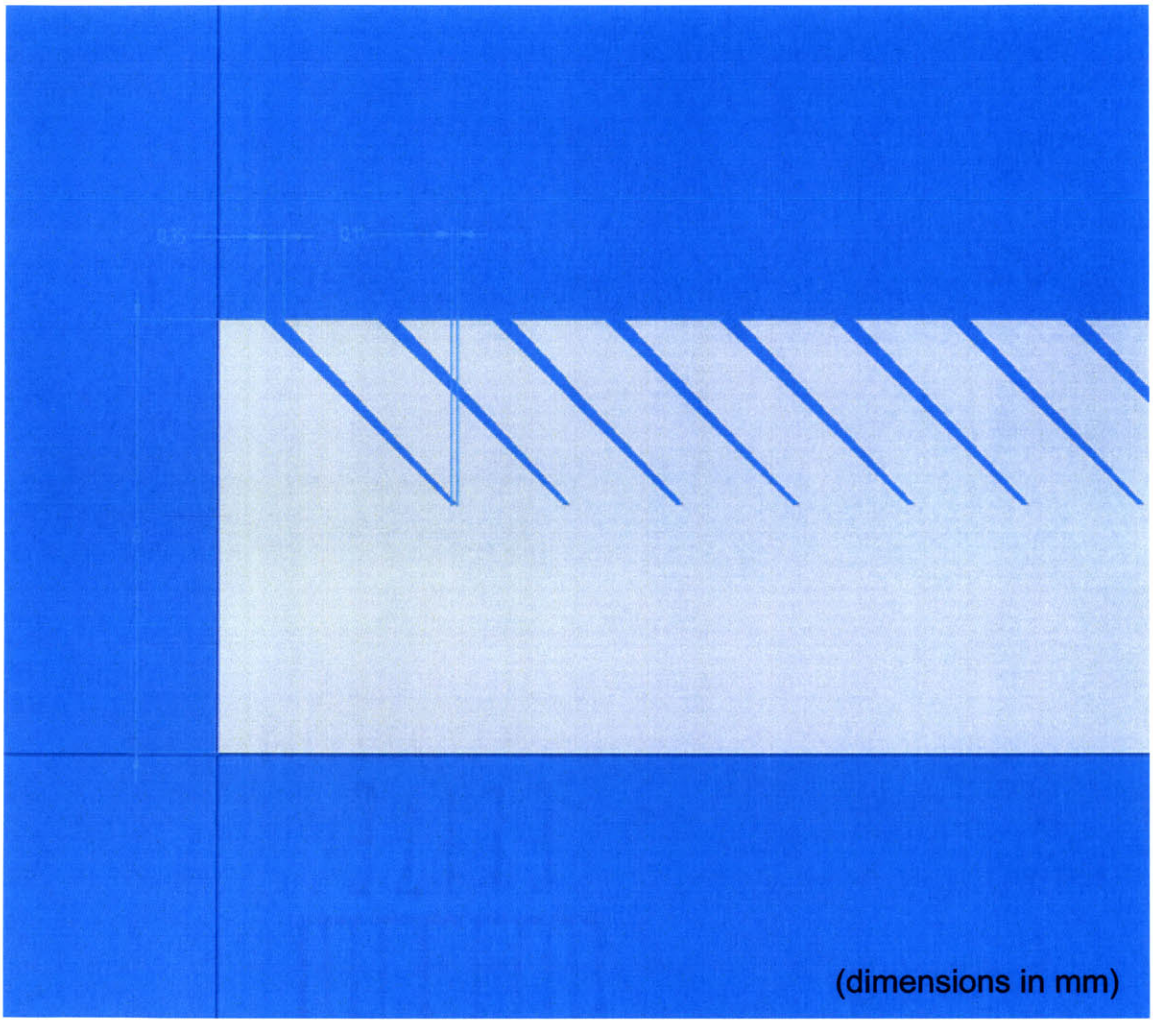

Figure 5-9: Close view of side section of the first iteration magazine design showing detail of fiber-holding notches.

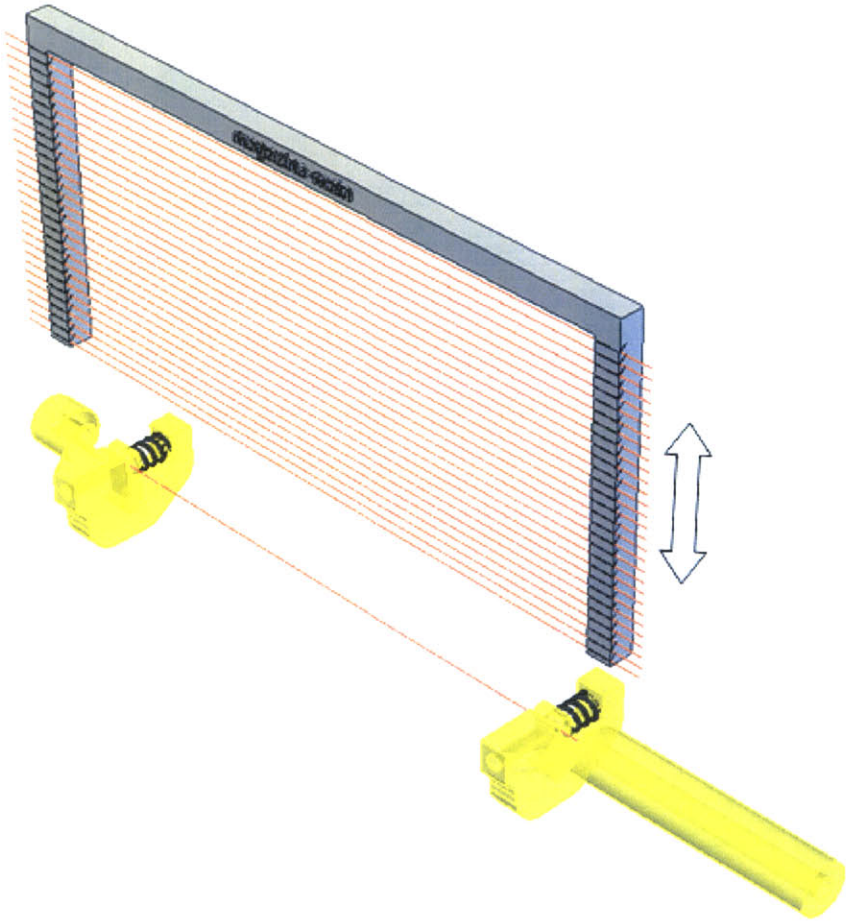

Figure 5-10: Solid model rendering of automatic loading procedure for first iteration magazine design. Arrow indicates loading motion of magazine.

magazine would be necessary to load a fiber into the gripper and to remove it once it had been loaded.

Several variations of prototypes of the first iteration design were constructed from epoxy resin using the 3D Systems Viper SLA. Most of the prototypes did not function well, but were useful for illustrating areas where improvement was needed. It was found that the configuration of the first iteration magazine prototypes was not optimized for maximum storage capacity in a minimum space. When the magazine was designed for a capacity greater than approximately 30 fibers, the form factor became ineffective. The design required that the magazine be open on one end for

fiber loading, so when the side arms became too long, they would flex easily while the magazine was handled. The flexing of the magazine meant that the fibers would become slack and therefore could not be loaded into the instrument properly.

Another more profound problem was the manufacturing of the fiber-holding notches. The smallest fibers tested by the machine would be as small as 40 μm in diameter. The 3D Systems Viper SLA was unable to create notches smaller than approximately 120 μm because of the limitations of the machine [41]. The magazines were redesigned with oversized dimensions to compensate for the inaccuracies of the laser curing system, which improved the characteristics of the notches slightly, but there were still issues with overcuring of the resin in the notches and the results were imperfect. In general, the notches were unable to hold fibers effectively.

Fiber Storage Method Design - Iteration 2

The wire EDM was tested as an alternative method to stereolithography manufacturing of the notches used for the first iteration magazine design. Prototypes were made from both aluminum and stainless steel. The stainless steel prototype is shown in Figure 5-11. The EDM-manufactured designs were modified to account for the fact that the smallest EDM wire available was 100 μm in diameter. In the resin prototypes, the notches were formed directly into the magazine as tapered grooves; yet in the EDM prototypes, the fiber-holding positions were designed as integrated spring-loaded flexures. This modification was meant to allow a variable range of fibers, including those smaller than 100 μm, to be loaded in the magazine.

In fact, EDM wires are available as small as 30 μm; however, the EDM process results in slight overcutting which would nevertheless lead to oversized notches for fibers smaller than 40 - 50 μm in diameter. Also, because aluminum and stainless steel are far stiffer than the resin material of the original prototypes, the flexures were intended to add flexibility for accommodating a variety of fiber sizes more effectively.

The EDM prototypes were very effective at holding the fibers in place, but they were very difficult to load. The surface finish which resulted from the EDM cutting process generated a high level of friction with the hair fibers which were tested in

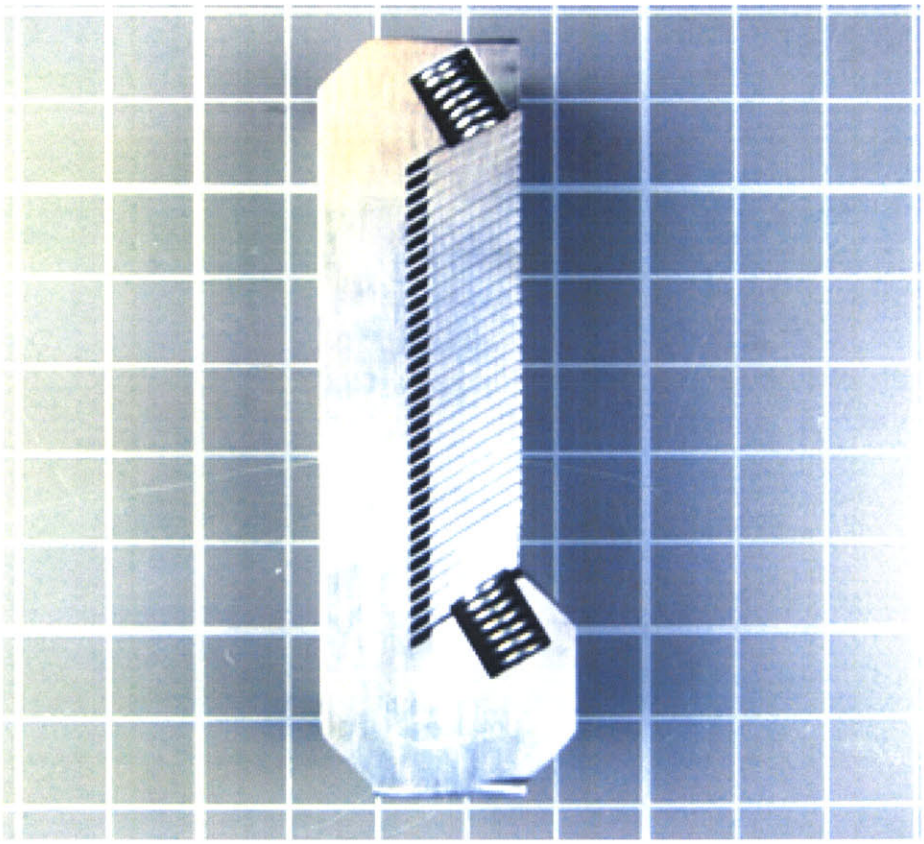

Figure 5-11: Image of EDM-manufactured steel magazine.

the magazine prototypes. The friction made it difficult to slide the fibers into place without damaging them and also made it difficult to remove the fibers as they would be loaded into the instrument.

Fiber Storage Method Design - Iteration 3

A third iteration magazine design attempted to combine gentle yet secure gripping of the fibers with manufacturability. The stereolithography process was again utilized because of the resin material's soft and mild interface with fibers, as compared to aluminum and stainless steel. The capability of the stereolithography machine to produce very accurate large scale features was exploited for the design. To overcome the problem of unmanufacturable feature sizes encountered with previous designs, a design with multiple interlocking parts was created as shown in Figure 5-12.

The notches in the third iteration design were formed by creating larger notches which, when interdigitated, would create precisely the amount of space necessary to hold a variety of fibers with diameters between 40 μm and 250 μm.

The design was the first to effectively hold the fibers in place and allow the fibers to be removed by the instrument without damage. The design did not solve the issues of capacity or robustness of form factor. Also, the design was found to be difficult to load by hand because the fibers were stored so closely together.

Fiber Storage Method Design - Iteration 4

The next generation fiber storage method sought to maintain the effective fiber holding strategies developed during the early design iterations, and attempted to improve the capacity, robustness, and ease of loading of the magazine as well. A semi-circular design, shown in Figure 5-13, was created to permit more fibers to be loaded without requiring a significant increase in space. The new design also resulted in a much more robust magazine by permitting structural cross-bracing throughout.

The new design required a significant modification of the original loading strategy. Rather than loading the fibers into the grippers by moving a linear magazine cartridge in one dimension, a two-degree-of-freedom (DOF) strategy would be required. One

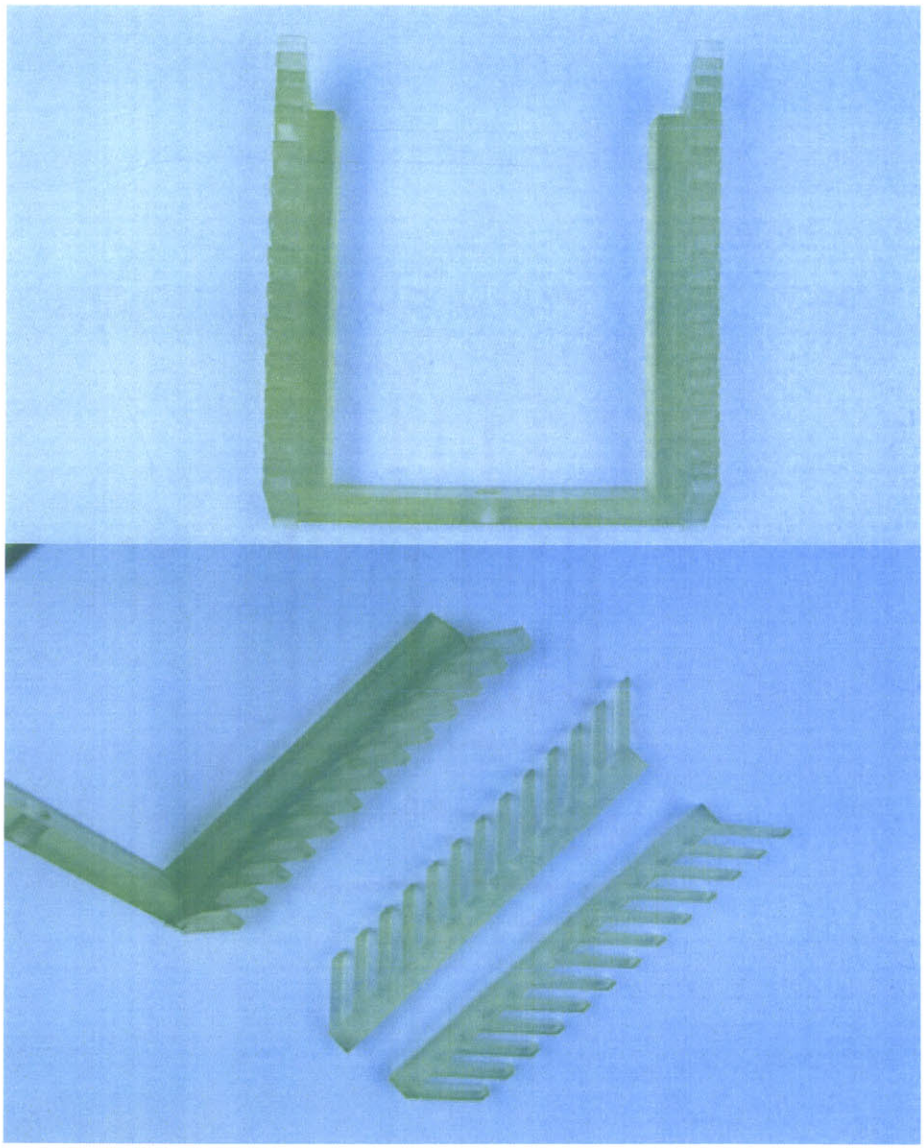

Figure 5-12: Images of SLA-manufactured interdigitated magazine. Shown assembled, with fibers in place (*top*), and disassembled (*bottom*).

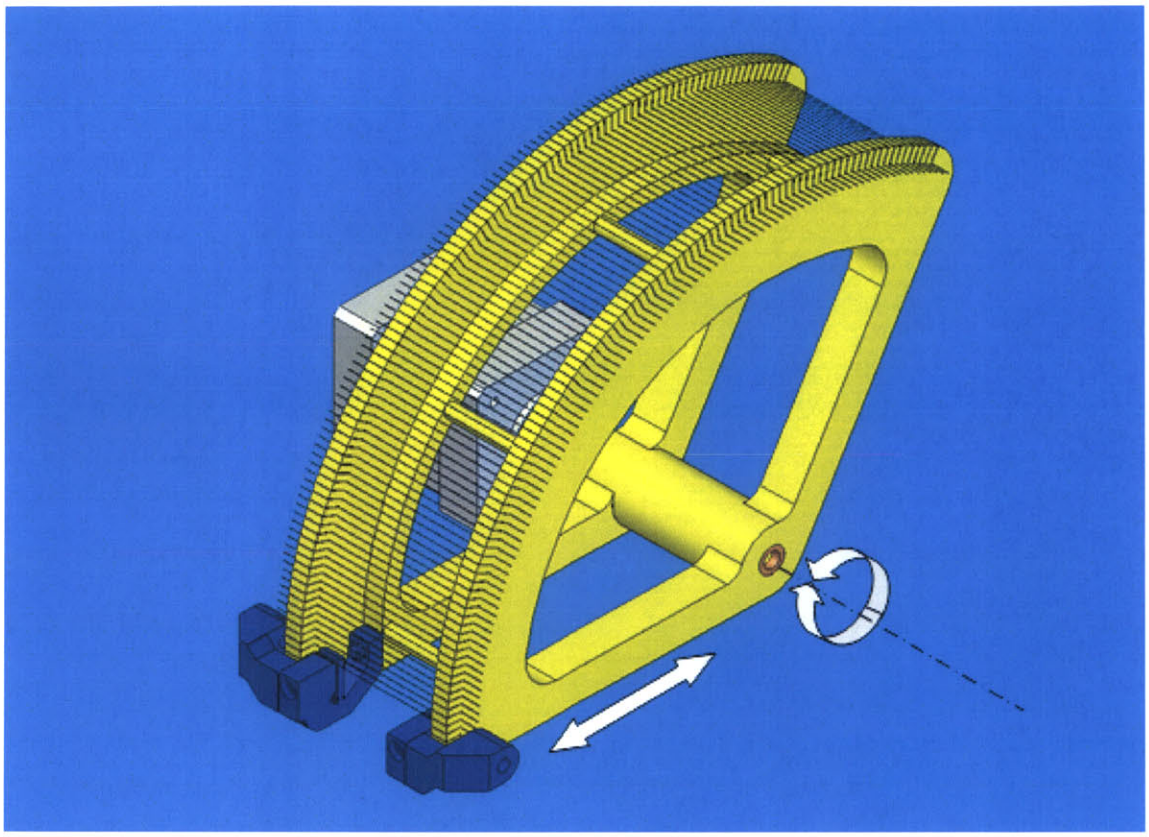

Figure 5-13: Rendering of fourth iteration magazine and loading mechanism. Directions of motion are shown by arrows.

DOF would provide rotational motion for indexing the specific fiber under test into position in the grippers, and another DOF would provide linear motion for placing and removing the fiber radially. The specific loading scheme is illustrated in detail in Section 5.1.3 which describes the final implemented magazine design.

The prototype was built using the stereolithography machine because it had not been optimized for manufacturing. In general, the prototype was a great improvement over the earlier designs. Although an extra DOF would be required for automated fiber loading, the magazine was easier to load by hand than the previous versions. Also, the more robust magazine structure was found to prevent warpage that could otherwise induce slack in the fibers, making them difficult for the instrument to load automatically.

The fourth iteration design did not offer any great improvement for a problem that had plagued the previous designs, namely holding the fibers in place. The new design utilized interlocking parts to create notches which could hold the fibers, the same strategy devised for the third iteration magazine. This method was not entirely effective and left substantial room for improvement.

Fiber Storage Method Design - Iteration 5

As the magazine underwent its fifth generation design, it approached a fully functional unit. The persistent problem of how to hold a large variety of fibers in the storage system was finally solved by this design. It was discovered that natural rubber is an ideal material for holding fibers [42]. When natural rubber is sliced with a sharp razor blade, a very fine notch is formed which is perfectly suited to gently securing a fine object such as the types of fibers the instrument will be testing. Natural rubber is soft enough to conform to a small fiber without causing mechanical damage or leaving a residue, is non-reactive with most materials, and is inexpensive. Figure 5-14 shows the fifth iteration of the magazine design with razor-sliced rubber grommets integrated around the radius for holding fibers in place.

The new design was further optimized for manufacture by transforming the solid structure into several parts. The side sections of the magazine were designed to

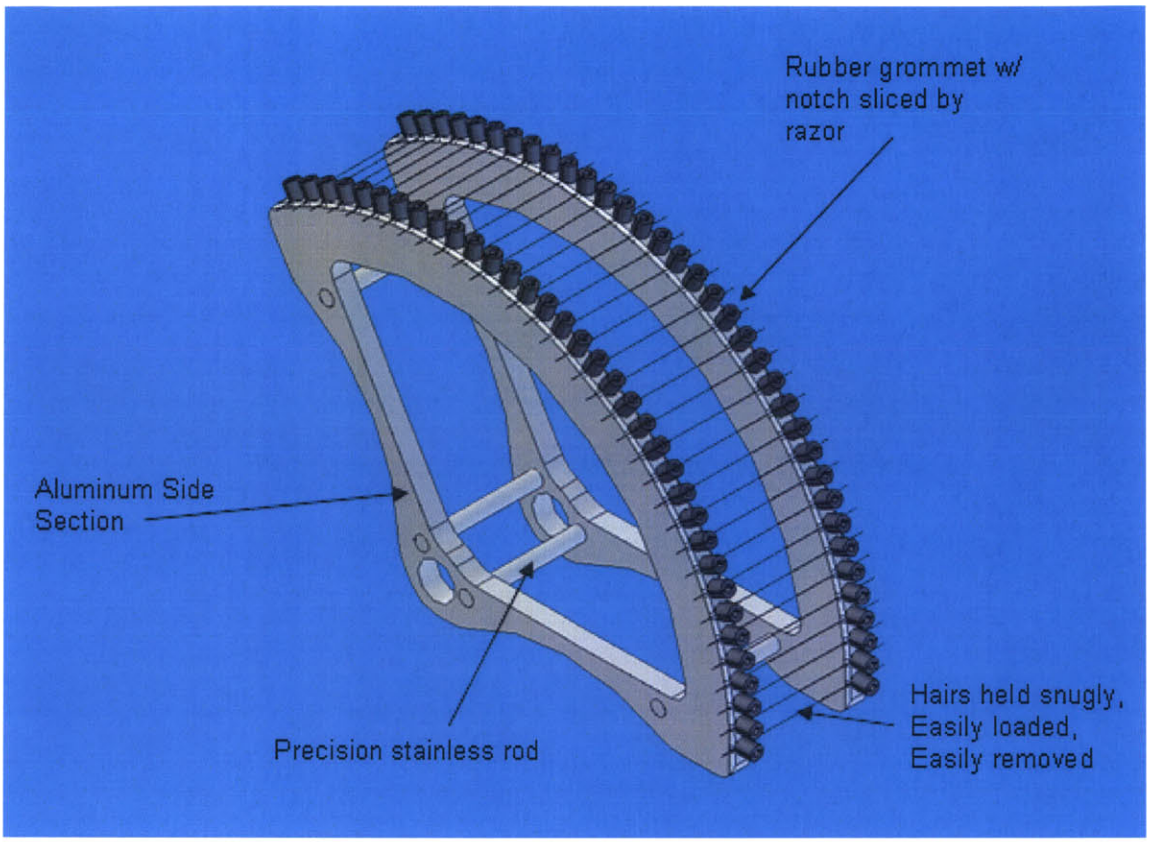

Figure 5-14: Rendering of fifth iteration magazine design. Novel features are indicated by arrows.

be essentially 2-dimensional so that they could be easily machined out of a robust material such as aluminum. Holes could then be drilled around the radius of each side section using computer-aided machine tools. Afterwards, the side sections could be joined by precision rods, and the rubber grommets could be fixed in place with epoxy and either sliced by computer-aided machining or by hand.

Because this design still needed revision, the above machining steps were not actually performed, and a prototype was instead created from epoxy resin using the 3D Systems Viper. The prototype was far more functional than all of its predecessors. Two problems persisted: capacity and the issue of how the magazine would be loaded into the instrument after it had been prepared with fibers for testing by a technician. The capacity of the magazine was merely 35 fibers. Ideally, the automated system should test more fibers. The semi-circular (120°) shape had not been chosen arbitrarily, but was in fact based upon geometric factors within the construction of the rest of the instrument at the time of development. The geometric design of the total instrument had to be modified to accommodate more fibers which meant increasing the outer radius of the magazine or increasing the sweep of the semi-circle to be greater than 120°.

For loading the magazine into the instrument after all of the fibers had been loaded into it, the mechanism had to be simple and repeatable.

Fiber Storage Method Design - Iteration 6

A separate subsystem was designed for the sixth generation magazine specifically to handle the task of securing the magazine to the instrument loading system. The magazine would have to be mounted on a rotational actuator to index the fibers into position for loading, so a spindle was designed for mounting to such an actuator and for coupling very repeatably to the magazine.

The magazine mounting mechanism was based on the principle of kinematic constraint. An object, for instance the magazine, in free space can translate in three dimensions (X, Y, Z) and can rotate in three directions (pitch, yaw, roll) [38]. In order to prevent the magazine from moving once mounted and to ensure that it would

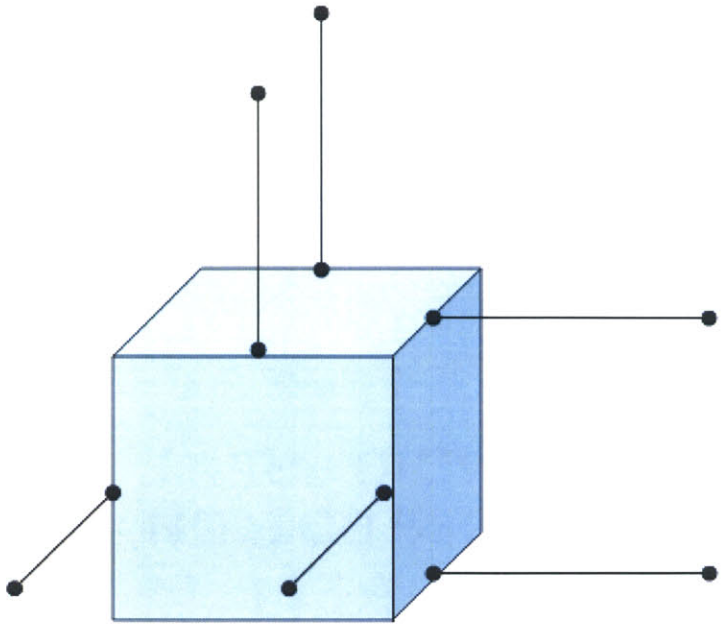

Figure 5-15: Schematic diagram of requirements for 6-DOF constraint of motion. Adapted from *Precision Machine Design*, Slocum, 1992.

set in an identical position each time it was loaded, each of the magazine's 6-DOF would have to be constrained. The constraint of each degree of freedom would be accomplished by a point contact between a hard sphere (4 mm ball bearing) and a hard, flat surface [38]. Figure 5-15 shows a schematic of the requirements for constraint of all 6-DOF.

A mechanism was designed to achieve full 6-DOF kinematic constraint while still allowing easy removal of the magazine from the spindle. A spring-torsioned ergonomic lever with a ball bearing affixed was mounted to the magazine to constrain 2-DOF, and two additional ball bearings were mounted to the magazine side sections, one on each side, to constrain the other 4-DOF. The design is shown in Figure 5-16.

For the sixth iteration magazine, the kinematic mounting mechanism was integrated with the previous magazine design. The prior design was modified further in the new version to include an increased capacity of 100 fibers. The greatly improved

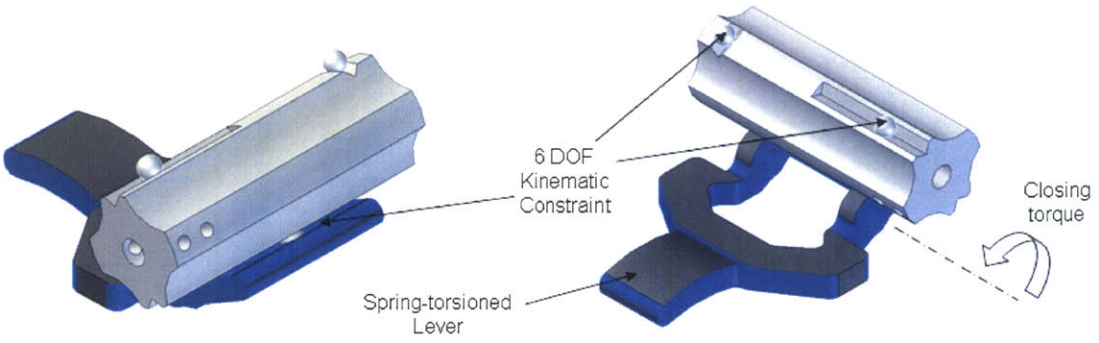

Figure 5-16: Kinematic magazine mounting unit. Novel features are indicated by arrows.

capacity was achieved by augmenting the magazine radius and increasing the sweep of the side sections to 240° from 120°. The penultimate fiber storage magazine design is shown in Figure 5-17.

This iteration of the magazine was never fully prototyped because it was realized that because of the asymmetry and large size of the magazine compared to the previous designs, the offset center of mass might strain the rotational actuator too much as it indexed the fibers for loading.

Implemented Fiber Storage Method

The final magazine design, shown in Figure 5-18, maintained all of the functionality of the previous design, and introduced a few critical improvements to make it fully and optimally functional. The center of mass was moved to the center of the magazine by redesigning the magazine to be a complete circle. This modification required some adjustment of the overall configuration of the instrument, but reduced the power requirements for the rotational indexing actuator significantly. Also, because a full circle was used, the spacing of the 100 fibers in the magazine capacity could be increased to allow for easier loading of the fibers by hand.

The implemented version of the final magazine, shown in Figure 5-19, was manufactured primarily from acrylic. A Trotec, Inc. laser engraver/cutter was used to cut

Figure 5-17: Magazine design - sixth iteration.

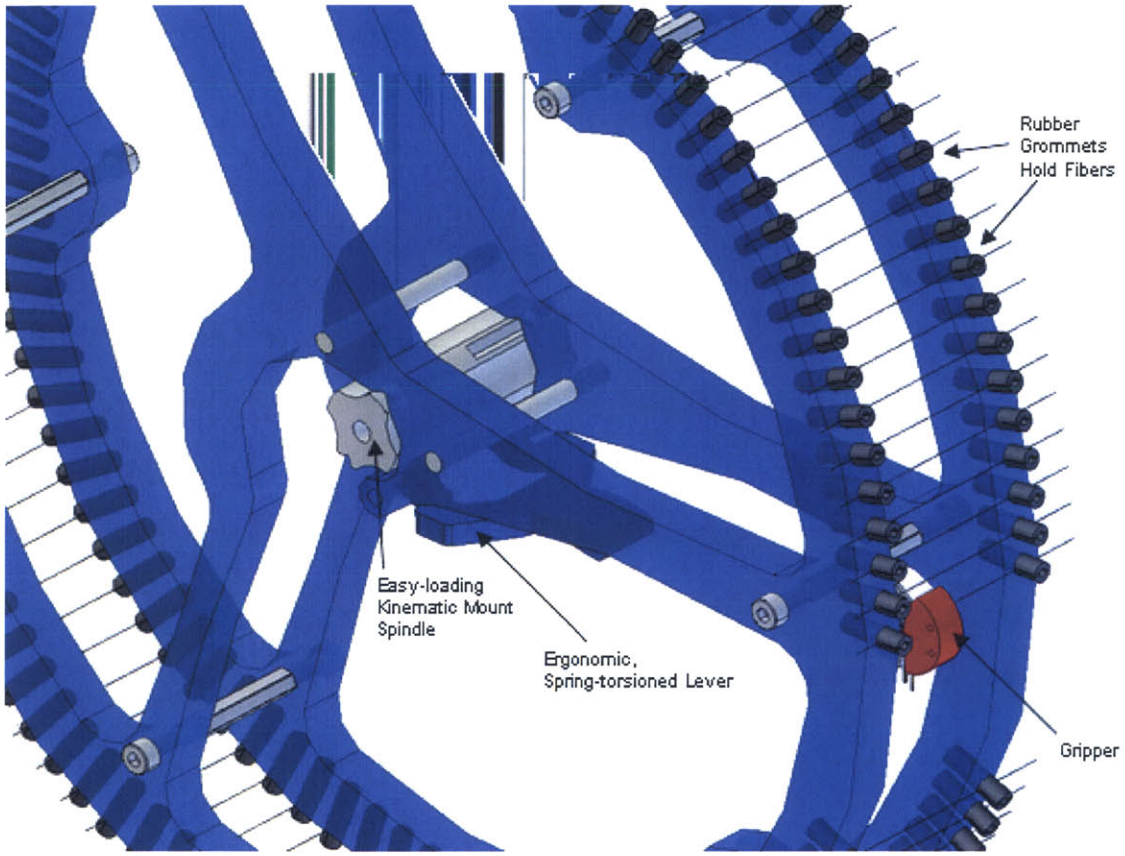

Figure 5-18: Rendering of the final magazine design.

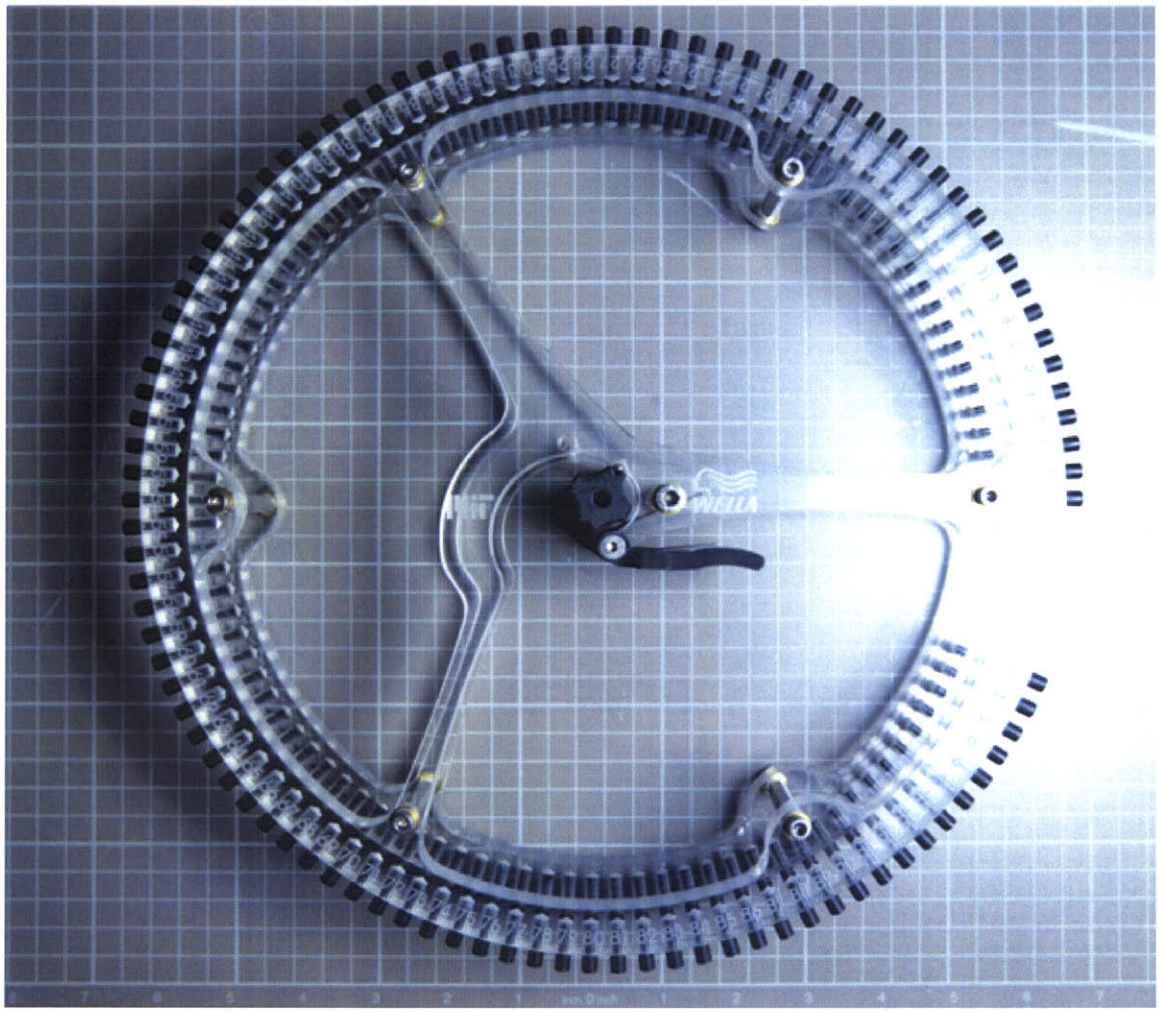

Figure 5-19: Image of the functional final magazine.

the side sections from large sheets of 10 mm thick acrylic. The Trotec laser cutting machine may be used to engrave or cut many different types of materials, such as plastics, rubbers, and woods, but generally not metals or stone [43].

The use of acrylic reduced the weight of the magazine by nearly half of what it would have been had it been constructed from aluminum. Also, the laser engraving feature of the Trotec permitted the number corresponding to each fiber position to be engraged on the face of the magazine to make the loading procedure more convenient.

The holes around the perimeter of the magazine were drilled using a MAZAK CNC mill-lathe turning center. The spring torsioned lever and the spindle for the kinematic mounting mechanism were manufactured using the 3D Systems Viper SLA. The parts

were substantial enough that the cured epoxy resin was a suitably strong material for each part. In the future, those parts may be injection molded.

Rubber grommets were used around the perimeter of the magazine for holding fibers in place before testing and were epoxied into the drilled holes of the magazine side sections. A special fixture was designed for the MAZAK, and a modified program was written to slice a notch into each grommet with a razor blade.

The side sections of the magazine were joined using hexagonal spacers to allow a user to adjust the width of the magazine to correspond to personal needs, for instance to test a longer or shorter fiber. The default fiber sample length for the instrument is 10 mm.

5.1.4 In-test Fiber Handling Design

Once the fibers are loaded into a suitable mechanism for pre-test storage, the instrument would be responsible for carrying out all fiber transport and testing in a completely autonomous way. The in-test fiber handling system design is the subject of this section.

Design Requirements

The in-test fiber handling system is a broad subsystem and would be responsible for several different functions within the instrument. The system is responsible for providing the motion to load fibers into the testing region, the motion for manipulating fibers during test, and the motion for moving the fibers to a suitable location for removal after testing.

First, an estimate was made for the minimum degrees of freedom required by the in-fiber testing system. This estimation was based upon the automation considerations described in Chapter 4. Four axes of motion would be required to provide the necessary testing motions for the instrument. Two of these axes would be linear translating axes mounted in parallel. The other two axes would be rotational translating axes mounted on axis with one another. Each rotational axis would be mounted to

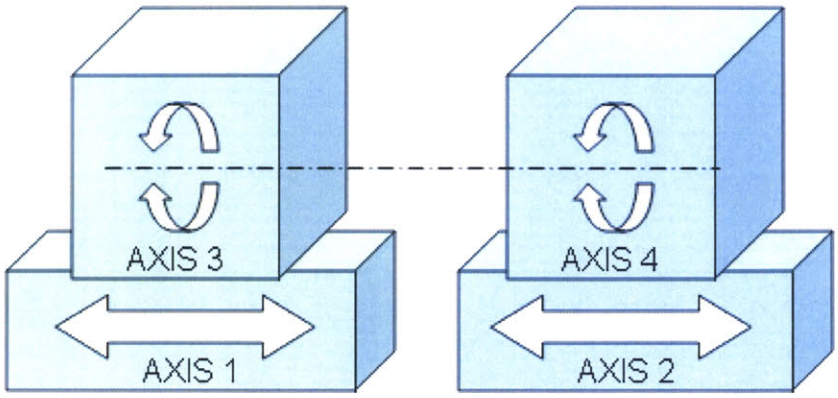

Figure 5-20: Schematic of the test stage configuration for the instrument. Dotted line indicates fiber testing axis.

one of the linear axes. Figure 5-20 shows a basic schematic of the configuration of the testing axes. The axial motions are represented by arrows in the diagram.

The specifications for these axes would be determined next. The amount of travel for the linear axes was a major consideration, and at the time the motion system was being designed, the specifications for the length of fibers to be tested had not been finalized. It was suggested that the instrument should be capable of measuring fibers up to 100 mm in length; therefore, the linear actuators would have to provide a minimum of 100 mm of motion each. Furthermore, since the instrument would be performing tensile tests on fibers such as hair which may elongate by as much as 100% when wet, the combined travel of the two axes would have to be greater than approximately 200 mm. The linear axes of the instrument were designed with a combined travel of 300 mm to accommodate any later changes of specification.

The rotational axes each have to provide a full 360° of continuous rotary motion. These axes would also have to be very accurate, repeatable, and relatively fast. Finally, the rotational axes must mount securely to the linear motion axes and must

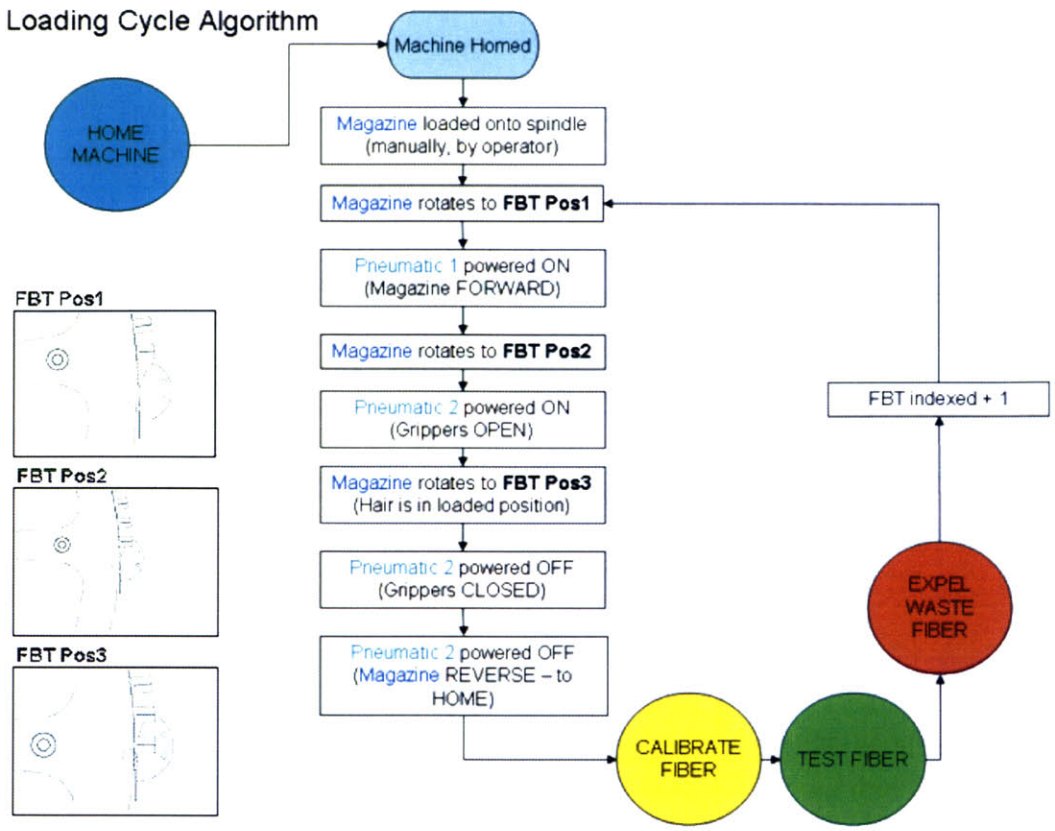

Figure 5-21: Flow chart for the loading of fibers into the instrument during the fiber testing cycle.

support mounting of testing components.

The in-test fiber handling system would also be responsible for providing the motion for automatically loading fibers from the fiber storage system into the grippers. The loading method, introduced in Section 5.1.3, would require two motion axes, one linear and one rotational, for manipulating the loading motion of the magazine and one linear motion axis for opening the grippers. Figure 5-21 shows the exact protocol for fiber loading.

Linear Motion Components

Several options were considered for providing linear motion. Linear electric motors and voice coil actuators were an attractive option because of their high speed and high operational bandwidth. However, the actuators were not deemed acceptable because

the types of units that could provide a sufficient amount of travel would not be accurate enough for the application. Inherent off-axis play is present in certain linear electric positioners such as voice coil actuators and serves to prevent stiction and to permit smooth motion. These off-axis deflections would result in fiber positioning errors. If used in combination with linear bearings to eliminate such error sources, these types of positioners would have been an acceptable option; yet, this design choice would have contributed unnecessary complexity to the machine. Additionally, these types of linear actuators would have required complex control strategies to manipulate them in the required sub-micron motion resolution range.

Another potential option was to use linear pneumatic actuators for the linear testing motions. These types of units could provide the high speed and bandwidth of linear electric actuators, as well as sufficient travel with very low off-axis deflection error. However, these actuators would also be difficult to control precisely in the sub-micron motion resolution range.

Stepper motor driven linear ballscrew stages were ultimately selected as the linear motion source for the testing region of the instrument. Parker-Hannifin manufactures linear stages which are capable of producing linear motion with a resolution of less than 0.1 μm and bi-directional repeatability of 1.3 μm over the entire length of travel for travels ranging from 50 mm to 2 m [44].

The Parker 404XR 150 mm travel linear stage was selected for the instrument to provide a combined 300 mm of travel between the two parallel mounted stages. The 404XR is a sleek and compact linear positioning stage (47.3 mm $\times$ 95 mm). The stage is capable of carrying relatively high loads over the distance of its travel, and its high strength extruded aluminum housing, square rail ball bearing system, and precision ground ballscrew drive result in a quick and accurate positioning capability [44]. Additionally, the low profile design of the stage makes it ideal for space restricted applications, such as the single fiber testing instrument. The stage is shown in Figure 5-22.

Compumotor Zeta57-83-MO stepper motors were selected to drive the Parker linear stages. These motors are directly compatible with the linear stages, are relatively

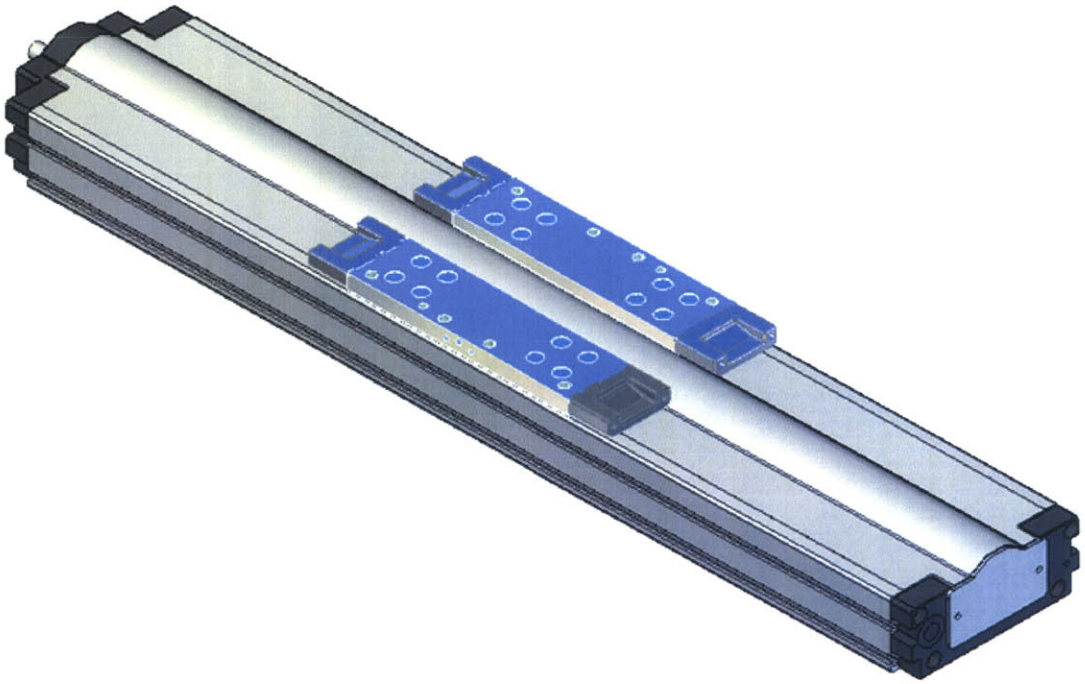

Figure 5-22: Parker 404XR linear stage. (Taken from http://www.parker.com, Parker)

inexpensive, and are capable of microstepping with 50,800 steps per revolution, which translates into less than 0.2 μm positioning resolution on the linear stages.

Rotational Motion Components

The rotational motion for the testing region of the instrument was provided by Parker 200RT Series (Model 20501) precision rotary tables with a 160:1 gear reduction. These stages are among the most precise rotational positioning systems on the market with highly repeatable indexing (12 arc sec) through 360° continuous travel made possible by a worm gear drive and dual race angular contact support bearings [45]. The tables are designed specifically to function with Parker linear stages for use in precision automation applications. The rotary stages feature a low profile design which minimizes the stack height and enables them to fit in many places where other motorized rotary devices cannot. Figure 5-23 shows the Parker 20501 rotary stage. The 20501 stages are also compatible with the Compumotor Zeta57-83-MO stepper motors which would be used to drive the linear motion of the instrument. The use of the same style motors to provide rotational motion would eliminate the complexity that might be associated with using a different type of motor to drive these axes.

Fiber Loading Motion Components

The fiber loading motion components would require the same precise repeatability as the testing axes, yet with comparably insignificant motion complexity. Two of the fiber loading motions, opening the gripper and advancing the magazine for fiber loading, would be binary state operations. Essentially, the positions of these axes would be in one of two states, forward or reverse. Pneumatic linear actuators therefore emerged as an ideal solution for providing fast, highly accurate, dual-state motion.

Festo linear pneumatic actuators were selected to perform the gripper-opening and magazine-advancing operations. Festo pneumatic actuators may be operated in the binary state configuration required for these motions and are easy to control and tune for custom applications. The actuators are highly accurate, repeatable, and inexpensive. For the gripper opening function, the Festo DFM-12-20-P-A-KF

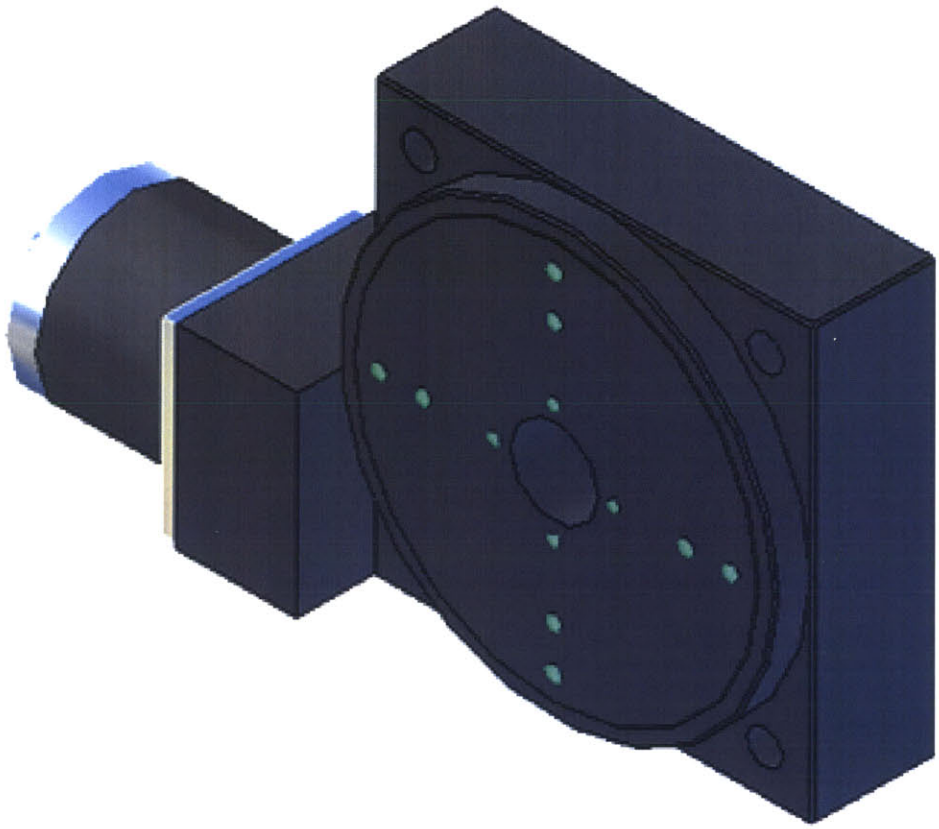

Figure 5-23: Parker 20501 rotary stage. (Taken from http://www.parker.com, Parker)

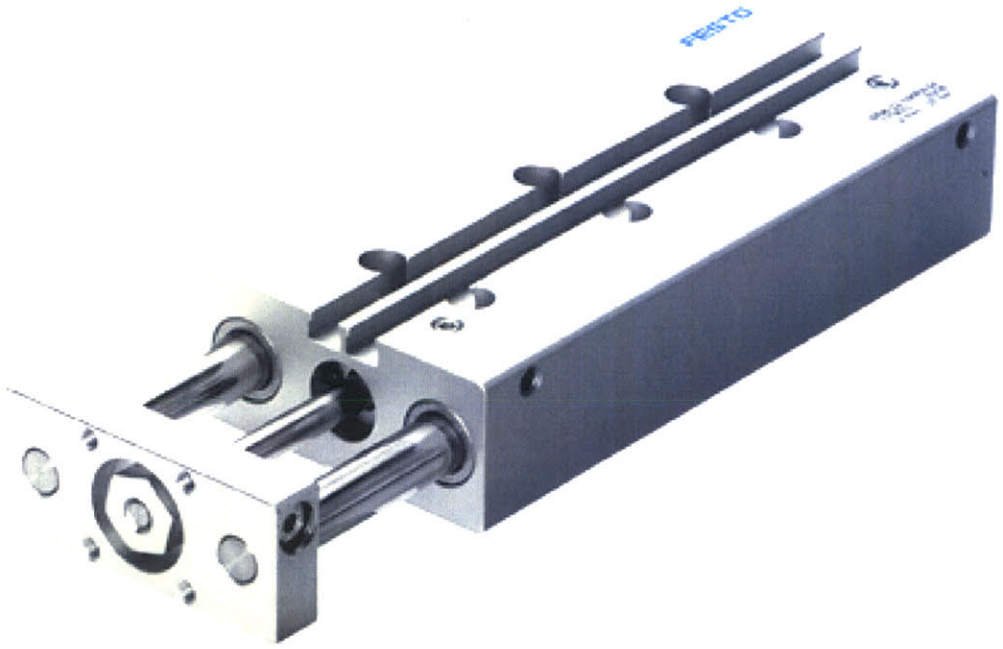

Figure 5-24: Festo 80 mm linear pneumatic actuator. (Taken from http://www.festo.com, Festo)

linear pneumatic actuator was chosen. The unit provides 20 mm of linear travel, sufficient for opening the grippers and then receding from the testing region. An 80 mm-stroke version of the same linear pneumatic actuator, the Festo DFM-12-80-P-A-KF, was chosen for advancing the magazine during loading. Both units minimize the space requirement for their respective travels in comparison with equivalent actuation systems. Also, the positioners are equipped with recirculating ball bearing guides to provide rigid, precise motion with low deflection under torque loads [46]. Figure 5-24 shows a picture of the 80 mm actuator.

The linear pneumatic actuators would be controlled by Festo CPE10-M1BH 5/2 pneumatic solenoid valves. These highly compact air valves are electrically-actuated, provide high flow rates, and offer low power consumption [47].

Aromat AQV212 PhotoMOS opto-electronic relays were used to control the electrical operation of the Festo control valves remotely from a computer generated digital

signal source. The relays are inexpensive and ideal for controlling solenoid loads [48].

The rotational indexing motion of the magazine would be provided by a Parker VS13B-DFR10 stepper motor. The stepper motor allowed for precise indexing of the magazine position for fiber loading. The motor also improved the simplicity of the design by providing sufficient torque to allow for attachment of the magazine directly to the motor shaft via the quick mount loading spindle described in Section 5.1.3. Also, the motor drive control of the magazine indexing axis would be similar to the control of other motion axes of the instrument, translating into simpler overall control of the instrument.

Motion Control

Motion control for the in-test fiber loading system would be provided via software. The interface between the stepper motors and software was achieved by a system comprised of National Instruments motion control cards, National Instruments universal machine interface boards, and Parker stepper motor drivers. Figure 5-25 shows a schematic representation of the instrument motion control system.

The National Instruments PCI-7344 motion controller card was chosen to provide high accuracy stepper motor control for the linear and rotational testing stages and the rotational indexing of the magazine. The PCI7344 card is a 4-axis controller, with each axis configurable for stepper or DC servo motor control, and features a 62 μs PID loop update rate. It may handle quadrature encoder or analog feedback [49]. A personal computer may be used to control the card via the provided National Instruments drivers. Five axes of stepper motor control would be required by the instrument; therefore, two PCI-7344 motion control cards were implemented. The three unused axes could be later used for expanding the functionality of the instrument.

The National Instruments UMI-7764 universal machine interface block was selected to provide connectivity between the PCI-744 cards and the Parker stepper motor power drives. The UMI-7764 interface provides a wiring and connection point for motion control and feedback signals via a single multi-axis input output (I/O) cable from the motion controller to the UMI. The interface block simplifies the inte-

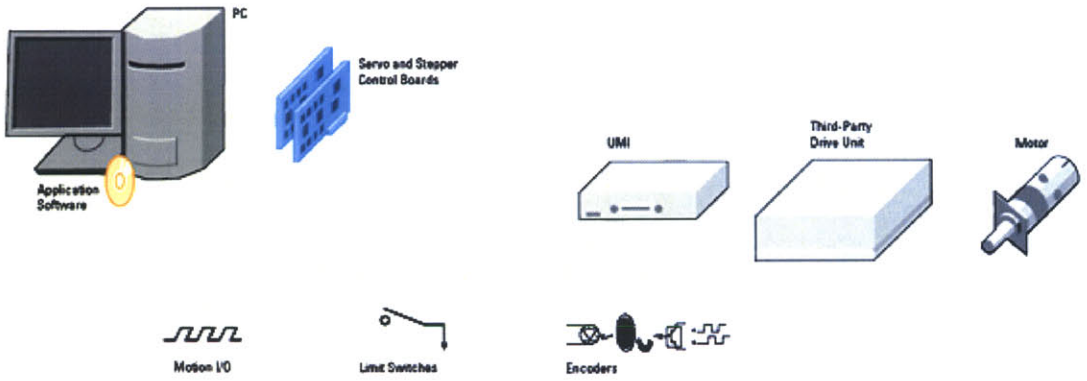

Figure 5-25: Schematic diagram of motion control configuration. (Diagram: National Instruments)

gration of third-party drivers, amplifiers, encoders, limits, and I/O with NI controllers by dividing these signals into per-axis and function-specific connections. Each UMI works with up to 20 MHz quadrature encoder rates, and incorporates a host PC power monitor that inhibits the motion driver if the host PC loses power during motion control. The UMI monitors the +5 VDC from the PC and activates the inhibit signals if the voltage falls out of tolerance [50].

Power would be provided to each stepper motor by a Parker E-AC microstepping drive. These drives are optimized to function with the Zeta57-series and VS13-series stepper motors utilized by the instrument. The drives feature a 3-state current control which allows each motor-drive pair to run cooler and more efficiently than comparable 2-state drive systems. The resolution of the drives may be selected up to 50,800 steps/revolution, and the drives provide between 0.02 A to 3.5 A (peak) to the motors based upon a 95 - 132 VAC power supply input. Additionally, the drives feature an automatic standby function which reduces motor current and heating at rest [51].

5.1.5 Post-test Fiber Disposal Design

After each test, all remnants of the tested fiber must be removed so that a new fiber might be loaded into the testing region of the instrument. The post-test fiber disposal system would be the final automated module designed for the automated single fiber testing instrument and is described in the following section.

Design Requirements

The post-test fiber handling system would be responsible for several different functions. Foremost, the system would be required to remove a tested fiber from the grippers following a round of testing regardless of the condition of the fiber. Additionally, the system would be expected to transport each tested fiber away from the testing region without the potential for a build-up of tested fibers which might obstruct the removal of subsequent fibers. Finally, the system would be responsible for storing an adequate capacity of waste fibers in an accessible container to provide easy access for technicians to ultimately discard the tested samples.

Fiber Disposal System Components

Vacuum was the first and most logical solution attempted for removing waste fibers from the testing zone. A Festo VADM-45 vacuum generator with a built-in solenoid control unit was tested first but was found to have inadequate volume flow rate to dislodge the fiber from the grippers and remove it [52]. It was found through trial-and-error testing that volume flow rate was the most critical factor for dislodging and transporting a fiber and that most compact commercial vacuum generators do not provide high volume air flow because they are optimized for generating vacuum.

A new component which provided an enormous increase in volume air flow rate was tested. The Anver TT05 transfer tube, a so-called transfer tube designed specifically for vacuum-based material transport applications and shown in Figure 5-26, is a device capable of providing 850 L/min volume air flow rates as compared to the 12 L/min volume flow rate associated with the Festo VADM-45 vacuum generator for

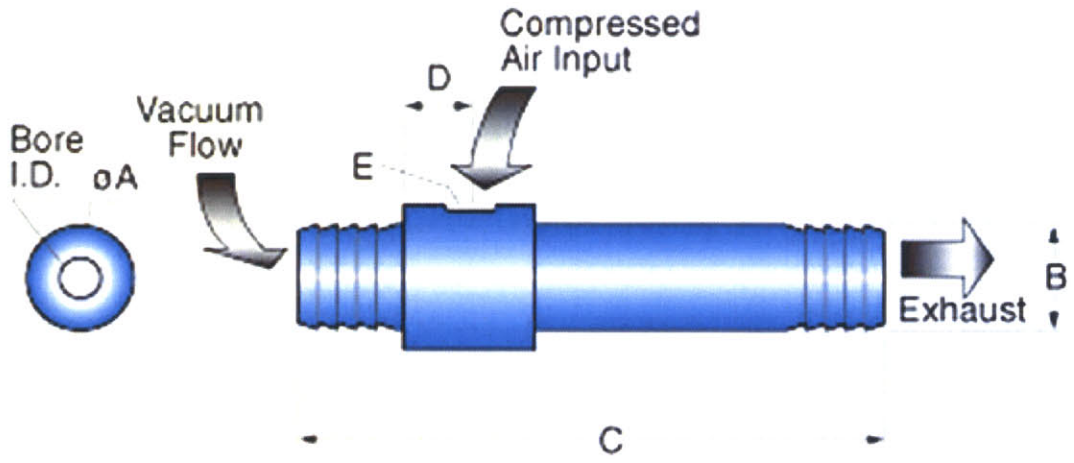

Figure 5-26: Schematic diagram of Anver TT05 vacuum transfer tube. (Diagram: Anver)

a supply line pressure of 0.689 MPa [53, 52]. Tests with the TT05 showed that, in most instances, the transfer tube could indeed remove a loose fiber from the grippers when placed in close proximity to the testing region.

It was found that some fibers would persist in the grippers and could not be easily removed by the vacuum flow generated via the transfer tube. An air blower was incorporated into the design of the fiber removal system which served to dislodge stubborn fibers from the grippers so that the vacuum system could eradicate them.

The fiber removal system would be operated by supplying the transfer tube and blower with an input of compressed air and would be controlled by the same variety of Festo control valve used for controlling the gripper-opening and magazine-advancing functions. The high flow volume Festo model CPE14-M1BH was used for this application.

Removed fibers would be transported by a 25 mm diameter rubberized vacuum hose into a fiber storage chamber. The chamber was comprised of a PVC tube with PVC end caps. One of the end caps was fixed in place by epoxy and served as the inlet port for the vacuum transport hose, and the opposite end cap could be screwed

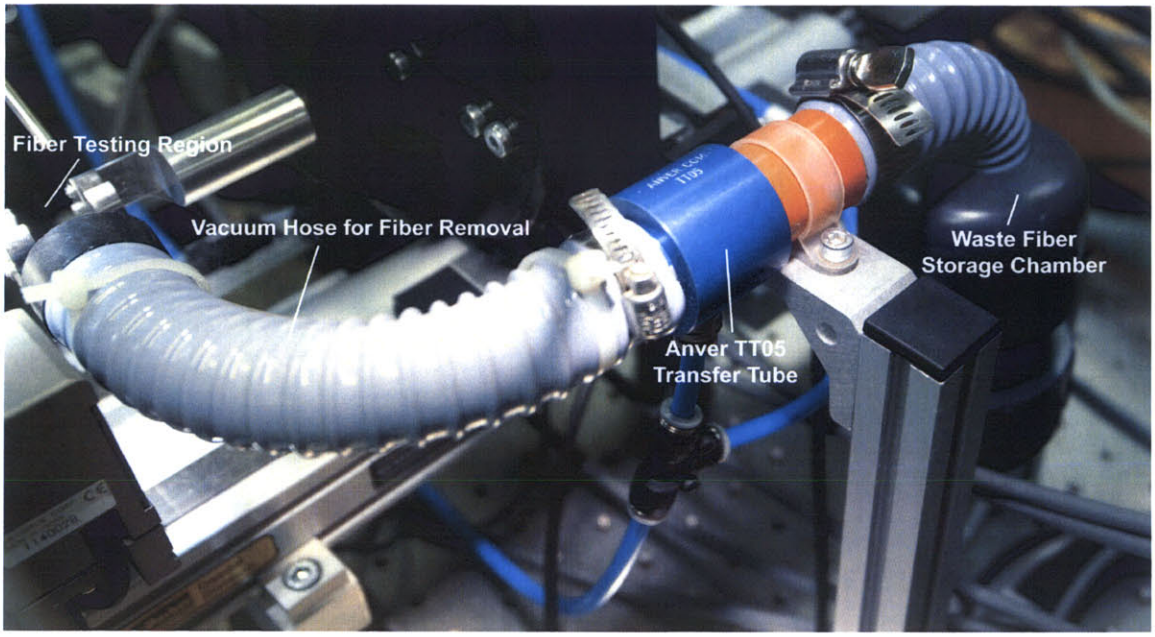

Figure 5-27: Image of complete waste fiber removal system with main components indicated.

on and off to allow for the removal of waste fibers. The removable end cap was also drilled with an array of holes to allow exhaust air to flow out and fitted with a foam filter to capture the waste fibers.

Chapter 6

Measurement System Design

Chapter 6 discusses the design and implementation of components related to the measurement modules of the machine. The measurement system of the single fiber testing instrument integrates many elements to provide simplified yet effective functionality. This chapter shall describe the early prototypical designs as well as the final designs for each measurement subsystem where applicable. Certain measurement modules have not been completely designed and implemented due to time considerations.

The data acquisition system is discussed first. Next, the position sensors are introduced. Afterwards, the design of the measurement systems for determining single fiber geometric properties, tensile properties, bending properties, surface roughness properties, friction properties, and torsion properties are presented respectively.

6.1 Data Acquisition System

The automated single fiber testing instrument would be responsible for measuring many low-level signals with great precision and low noise. The instrument would also require digital control of many signals to facilitate much of its automated operation. Both of these functionalities would be required to interface simply with custom software to create a seamless final operation of the instrument. In order to satisfy these diverse system demands, a multifunctional data acquisition (DAQ) system was selected, the National Instruments PCI-6052E. The National Instruments PCI-6052E

is a 16-bit multifunction DAQ device with analog and digital input/output (I/O) capability. For analog signal input, the PCI-6052E features a 333 kS/s maximum sampling rate, ±0.05 V to ±10 V input voltage range, and 16 single-ended analog input channels that may be configured as 8 differential analog inputs. The PCI-6052E provides 2 analog output channels, each with 16 bit resolution, a maximum 333 kS/s output rate, and ±10 V output range. Digital I/O on the PCI-6052E is provided by 8 channels which each may be configured as an input or output. Finally the device features two 24-bit counters for signal timing as well as analog and digital triggering [54].

All analog and digital connections would be easily interfaced between the instrument and the PCI-6052E DAQ via a National Instruments SCB-68 I/O connector block. The SCB-68 is a shielded connector block with 68 screw terminals for easy I/O connections. The connector block also features two general-purpose breadboard areas which allow for the addition of custom circuit components for signal conditioning [55]. The National Instruments DAQ components would be controlled directly from the custom software application using the included NI-DAQmx drivers.

6.2 Position Sensors

All of the measurements performed by the single fiber testing instrument would require precise knowledge of fiber position and orientation. Additionally, the consistent automated functionality of the instrument would be dependent on position feedback. This section describes the position encoders selected to measure linear and rotational positions for the instrument.

6.2.1 Linear Position Sensors

Renishaw RGH24Y optical encoders were selected to measure the axial position of the linear motion stages in the instrument. The RGH24Y encoders measure position via a non-contact open optical system based on readhead and a self-adhesive glass scale which mounts directly to the linear stages. The encoders feature 0.1 μm res-

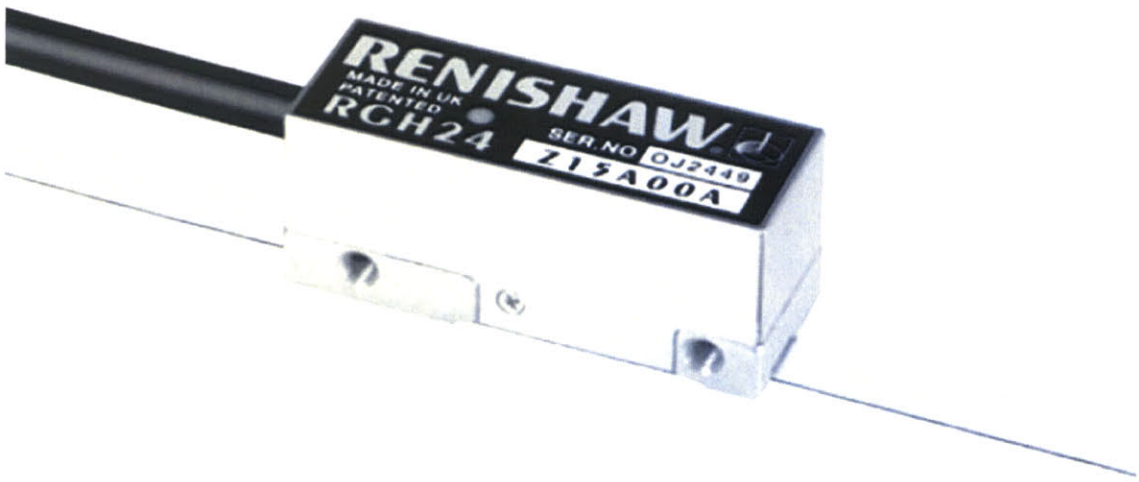

Figure 6-1: Renishaw RGH24 optical linear position encoder readhead and glass scale. (Taken from http://www.renishaw.com, Renishaw)

olution, integral interpolation, digital and analog output configuration options, and high tolerance to scale contamination [56].

6.2.2 Rotational Position Sensors

Renishaw RM36I 12-bit non-contact rotary magnetic encoders were selected to measure the angular position of the rotational motion stages in the instrument. An RM36I was also mounted to the stepper motor which controlled the indexing position of the magazine during automated fiber loading.

The RM36I encoders measure incremental angular position via a non-contact, frictionless magnetic system based on a "magnetic actuator" which mounts to the moving shaft and a separate, stationary encoder body. The encoders feature 4096 counts/revolution which translates into $\pm 0.3°$ rotational positioning accuracy [57]. When used in tandem with the Parker rotational stages with their 160:1 reduction ratio, the rotational positioning accuracy improves to $\pm 0.00188°$.

Figure 6-2: Renishaw RM36 magnetic rotary position encoder readhead and "magnetic actuator." (Taken from http://www.renishaw.com, Renishaw)

6.3 Geometric Property Measurement Design

The design of the measurement subsystem for determining the cross-sectional geometry of single fibers is discussed in this section. The cross-sectional geometry must be known in order to determine many other mechanical properties of a fiber. An effective geometry measurement system is therefore of great importance to the success of the instrument.

6.3.1 Diameter Measurement System Principles

The instrument would determine the cross-sectional geometry of single fibers by measuring the diameter of the fibers. A diameter measurement system based on mechanical contact was considered first, because it might allow researchers to examine features of a fiber cross-sectional geometry such as cavities and voids that could not be detected by most other methods [22]. The contact-based design was deemed too complicated, however. Contact with the fiber might affect the diameter measurement by distorting the fiber under test in a non-quantifiable fashion and more importantly, a contact measurement would be quite difficult to implement.

A non-contact geometry measurement design was selected as the preferred method. The benefits of a non-contact measurement included the ability to perform measurements quickly and without damage to the fiber. Also, the non-contact method would allow a continuous scan of the dimensions of a fiber which could later be digitally reconstructed into a 3-dimensional model of the fiber.

6.3.2 Geometry Measurement Components

The non-contact measurement system would be based on optical examination the fiber. A number of devices were considered for performing the non-contact geometry measurements on hair fibers. Concepts were considered for creating a proprietary technique for performing the optical diameter measurements, but ultimately, two commercial devices designed specifically for measuring the diameter of fine fibers with great accuracy were evaluated.

Mitutoyo LSM500 Ultra-fine Laser Scan Micrometer

Mitutoyo is a leading manufacturer of metrology devices and offers an excellent system for the non-contact measurement of fine objects such as single fibers. The LSM500 Ultra-fine Laser Scan Micrometer measures the diameter of objects between 50 μm and 2 mm with a measurement accuracy of ± 0.3 μm and repeatability of ± 0.04 μm. The design operates by scanning a laser beam at high speed across the object of interest in a measurement region and onto a photoelectric receiver element [58].

An FDA Class II/IEC Class 2 semiconductor laser beam (maximum power: 1.3 mW) is emitted from a diode oscillator and directed at a 16-sided polygon mirror which rotates at high speed. The direction of the beam reflected by the mirror is changed via a collimator lens and aimed straight at the fiber under test. As the polygon mirror rotates, the horizontal laser beam travels downward and, if it is not obstructed by the fiber, reaches the receiver. The output voltage of the photoelectric receiver element varies proportionally with the amount of light which reaches the photoelectric cell. The dimension of the fiber is represented by the period required to count the pulses generated during the beam obstruction by the fiber [58]. Figure 6-3 shows a schematic of the principle of measurement. 1 The Mitutoyo LSM-500 may be controlled from a custom software application by the LSM-6000 display unit via RS-232c serial communication at an experimentally-determined measurement rate between approximately 25 ms and 100 ms.

Keyence LS-7010M CCD Micrometer

Keyence is an alternative manufacturer of world-class metrology devices. The Keyence LS-7010M CCD micrometer was evaluated against the Mitutoyo LSM-500 laser scanning micrometer as an alternative system for non-contact optical measurement of fine fibers. The LS-7010M offers many advantages over the Mitutoyo unit.

The LS-7010M has a broader measurement range than the LSM-500, and is capable of measuring objects with dimensions as small as 0.04 μm and as large as 6 mm. Also, the Keyence unit features a 60 mm wide measuring region compared to the

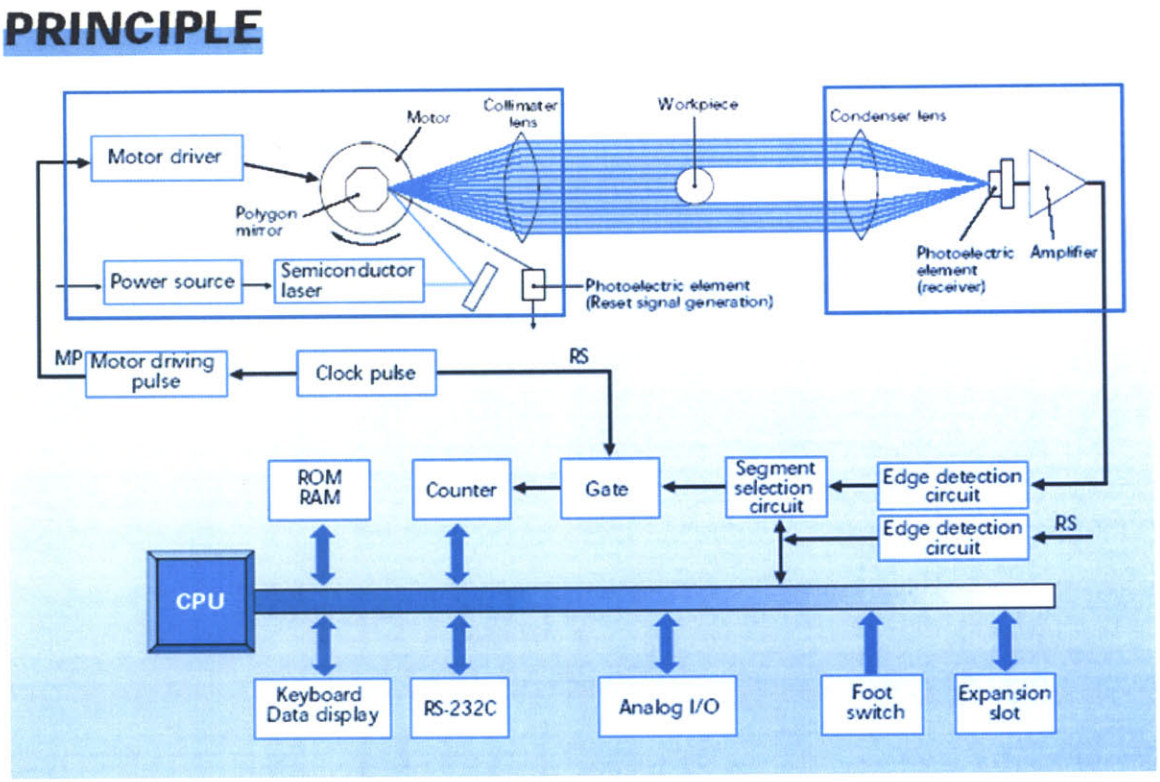

Figure 6-3: Principle of operation for the Mitutoyo LSM500 laser scanning micrometer. (Taken from http://www.mitutoyo.com, Mitutoyo)

34 mm wider opening of the LSM-500. This nearly two-fold increase in space would be a major advantage for configuring the system to accommodate additional testing functionalities. The measurement characteristics of the LS-7010M are only slightly inferior to the LSM-500 with ± 0.5 μm accuracy and ± 0.06 μm repeatability [59].

The LS-7010M measurement system consists of a transmitter and receiver measuring head. The transmitter features a high-intensity gallium nitride (GaN) LED that emits a uniform, low noise, short wavelength green light. The LED is much safer than the laser alternative of the LSM-500. The receiver unit of the LS-7010M contains a telecentric optical system which utilizes only parallel collimated light to form an image, ensuring accurate measurement by preventing fluctuations in lens magnification due to changes in the position of the fiber under test. A high-speed linear CCD allows continuous exposure to all received light and enables an extremely fast sampling rate of 2400 scans/second. Finally, the receiver incorporates a CMOS monitor camera which provides a realistic image of the fiber under measurement [59].

A much faster data acquisition rate of approximately 420μsec is achievable with the Keyence unit with the Keyence LS-7501 controller. The controller interfaces with a custom software application via RS-232C and includes a visual display of the fiber being measured.

In general, the Keyence LS-7010M CCD micrometer outperformed the Mitutoyo LSM-500 laser scanning micrometer and was selected as the geometry measurement system for the single fiber testing instrument.

6.4 Tensile Properties Test Design

The design of the measurement subsystem for determining the tensile properties of single fibers shall be discussed in this section. The tensile properties are a collective measure of the deformation effects of stretching a fiber. In general, these effects are determined by so-called load-elongation methods, otherwise known as stress-strain methods, which measure the load on a fiber as it is stretched [6].

6.4.1 Tensile Properties Measurement Principles

The tensile testing system would be responsible for elongating the fiber at a prescribed rate and for measuring the load on the fiber as it stretched. The fiber elongation functionality would be carried out by the linear motion axes described in the previous chapter concerning the automation of the instrument. This section shall describe the load measurement components.

6.4.2 Tensile Properties Measurement Components

The GSSensors XFTC300-2N load cell was selected for measuring the load on the fiber during elongation. The load cell is capable of 2 N full-scale force measurement for both tensile and compressive loads in static and dynamic applications. The XFTC300-2N has been designed for high stiffness to eliminate measurement error associated with coupling of the load cell with the measured load. The load cell features threaded male mechanical fittings, making it ideal for the custom application and provides a high overload capacity (three-times overload without damage, six-times overload without destruction) to manage excessive force application. The sensor is small and light weight, as well, making it ideal for the tight space conditions of the single fiber testing instrument [60].

The performance of the XFTC300 at low ranges and frequencies is optimized by a sensing element with a fully temperature-compensated Wheatstone bridge equipped with high stability micro-machined silicon strain gages [60]. The XFTC300-2N load cell is shown in Figure 6-4.

To amplify the level of the signal for input into the NI-6052E DAQ card, the load cell was paired with a factory-matched and calibrated GSSensors XAM-BV bipolar amplifier. The XAM-BV is a highly compact bipolar voltage amplifier with a diameter of only 15 mm and length of 55 mm. The amplifier accepts unregulated power between 5 V and 18 V and provides for adjustment of the DC-level and gain of the output signal. The amplifier also features very low noise with a 95 dB common mode rejection ratio (CMRR) [61].

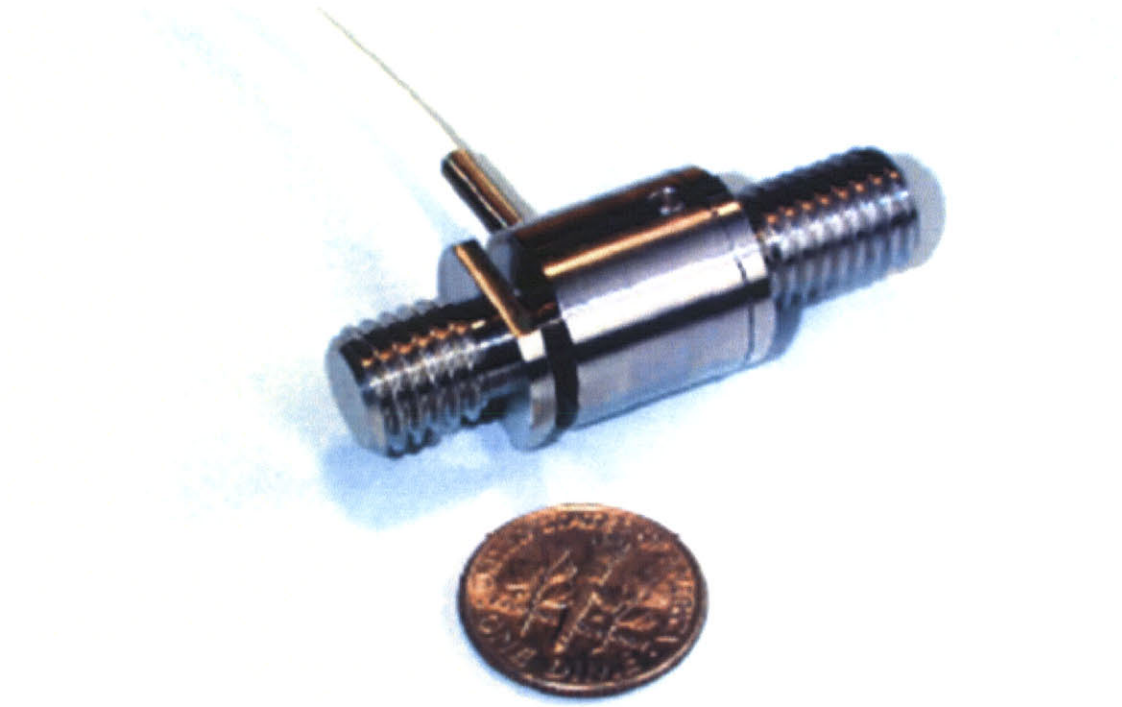

Figure 6-4: Image of the GSSensors XFTC300 load cell. (Taken from http://www.gssensors.com, GSSensors)

6.4.3 Load Cell Protection Unit

The extremely high sensitivity of the XFTC300 load cell also means that it may be damaged very easily. A protection system would have to be created to protect the load cell from overload and to incorporate it into the automated testing protocol of the instrument.

Load Cell Mounting Design Requirements

Tensile testing would involve stretching a fiber which had been loaded into the grippers. During the elongation cycle, the force on the fiber would be measured by the XFTC300 load cell. The grippers were designed to be opened for fiber loading by a force applied perpendicular to the axis of the fiber. Consequently, this was the same axis along which the load cell would have to be mounted to measure the tensile loading forces on the fiber. Figure 6-5 shows this fiber loading and testing configuration.

The load cell would be required to permit precise force measurement along the fiber axis but would have to be protected in all other directions. Five degrees of freedom of protection would be required in all, including all three degrees rotation and two degrees of off-axis translation. The protection mechanism would be designed to permit only translation on-axis with the fiber under test. Also, friction and inertia of the mechanism would be minimized so as not to affect the measurements.

Load Cell Mounting Structure

A mounting structure, shown in Figure 6-6, was designed to completely enclose the load cell and to prevent inadvertent human contact from damaging it. Restriction of all off-axis translational motion and all rotational motion was accomplished by means of a plain bearing with a notch and pin. A Rulon J plain bearing was used as the sliding contact material; and a Delrin structure was designed to mount the load cell to the gripper. The friction between Delrin and Rulon J is extremely low, and Delrin is also a very stiff yet lightweight material, making it optimal for the tensile testing structure.

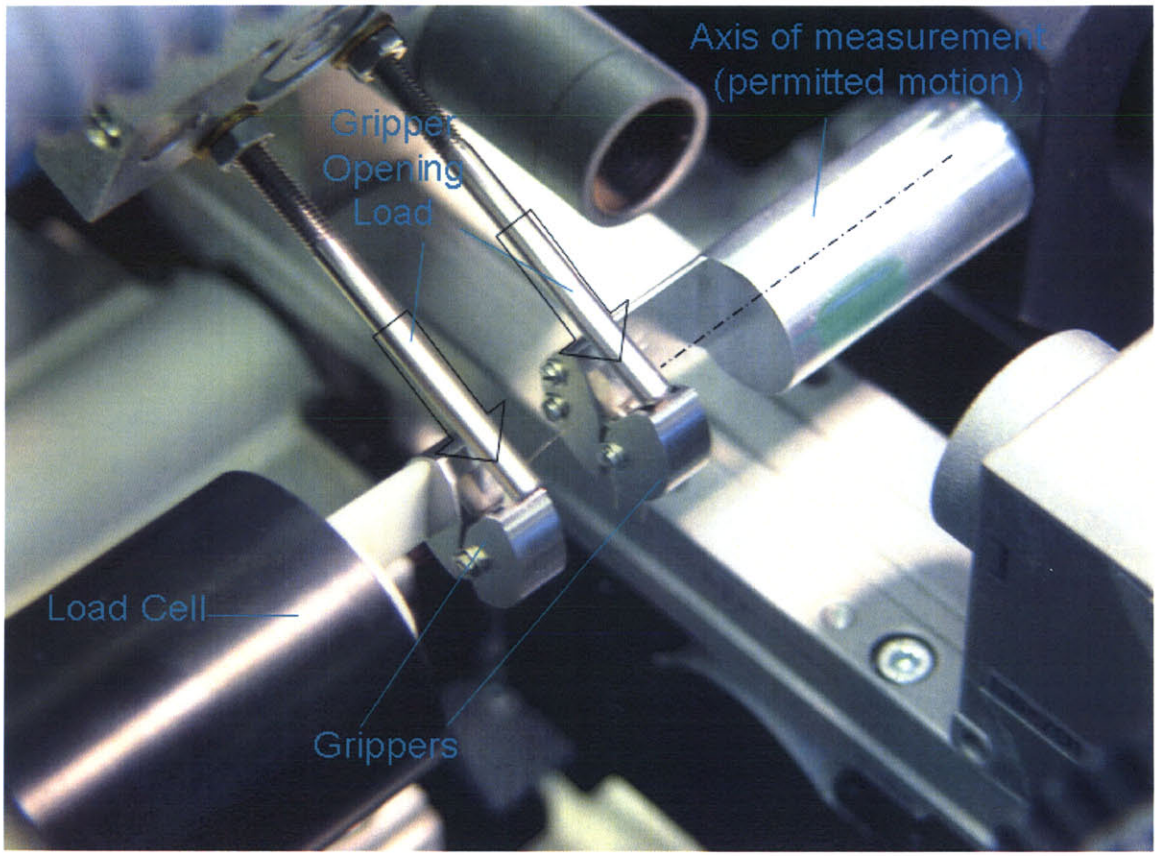

Figure 6-5: Annotated image of the gripper opening mechanism in the single fiber testing instrument.

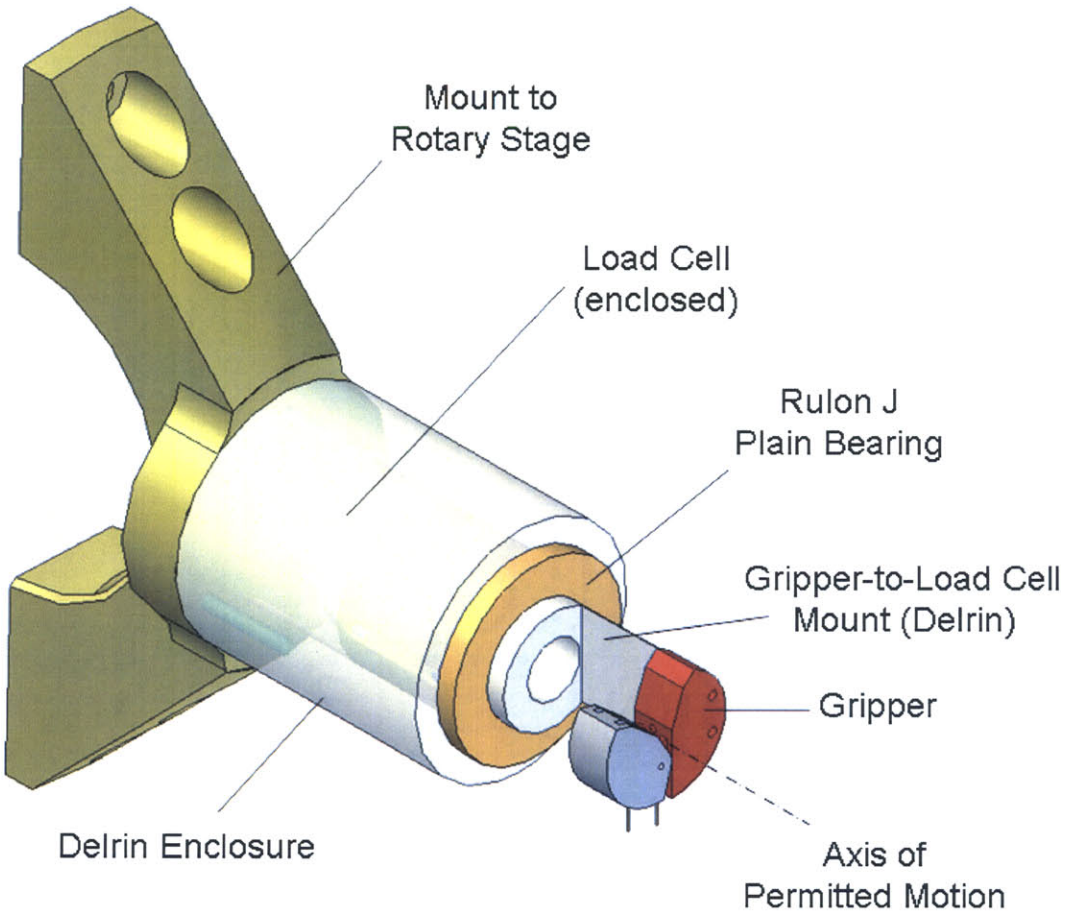

Figure 6-6: Rendering of the load cell mounting assembly.

6.5 Bending Modulus Test Design

The design of the measurement subsystem for measuring the bending properties of single fibers is discussed in this section. The bending properties are determined by measuring the deformation effects of compressing a fiber.

6.5.1 Bending Measurement Principles

The bending measurement system would be responsible for compressing the fiber under test at a prescribed rate and for measuring the load on the fiber during compression. The fiber compression functionality would be carried out by the linear motion axes described in the previous chapter concerning the automation of the instrument. This section shall describe the load measurement components.

6.5.2 Bending Measurement Design Requirements

As described in Section 3.2.5, measurement of the fiber bending modulus will be approximated from the Euler column buckling load for a fixed-fixed boundary condition. The fiber may be compressed while fixed in the grippers and the compressive load may be measured as a function of time and position.

For human hair, the maximum corresponding compressive loads are between 1.0 μN and 6.8 μN so the load measurement system must be very sensitive in the small force range [62]. Also, it is important that the load measurement system has very low inertia so that it couples minimally with the buckling load measurement.

6.5.3 Bending Measurement Components

In the current iteration of the instrument, the measurement of the buckling load for determination of the bending modulus is carried out by the same load cell setup which performs the tensile property measurements. While the load cell is certainly sensitive enough to perform this measurement, and its use for measuring compressive loads as well serves to minimize the number of sensors and complexity of the instrument, it is

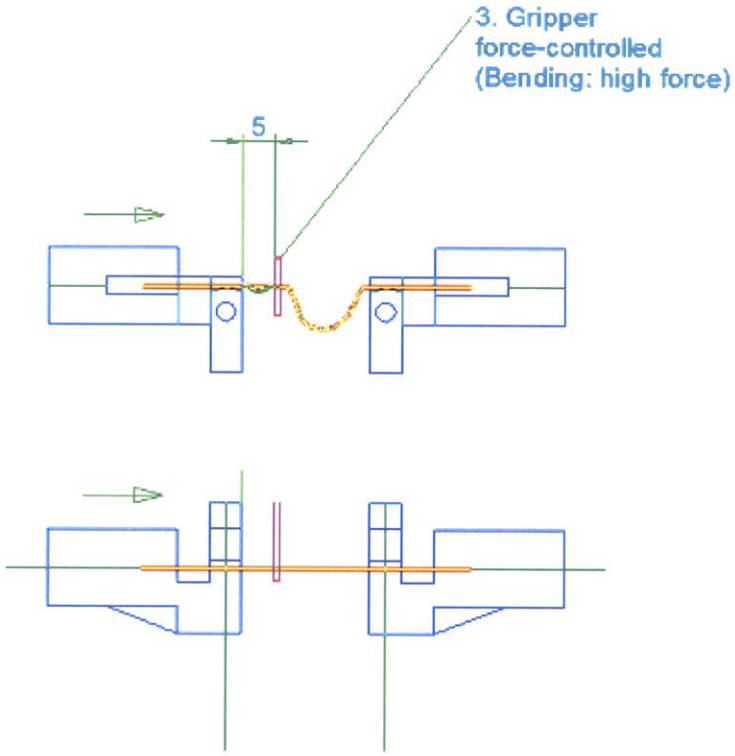

Figure 6-7: Alternative single fiber bending measurement configuration with additional load measuring unit. (Taken from personal communication, Wella AG)

not the ideal scenario. Because the gripper is attached to the load cell, it is massive and its inertia will likely have a profound effect on the quality of the buckling load measurements.

A preferential method would utilize a separate load cell that could be ushered in and out of the testing region. The additional load cell would be able to fix temporarily to the fiber under test securely and without damaging it. The setup would be very low in mass and highly sensitive in the low range of approximately 0.1 N with a resolution better than 0.01 N [63]. Figure 6-7 shows this suggested bending measurement configuration.

6.6 Surface Roughness Test Design

Automated measurement of the surface roughness of fibers is one of the most challenging duties of the single fiber testing instrument. The measurement system has not been fully designed. However, this section shall describe the important measurement principles and design requirements for designing a surface roughness measurement system. Suggestions are also made for components which may be used to carry out the measurement of automate fiber surface roughness.

6.6.1 Surface Roughness Measurement Principles

Chapter 3 defined surface roughness as a quantitative measure of the profile of a surface. The typical method for measuring the roughness of a surface is the tactile stylus method, in which a cantilever tip is passed over the surface of interest, and the vertical deflections of the tip are measured as a function of the horizontal position along the surface. The method produces a 2-dimensional profile of the surface which may then be examined based upon international test standards to determine the roughness.

6.6.2 Surface Roughness Design Requirements

In order to accurately measure the profile of a surface to determine its roughness, very precise horizontal and vertical position measurement transducers are required. Futhermore, it is very important that the surface under measurement remains stationary during testing and that vibration is kept to a minimum as any deflection of the cantilever measurement tip will directly affect the measurement of surface roughness. Finally, it is necessary to scan the surface over an appropriate length, dependent on the standard which shall be used to determine the roughness measurement and the surface characteristics of the sample. Typically, rougher surfaces require greater scan distances and smoother surfaces require shorter scan distances as shown in Table 3.1. Perhaps because of these diverse and complex design requirements, no devices have been developed in the past for the automated measure of fiber surface roughness.

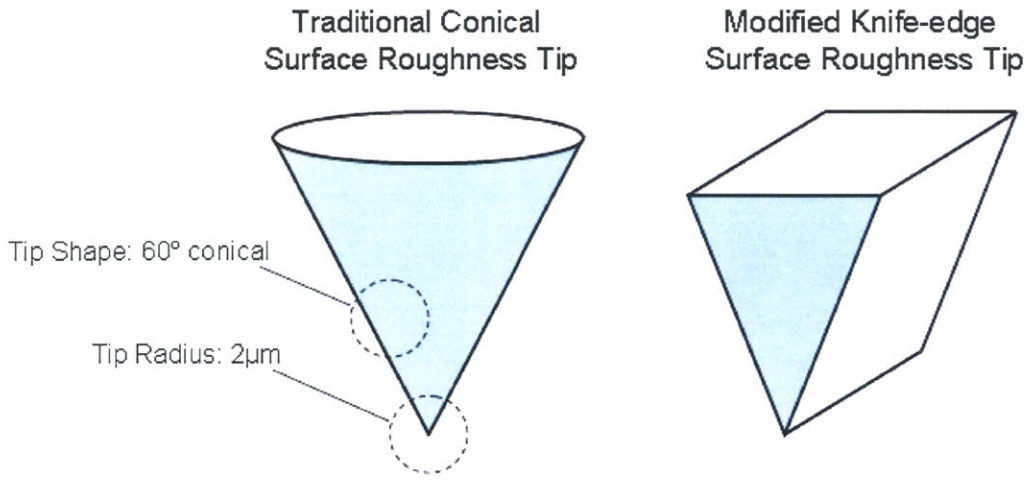

Figure 6-8: Alternative measurement tips for single fiber surface roughness measurement.

6.6.3 Surface Roughness Measurement Components

Mitutoyo markets a series of devices for measuring surface roughness. One device, the Surftest SJ-401, is a handheld unit that uses a cantilever scanning tip and differential inductance method to measure surface roughness with a resolution of 0.01 μm [64]. Such a unit might be integrated into the instrument at a later point. Yet a problem persists with the surface roughness measurement of single fibers that the surface of a fiber is cylindrical, and not flat. The scanning tips for the SJ-401 and for most other commercial surface roughness measuring systems are conical as shown in Figure 6-8. To measure the surface roughness profile of a single fiber, the geometry of the scanning tip would have to be modified to be more like a knife blade so that the tip would maintain constant contact with the surface of the fiber as shown in Figure 6-8.

An optical imaging system may be used as an alternative to a contact-based surface roughness measurement. Scanning electron microscopy (SEM) has been used to measure the surface roughness of single fibers [65]. The instrument has been designed to incorporate a digital video microscope system comprised of a Sony DFW-SX900

high resolution SXGA 1280 $\times$ 960 pixel color digital video camera, an InfiniTube Standard 200 mm infinity correction optic, and a Mitutoyo APO 100$\times$ objective lens. With this setup it is may be possible to visually estimate surface roughness of fibers. Nevertheless, it will be extremely difficult to automate the process of visual surface roughness estimation.

6.7 Friction Test Design

Automated measurement of the friction properties of single fibers is another challenging endeavor. As with the surface roughness module, the measurement system for this module has not been fully designed for the single fiber testing instrument. This section shall describe the important measurement principles and design requirements for designing a friction measurement system. In addition, a method is suggested which may be fully designed in the future to carry out the automated measurement of single fiber friction properties.

6.7.1 Friction Measurement Principles

Fiber friction has been defined in Chapter 3 as the force of resistance when a fiber and a foreign body are placed in sliding contact. Friction may be quantified simply as a force of resistance against sliding, or more commonly, in terms of a coefficient of friction, μ, which relates the resistance force to the contact force between a fiber and a particular material. Friction forces may be static, in reference to bodies which are not sliding, or kinetic, in reference to bodies which are actively sliding.

The important variables for performing a friction measurement are the normal force of contact between two bodies of interest and the force of resistance against sliding the two bodies together. Advanced studies of friction may be interested in the true area of contact between surfaces, as well.

6.7.2 Friction Measurement Design Requirements

Friction properties may be measured in many ways for single fibers, as described in Chapter 3. The design of any effective fiber friction measurement device will entail a few basic requirements. Foremost, the system must measure the frictional force precisely. The system must also provide a consistent surface contact area to ensure consistent surface interaction between fibers and friction specimens. The system must apply a constant, well-known amount of normal force and should accommodate variation of this normal force within a useful range.

In addition, one of the principle reasons to investigate the frictional properties of fibers is to understand the interactions with different materials. Therefore, the friction measurement system should accommodate the testing of various material types. For instance, researchers at Wella would like to be able to test the friction properties of hairs with other keratinous fibers, skin surrogates, and comb materials such as nylon and aluminum [66].

6.7.3 Friction Measurement Components

A new friction mechanism is proposed for incorporation in the single fiber testing instrument which shall allow the measurement of the friction properties of a fiber while the fiber remains in the testing region. Figure 6-9 shows a schematic diagram of the proposed mechanism.

The friction measurement module is comprised of a beam with a friction specimen on one end and a mass on the opposite end. The beam is stiff and can rotate freely about an axis of rotation at its center. The friction specimen may be set into contact with the fiber under test by moving the entire friction measurement module into the testing region between the grippers. The weight of the variable mass, shown by the blue arrow, supplies a precise normal force on the fiber, shown by the black arrow, by reason of a moment created through the axis of rotation of the beam. The fiber may then be moved with a precise velocity by the linear motion stages while still in the grippers. A frictional resistance force, shown by the red arrow, will result between

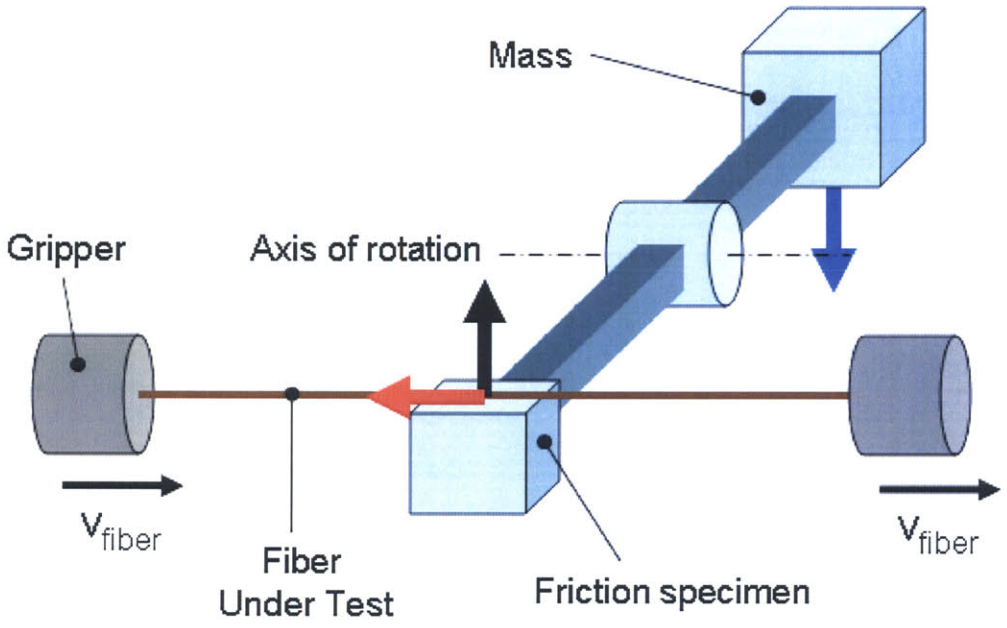

Figure 6-9: Proposed design for measurement of single fiber friction properties.

the fiber under test and the friction specimen.

The friction specimen may be designed as a user-adjustable cartridge. Cartridge variables may include various materials and friction testing tip shapes such as sharp tips, hollow half-cylindrical tips, and saddle tips.

The frictional load on the fiber may be measured directly by the load cell used for determining the tensile forces in the fiber. A better alternative, however, would be to use a separate, independent load cell for the reasons discussed in Section 6.5.3 for the bending modulus measurement system. A separate load measuring device could be designed to have lower inertia and higher sensitivity in the ranges of importance for the friction measurement.

6.8 Torsional Modulus Test Design

The final measurement module design discussed shall be the torsional modulus test. A new contact-based mechanical method has been proposed in Chapter 3 for measuring the torsional modulus of a fiber as opposed to traditional torsional pendulum method. The principles of this measurement are reiterated in this section, and the design requirements and the components necessary to create a prototype of the new design are presented.

6.8.1 Torsional Modulus Measurement Principles

The basic principle of the new proposed torsional modulus measurement is that a fiber is gripped at both ends, and that the ends are rotated together at a constant rate while the fiber is held fixed at its center. A moment will be generated in the fiber to counter the rotation of its ends, and this moment will be measured by the proposed measurement system. The torsional modulus may then be determined from geometric variables of the fiber which will be determined by the geometry measurement module of the instrument.

6.8.2 Torsional Modulus Design Requirements

The proposed torsional modulus measurement method will be far more convenient than the pendulum method; however, in order to produce accurate results, several design requirements must be carefully observed. An extremely sensitive load sensor will be required to measure the minute moment resulting from twisting the fiber. The angular torque τ will correspond to a measured force via the relationship

$$\tau = F \times R, \tag{6.1}$$

where F is the force measured by the load sensor and R is the total distance between the center of the fiber and the center of the sensing element.

The angle of rotation of the fiber must be uniform and precise. The fiber must be located exactly on the axis of rotation, as well, to prevent deviations in the force measurement as it is turned. The cross-sectional dimensions of the fiber must be well-known at the point of contact between the fiber and the measurement unit. Finally, it will be quite important that the fiber does not slip on the measurement unit. Even a small angle of slip between the pair will compromise the quality of the measurement significantly.

6.8.3 Torsional Modulus Measurement Components

A prototype design of the proposed mechanism has been created based upon available components. The moment on the twisted fiber is measured using a SensorOne AE801 force transducer. The AE801 is a highly sensitive and compact silicon beam strain gage force sensor with a maximum detection range of 0.12 N. The sensor is constructed from a single crystal silicon beam with one ion implanted resistor on each side. The whole sensor assembly is mounted in a miniature header as shown in Figure 6-10. A deflection of the sensor beam results in a change in the resistance values with one resistor increasing in value and the other decreasing [67]. With appropriate signal conditioning of the AE801 sensor output, calculations have shown that it will be possible to resolve loads as small as 0.4 mN with the AE801 sensor using the 16-bit

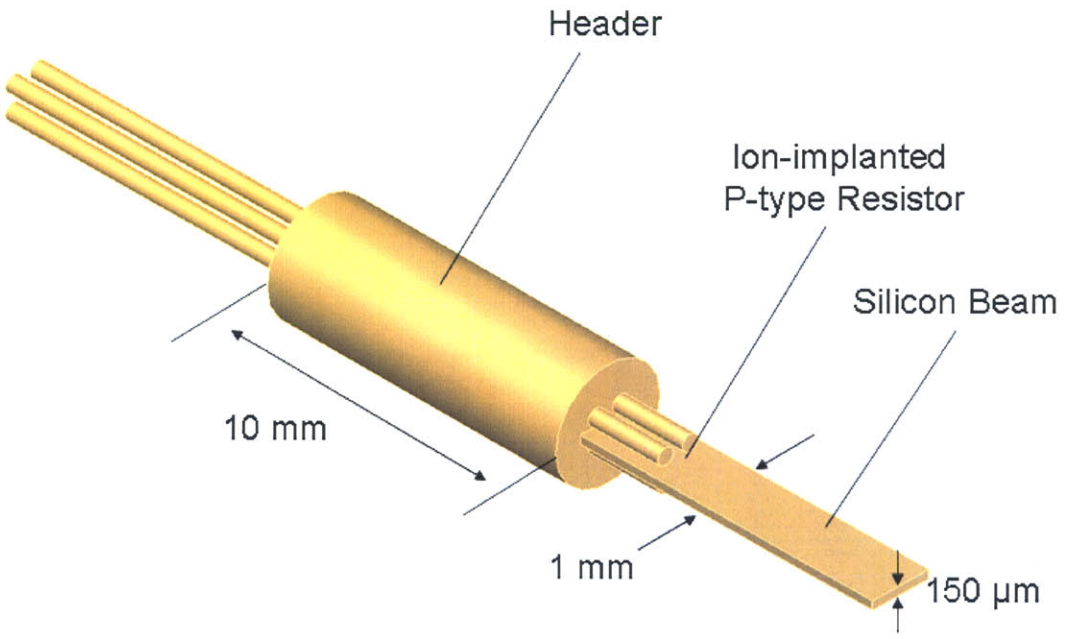

Figure 6-10: SensorOne AE801 silicon beam sensing element. (Adapted from http://www.sensorone.com, SensorOne)

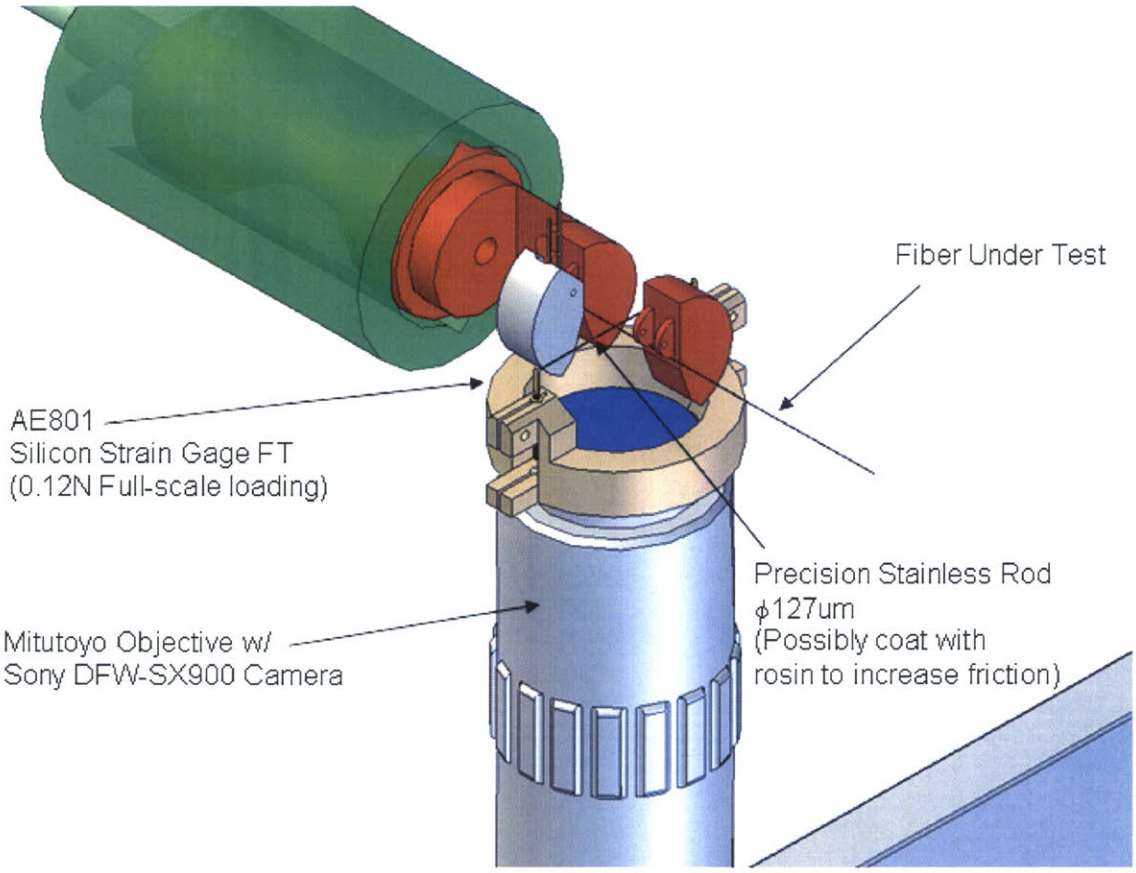

Figure 6-11: Prototype design for in-situ measurement of single fiber torsion properties.

National Instruments PCI-6052E DAQ card. Further calculations based upon the torsional modulus equations shown in Chapter 3 suggest that the sensor will allow measurement of the torsional modulus of fibers to 0.01 GPa.

Figure 6-11 shows a rendering of the proposed mechanism. The torsion measurement module is to be mounted to the video microscope imaging system of the instrument so that the fiber slip may be monitored. In the rendering, two AE801 strain gages are mounted in parallel with a roughened stainless rod mounted between the two. Further study will be required to determine whether a design based on the use of two parallel sensors is superior to using only a single AE801 sensor to measure the torsional modulus.

No-slip contact between the sensor and the fiber is achieved through contact with

a roughened surface element affixed to the end of the AE801 sensor. If the fiber slips with this design, an alternative means such as adhesive, electrostatics, or mechanical gripping will be necessary.

Chapter 7

Software

The automation and testing functionality of the single fiber testing instrument would not be possible without a software system to control the operation of all of the hardware and components. Software would also be responsible for the interface between a user and the instrument. This chapter shall discuss the main considerations that drove the development of the instrument software.

7.1 Main Software Platform

The multifunctionality of the instrument required the use of an advanced main computing platform. A high performance 3.2GHz Pentium 4 Dell XPS personal computer was used to develop and run the instrument control software. The software and the graphic user interface of the instrument were developed in the Visual Basic.NET 2003 programming environment. National Instruments Measurement and Automation Explorer and the associated National Instruments motion and DAQ device drivers were used to configure and ultimately control the motion and DAQ systems of the instrument from the custom software application.

7.2 Graphic User Interface

The graphic user interface (GUI) for the automated single fiber testing instrument was designed for optimum simplicity and usability by a trained technician. The GUI would be responsible for allowing a user to configure the instrument prior to automated testing and was designed to handle pre-test input such as user information, fiber type, number of fibers to be tested, the tests to be performed. Advanced features such as user-adjustable test parameters would also be integrated into the GUI. The GUI was designed to be robust against erroneous inputs during these user input processes.

The GUI was also designed inform a user of testing status, including the fiber under test and measurement readouts for on-instrument sensors. Finally, the GUI would be responsible for posting and saving the results of measurements of tested fibers.

7.3 Data Storage

The large amounts of data generated by the instrument would be stored as plain text data files. During each round of testing, an independent file would be created for each tested fiber. Each file contained information about the fiber type, the fiber number in the test sequence, the date of the test, the user who operated the instrument during the test, and all of the raw data associated with the measured properties of the fiber.

The user would be responsible for processing the data himself after a round of testing. Future work would require that the instrument control software would perform appropriate analyses to determine single fiber properties from the raw data as well as statistics on large sets of tested fibers. Many of the testing protocols have not been well-established to permit this action at present.

Chapter 8

Conclusion

In conclusion, the design and development of the automated single fiber testing instrument has been quite successful. The automation system is fully functional and is capable of precisely and delicately manipulating a wide variety of single fiber types for automated testing of up to 100 fibers. The measurement system of the instrument is also quite functional and provides full measurement capabilities for automatically determining fiber geometry, tensile strength, elastic modulus, elongation to break, Poisson's ratio, bending modulus, and for performing microscopic fiber still and video imaging.

Some single fiber measurements including frictional properties and torsional modulus have not been fully implemented, but have been carefully considered. Well-structured designs have been proposed for how to perform these measurements and which should make their development possible in the near future.

Measurements of single fiber surface roughness properties remain an elusive goal of the instrument, and it is hoped that the research provided by this thesis will inspire the development of an operational system for measuring these properties in the future.

More work must be done to further develop each test performed by the instrument. Protocols for each test need to be rigidly established. The sensing systems in the instrument must be calibrated and optimized for reduction of signal noise. Furthermore, each test must be verified for effectiveness.

Additionally, the software which controls the instrument has not been thoroughly

debugged or optimized for robustness. The user interface may require improvements which will become evident as soon as a technician unfamiliar with the instrument first uses it.

Upon completion, the instrument will be unlike any other on the market or perhaps in existence. The automated single fiber testing instrument shall be fully capable of automatically testing a large number of single fibers for geometric properties, tensile properties, elastic properties, surface roughness properties, friction properties, bending properties, and torsional properties. A host of other measurements such as resistance, thermal conductivity, fatigue strength, and others may be easily incorporated into the automated functionality of the instrument as well. The instrument will be an invaluable tool to countless researchers who presently rely on many different manually-operated machines to characterize the properties of single fibers.

Bibliography

[1] Annette Schwan-Jonczyk. *Wella Hair Structure.* Wella AG, Darmstadt, Germany, 1st edition, 1999.

[2] Mahr GmBH, P.O. Box 1853 D-37073 Göttingen. *Perthometer Definitions, Surface Texture Parameters.*

[3] http://www.diastron.com/docs/hair.htm.

[4] http://www.textechno.com.

[5] John Gray. P & g - the world of hair (hair structure - follicle - hair bulb). http://www.pg.com/science/haircare.

[6] C. R. Robbins. *Chemical and Physical Behavior of Human Hair.* Springer-Verlag, New York, New York, 4th edition, 2002.

[7] M.J. Adams, B.J. Briscoe, and T.K. Wee. The differential friction effect of keratin fibres. *J. Phys. D: Appl. Phys.*, 23:406–414, 1990.

[8] J.D. Leeder and J.H. Bradbury. No title. *Nature*, 218:694, 1968.

[9] P. Kintz. *Drug Testing in Hair.* CRC Press, Boca Raton, Florida, 1996.

[10] K. Meinert. Wella testing methods. Email, October 2002.

[11] R.F. Stamm, M.L. Garcia, and J.J. Fuchs. The optical properties of human hair. *Int. J. Cosmet. Chem.*, 28:571, 1977.

[12] Wella AG. Measurement of hair shine. *FKM Final Report*, page 9f, 1997.

[13] A. Böther, B. Primmel, and W. Seidel. Haarkosmetich bedingte volumenänderungen bestimmen. *Parfümerie und Kosmetik*, 79(10):26, 1998.

[14] C. R. Robbins. *Chemical and Physical Behavior of Human Hair.* Springer-Verlag, New York, New York, 3rd edition, 1994.

[15] M.A. Pykett and J.A. Swift. No title. *Parfümerie und Kosmetik*, 79(38), 1998.

[16] N.R. Mann, R.E. Schafer, and N.D. Singpurwalla. *Methods for Statistical Analysis of Reliability and Life Data.* John Wiley & Sons, New York, New York, 1974.

[17] Wella AG. Wella methods - short description. Email, August 2003.

[18] C.R. Robbins and G.V. Scott. No title. *J. Soc. Cosmet. Chem.*, 29:783, 1978.

[19] G.V. Scott and C.R. Robbins. No title. *J. Soc. Cosmet. Chem.*, 29:469, 1978.

[20] P. Busch and W. Höfer. No title. *Parfümerie und Kosmetik*, 72(10):632, 1991.

[21] W. Krause. *Konstruktionselemente der Feinmechanik.* Carl Hanser Verlag, Munich-Vienna, 2nd edition, 1993.

[22] K. Meinert. Wella single fiber testing methods. Email, October 2002.

[23] W.B. Bickford. *Mechanics of Solids.* Richard D. Irwin, Burr Ridge, Illinois, 1993.

[24] http://www.mahr.com.

[25] http://www.outokumpu.com/pages/Page____5852.aspx.

[26] G. Kristofek. Mit-wella meeting minutes. Email, November 2004.

[27] Mitutoyo, 20-1, Sakado 1-chrome, Takatsu-ku, Kawasaki, Kanagawa, Japan. *SV2000/3000 Surface Roughness Measuring System Main Unit User's Manual*, 178 edition.

[28] N.P. Suh. *Tribology.* MIT Press, Cambridge, Massachusetts, 1992.

[29] M.J. Adams, B.J. Briscoe, and T.K. Wee. The differential friction effect of keratin fibres. *J. Phys. D: Appl. Phys.*, 23:406–414, 1990.

[30] A. Schwartz and D.J. Knowles. No title. *Soc. Cosmet. Chem.*, 34:301, 1983.

[31] C.R. Robbins and G.V. Scott. No title. *J. Soc. Cosmet. Chem.*, 31:179, 1980.

[32] http://www.instron.com.

[33] Wella AG. Biegesteifigkeitsmessung von einzelhaaren. Email, May 2004.

[34] G. Kristofek. Wella hair fiber testing machine specs. Email, November 2002.

[35] http://www.inanowin.com/pdf/Nano%20Positioning%20System %20PDF/Special%20system/Piezo%20gripper.pdf.

[36] http://www.techno-sommer.com.

[37] http://www.3dsystems.com/products/sla/viper/index.asp.

[38] A. H. Slocum. *Precision Machine Design.* Society of Manufacturing Engineers, originally published by Prentice-Hall, Dearborn, Michigan, 1992.

[39] T. Fofonoff. Microelectrode array fabrication by electrical discharge machining and chemical etching. *IEEE Trans. On Biomed. Eng.*, 51(6):890, 2004.

[40] http://www.matweb.com.

[41] http://www.3dsystems.com/products/sla/viper/specs.asp.

[42] M. Arista. Personal Communication, June 2004.

[43] http://www.trotec.net.

[44] http://www.daedalpositioning.com/404XR_406XR_Manual.pdf.

[45] http://www.daedalpositioning.com/Products/Rotary_Positioners__ 5504__32.html.

[46] http://catalog.festo.com/data/CAT_PDF/001/DFM_0410_EN.pdf.

[47] http://catalog.festo.com/data/CAT_PDF/001/CPE_0410_EN.pdf.

[48] http://www.aromat.com/pcsd/product/pmos/pdf_cat/aqv21_.pdf.

[49] http://www.ni.com/pdf/products/us/4mo636-637.pdf.

[50] http://www.ni.com/pdf/products/us/4mo640-641.pdf.

[51] http://www.compumotor.com/products/Stepper_Drives_and_Motors_5325_30_32_80_567_29.html.

[52] http://catalog.festo.com/data/CAT_PDF/001/VADM_0410_EN.pdf.

[53] http://www.anver.com/document/vacuum%20components/vacuum%20generators/Transfer%20Tubes/tt05!.htm.

[54] http://www.ni.com/pdf/products/us/4daqsc199-201_ETCx3_212-213.pdf.

[55] http://sine.ni.com/apps/we/nioc.vp?lang=US&cid=1180.

[56] http://www.renishaw.com/client/product/UKEnglish/PRD-855.shtml.

[57] http://www.renishaw.com/client/product/UKEnglish/PRD-6076.shtml.

[58] http://www.mitutoyo.ca/Links/New%20Products/Laser%20Scan%20Micrometer.pdf.

[59] http://world.keyence.com/products/thrubeam/ls_7000/ls_7000.html.

[60] GS Sensors, 116 W. Chestnut St., Ephrata PA 17522. *XFTC300-U Series Miniature Load Cell.*

[61] GS Sensors, 116 W. Chestnut St., Ephrata PA 17522. *Miniature In-line Voltage Amplifiers XAM Series.*

[62] K. Meinert. Re: Mit-wella meeting minutes 11-2-04. Email, November 2004.

[63] K. Meinert. Wella testing - bending force values. Email, November 2004.

[64] http://www.mitutoyo.com/catalog/pdf/B-08.pdf.

[65] TRI/Princeton. Tri/princeton research: Textile science - single fiber, yarn, and fabric studies. http://www.triprinceton.org/research/textile_sci.html.

[66] G. Kristofek. Mit-wella meeting minutes. Email, June 2004.

[67] http://www.sensorone.com/AE801_Home.asp.